

Renewable, Flexible, and Storage Capacities: Friends or Foes?

Xiaoshan Peng^{*}, Owen Q. Wu^{*}, and Gilvan C. Souza^{*}

^{*}Kelley School of Business, Indiana University, Bloomington, IN, USA

^{**}Haslam College of Business, University of Tennessee Knoxville, TN, USA

March 3, 2024

Problem Definition: Over 97% of the power generation capacity to be installed from 2021 to 2050 in the U.S. is expected to be powered by wind, solar, and natural gas. Meanwhile, large-scale battery systems are planned to support the power systems. It is paramount for policymakers and electric utilities to deepen the understanding of the operational and investment relations among the renewable, flexible (natural gas-powered), and storage capacities. In this paper, we optimize both the joint operations and investment mix of these three types of resources, examining their investment relations (i.e., investment substitutes or complements). **Methodology/results:** Using stochastic control theory, we prove the structure of the optimal storage control policy. From the optimal control policy, we identify different pairs of charging and discharging operations. We find that whether storage complements or substitutes other resources hinges on the operational pairs involved and whether executing these pairs is constrained by charging or discharging. Through extensive numerical analysis using data from a Florida utility, government agencies, and industry reports, we demonstrate how storage operations drive the investment relations among renewable, flexible, and storage capacities. **Managerial implications:** Several distinct relations are identified: storage and renewables are substitutes in meeting peak demand; storage complements renewables by storing surplus renewable output; renewables complement storage by compressing the peak period, making it easier for the storage to shave the peak demand and displace flexible capacity.

Key words: Renewable energy, flexible generation, energy storage, capacity investment, stochastic optimal control

1. Introduction

Electricity and heat generation are the largest contributors to global greenhouse gas (GHG) emissions, accounting for 32% of global GHG emissions.¹ In the U.S., electricity generation makes up 25% of total GHG emissions, down from 33% in 2010 ([U.S. Environmental Protection Agency 2024](#)). The reduction has been achieved partly by a shift from GHG-intensive coal toward renewables and natural gas ([Drake and York 2021](#)). According to the American Public Power Association ([Buttel 2023](#)), from 2015 to 2022, a total of 234.8 GW of new power generation capacities were built in the U.S., of which 34.1% was powered by natural gas, 34.1% by wind, 29.7% by solar, 1.2% by other renewables and wastes, and 0.6% by nuclear. Going forward, the U.S. Energy Information Administration ([EIA 2021a](#)) projects that between 2021 and 2050, about 950 GW of new electricity generation capacity will be installed, of which 46% are expected to come from solar, 12% from wind, and 39% from natural gas. Evidently, an increasing share of power generation will be from solar and wind power, whose intermittent output is buffered by natural gas-powered capacity.

Intermittency of renewable generation is also increasingly managed by energy storage, which, despite being a net energy consumer, plays a crucial role in balancing supply and demand. Recent investments in energy storage, particularly in batteries, have surged. By the end of 2019, U.S. had installed 1 GW of utility-scale battery, with 83% added between 2015-2019 ([EIA \(2021b\)](#)). However, utility-scale battery capacity soared to 7.8 GW by October 2022 ([EIA 2022b](#)) and reached approximately 16 GW by the end of 2023 ([EIA 2024](#)). Future projections are robust, with plans to introduce an additional 15 GW in 2024 and about 9 GW in 2025 ([EIA 2024](#)).

The composition of energy resources is largely decided by utility firms aiming to minimize the total cost of serving their customers ([Anderson 1972](#)), among other policy considerations. Their decisions are shaped by government incentives and regulations, such as the U.S. federal investment tax credit for solar and California's mandates on minimum storage investments by utilities. Given the substantial projected investments in energy resources—storage, renewable, and flexible resources—it is critical for the government and the energy sector to grasp the relationship between these resources in terms of both investment and operations.

On the investment front, it is vital to understand how policies directed toward one type of energy resource may influence investments in others—whether these energy resources act as investment complements or substitutes (or figuratively, whether they are friends or foes). For example, federal tax credits intended to reduce solar investment cost may affect investments in battery and flexible resources; government funding for electricity storage R&D may lower future storage costs, influencing

¹Based on data compiled by [World Resources Institute \(2024\)](#), the top GHG contributing sectors in 2020 were: electricity/heat (32.0%), transportation (15.3%), manufacturing/construction (13.1%), and agriculture (12.3%).

investments in renewable and flexible resources. Investment decisions depend on operating policies, which can be seen evidently through examples. Operationally, battery can store surplus renewable energy, suggesting that battery and renewable capacities may be complementary investments. On the other hand, peak demand can be satisfied by flexible, renewable, and/or battery resources, indicating these capacities could be substitutable investments. In this paper, we aim to address the following pivotal questions: Under given resource capacities, what is the optimal operating policy for energy storage, renewable and flexible resources? Under the optimal operating policy, how do the relations among the optimal investments in these three resources (as investment substitutes or complements) change with investment costs?

Investments in power generation resources have received considerable research attention. While we provide a detailed review in Section 2, here we briefly discuss two pertinent studies. [Kök et al. \(2020\)](#) analyze the investment relations among renewable, flexible, and inflexible resources. In their setting without storage, costs can be decoupled across periods, allowing for static optimization of resource operations. [Kaps et al. \(2023\)](#) consider investments in renewable and storage resources by approximating storage operation dynamics and deriving upper and lower bounds on storage investment. To the best of our knowledge, our research is the first to examine the joint investment in renewable, flexible, and storage resources while optimizing storage operations in a stochastic and dynamic setting. We employ stochastic optimal control theory to optimize resource operations. This method has rarely been applied in economic analysis for energy systems (see Section 2). We demonstrate the advantages of this method for optimizing energy generation and storage operations: The continuous-time model not only reflects the reality of instantaneous balancing of supply and demand in electricity systems, but also enables a more concise characterization of the optimal control policy compared to a discrete-time model.

In this paper, we also introduce a novel approach to analyzing how energy storage operations drive resource investment relations. For every unit of energy charged or discharged, we identify the source of energy for charging or the energy displaced by discharging. We then pair up units of charged or discharged energy to deepen our understanding of how the storage policy (optimized using the control theory) creates value and drives the investment relations among battery, renewable, and flexible resources.

By tightly connecting operations to investments, this paper offers several practical insights. In areas with high existing natural gas generation and low renewable penetration, promoting renewable investments can discourage battery investments and vice versa, as they act as substitutes in meeting peak demand. However, this substitution relation reverses in two situations. First, when renewable generation occasionally exceeds the demand, batteries complement renewables by time-shifting the

surplus output: the batteries may operate predictably (e.g., storing excess solar every morning) and/or serve as a buffer against uncertainties in demand and renewable output. Second, anticipating power plant retirements, utilities may consider using batteries to meet part of the peak load, thereby reducing the need for new flexible capacity. In such a situation, increasing renewable capacity (even if renewable output never exceeds demand) can compress the peak-load period, making it easier for batteries to shave the peak load. Thus, renewables and batteries together can substitute flexible capacity, in contrast to the complementary relation between flexible and renewable capacities identified by [Kök et al. \(2020\)](#).

2. Literature Review

There is a vast literature on energy operations, with general reviews provided by [Parker et al. \(2019\)](#), [Sunar and Swaminathan \(2022\)](#), and [Mak \(2022\)](#). Our work considers the context of regulated utilities investing in flexible fossil fuel capacity, renewable, and storage capacities. Establishing an optimal investment strategy requires an optimal operating policy for these resources. Four streams of research are particularly relevant to our study: 1) optimal operations of stand-alone storage units, 2) joint operations of renewables and storage, 3) investments in renewable energy capacity (without considering storage) and the impact of government policies, and 4) optimal capacity investment in a renewable-storage combinations. We review each of these streams below.

First, optimal operations of stand-alone storage units in electricity markets have received significant research attention. [Paine et al. \(2014\)](#) analyze the optimal operation of a pumped hydro storage unit under different compensation rules by independent system operators. Using different modeling approaches, [Secomandi \(2010\)](#) and [van de Ven et al. \(2013\)](#) establish the optimality of a dual-threshold policy for a storage unit with charging and discharging constraints on a market with positive electricity prices. [Zhou et al. \(2016\)](#) allow for the possibility of negative prices and show that the dual-threshold policy may not hold. [Xi et al. \(2014\)](#), [Jiang and Powell \(2015\)](#), and [Cruise et al. \(2019\)](#), among others, focus on algorithmic and computational aspects. [Wu et al. \(2022\)](#) optimize charging schedules for electric vehicles to minimize charging costs and customers' inconvenience cost. In this paper, storage is not stand-alone but is jointly optimized with flexible and renewable generation, in terms of both operations and investments.

The second research stream considers operations of storage-renewable combinations. [Korpaas et al. \(2003\)](#), [Castronuovo and Lopes \(2004\)](#) and [Del Granado et al. \(2014\)](#) use a deterministic optimization approach to find the optimal operation of a storage-renewable combination in a day-ahead market given forecasts of wind generation and spot market prices. [Castronuovo and Lopes \(2004\)](#) and [Del Granado et al. \(2014\)](#) use sensitivity analysis to calculate the value of storage, with the latter study concluding that storage and wind are economic complements. To explicitly capture

uncertainty in electricity market prices and wind generation, [Garcia-Gonzalez et al. \(2008\)](#) propose a two-stage stochastic program to optimize the joint operation of a pumped hydro-wind system. [Kamdem and Shittu \(2017\)](#) use Bender's decomposition in a two-stage stochastic program for a grid-connected micro-grid with many dispatchable units and a constraint on emissions. [Harsha and Daleh \(2015\)](#), [Zhou et al. \(2019\)](#) and [Avci et al. \(2021\)](#) use Markov decision processes to derive optimal operating policies of a wind-storage unit connected to a grid. [Zhou et al. \(2019\)](#) and [Avci et al. \(2021\)](#) allow for negative electricity prices and transmission constraints; given the difficulty in characterizing optimal operating policies under these conditions, they propose well-performing heuristics. [Kim and Powell \(2011\)](#) explores a wind farm's optimal commitments in energy markets, in the presence of storage and conversion losses. Our contribution to this stream includes analyzing joint operations of storage, renewable, and flexible resources under stochastic conditions, applying stochastic control to characterize the optimal policies.

The third stream of research studies energy markets with renewable generation and investments in renewable capacity. Renewable energy integration into energy markets have been examined from the perspectives of supply function competition ([Al-Gwaiz et al. 2017](#)), forward markets ([Sunar and Birge 2019](#), [Peura and Bunn 2021](#)), aggregation ([Gao et al. 2024](#)), and consumer adoption ([Huang et al. 2023](#)). On renewable capacity investment, some research considers computational issues ([Parpas and Webster 2014](#), [Bruno et al. 2016](#)), while the majority focuses on how renewable investors (including households) invest in response to factors such as random demand and a price-setting utility ([Angelus 2021](#)), third-party ownership ([Guajardo 2018](#)), feed-in-tariffs ([Alizamir et al. 2016](#), [Babich et al. 2020](#), [Goodarzi et al. 2019](#), [Ritzenhofen et al. 2016](#)), net metering ([Hu et al. 2015](#), [Sunar and Swaminathan 2021](#)), tariff structure ([Singh and Scheller-Wolf 2022](#)), timing of government support ([Welling 2016](#)), and competition ([Siddiqui et al. 2016](#), [Weigelt and Shittu 2016](#)). As in our research, [Aflaki and Netessine \(2017\)](#), [Kök et al. \(2018\)](#) and [Kök et al. \(2020\)](#) study a utility firm's investment in renewable and conventional generation. The key distinction of our research lies in the inclusion of battery storage investments, necessitating the development of an optimal storage operating policy as an input to the capacity investment decisions.

Finally, a stream of literature delves into optimal or near optimal investment strategies in energy storage and renewables. [Fertig and Apt \(2011\)](#) simulate different storage capacities for wind farms in Texas to meet demand of a large Texas city. [Budischak et al. \(2013\)](#) simulate a large number of scenarios where batteries could be used with a portfolio of renewables in different locations to meet electricity demand. [Kuznia et al. \(2013\)](#) and [Billionnet et al. \(2016\)](#) propose two-stage stochastic mixed-integer programs to find optimal investments in renewable and storage capacities; [Brown et al. \(2008\)](#) use a similar approach to find optimal pumped storage capacity. [Qi et al. \(2015\)](#) use

a facility location model to optimize capacities of a transmission network serving wind generators, where batteries can store wind generation exceeding transmission capacity. Wu et al. (2023) identify optimal storage investment strategy in a tree network. Sharma et al. (2019) find the optimal battery size for a home with a given solar capacity through simulation optimization. Cho et al. (2023) analyze optimal investments of renewable and storage in the residential sector with time-of-use tariffs. Bertsimas et al. (2023) develop a robust optimization method for optimizing renewable and storage capacities, and implement it practice. Finally, Kaps et al. (2023) find the optimal renewable and storage capacities under deterministic demands with two levels (day and night) and uncertain renewable output modeled by a uniform distribution. They approximate storage operation dynamics and derive optimal capacity investments in closed form. In our research, under stochastic demand and renewable generation, we determine the optimal battery operating policy as a foundation for the high-level problem of optimizing capacity investments. We show that the two problems—operations and investment—are tightly connected by our new perspective to understand how storage operations drives resource investments. Our approach captures the value of battery in time-shifting of demand, buffering demand and renewable uncertainties, encouraging renewable investment, and reducing reliance on flexible fossil-fuel generation.

3. The Model

We consider the problem of an electric utility firm investing in three types of resources—renewable and flexible power generators, and battery storage, given their technologies and investment costs. After these new resources are installed, the utility operates its resource portfolio to meet fluctuating electricity demands. Our model excludes investments in nuclear or coal-fired power generators. The existing nuclear or coal-fired plants are assumed to produce a (predetermined) constant power.

3.1 Resource Investment

We assume that a utility-scale battery storage technology is given, and its key technological parameters include round-trip efficiency α (the proportion of energy output relative to energy input), battery duration L (amount of time a battery can discharge at its power capacity before depleting its energy capacity), charging duration L^c (time it takes to fully charge a depleted battery), and maximum depth of discharge l_{\max} (maximum proportion of the battery’s total energy capacity that can be used, recommended to ensure longevity and performance). The utility’s battery investment decision is the battery’s *operating energy capacity* B (in energy units, MWh), which is the effective energy capacity that is available for operational purposes to maintain battery longevity. This is equivalent to deciding the *discharging power capacity* y_{out}^B (maximum power output, in power units, MW) or the *charging power capacity* y_{in}^B (maximum power input, MW). These three metrics, B , y_{out}^B ,

and y_{in}^B , are proportional and linked by the battery's technological parameters. One must install a total energy capacity of B/l_{max} to obtain an operating energy capacity of B . The corresponding power capacities are $y_{\text{out}}^B = B/(l_{\text{max}}L)$ and $y_{\text{in}}^B = B/(l_{\text{max}}L^c\alpha)$.

We assume that the utility's current renewable, flexible, and storage capacities are y_0^R (MW), y_0^F (MW), and B_0 (MWh), respectively. The utility's investment problem is to bring the renewable, flexible, and storage capacities up to $y^R \geq y_0^R$, $y^F \geq y_0^F$, and $B \geq B_0$, to minimize the sum of the investment cost and the expected discounted operating cost after the investment.

Let k^R , k^F , and k^B denote the investment cost per unit of renewable, flexible, and storage capacities, respectively. Linear investment cost functions are suitable for utilities to estimate the investment expenses (see [Kök et al. 2018](#) for a discussion). Let $C(y^R, y^F, B)$ denote the minimum expected discounted cost of meeting demand using capacities (y^R, y^F, B) over a planning horizon of length T . Then, the utility's investment problem can be written as

$$\begin{aligned} \min_{\{y^R, y^F, B\}} \quad & k^R(y^R - y_0^R) + k^F(y^F - y_0^F) + k^B(B - B_0) + C(y^R, y^F, B), \\ \text{s.t.} \quad & y^R \geq y_0^R, \quad y^F \geq y_0^F, \quad B \geq B_0. \end{aligned} \quad (1)$$

To answer the research questions proposed in Section 1, we will analyze how the utility's optimal capacity decision (solution to (1)) is impacted by the cost parameters (k^R, k^F, k^B) , which are affected by government policies. In the rest of this section, we formulate the resource operating problem embedded in (1) and define the operating cost function $C(y^R, y^F, B)$. This function embodies the operating characteristics of the renewable, flexible, and storage resources. For the purpose of addressing the research questions in this paper, we focus on one-time investment, similar to [Aflaki and Netessine \(2017\)](#) and [Kök et al. \(2018\)](#).

3.2 Modeling Uncertainties

Let $R_t \in [0, 1]$ denote the *capacity factor* of the renewable capacity at time t , i.e., the renewable capacity can produce a power of $y^R R_t$ (MW) at time t . Let $D_t \geq 0$ (MW) denote the electricity demand at time t minus the predetermined output from the existing inflexible resources. To capture the reality that the demand and available renewable power have both seasonal and uncertain fluctuations, we model R_t and D_t as a composition of deterministic and stochastic processes:

$$R_t = f_r(\bar{R}_t, r_t), \quad D_t = f_d(\bar{D}_t, d_t), \quad t \geq 0, \quad (2)$$

where f_r and f_d are twice continuously differentiable functions; \bar{R}_t and \bar{D}_t are periodic deterministic processes with period t_0 (in the numerical analysis, we set $t_0 = 168$ hours or 1 week); r_t and d_t are diffusion processes governed by the following equations:

$$dr_t = \mu_r(r_t) dt + \sigma_r(r_t) dW_{r,t}, \quad dd_t = \mu_d(d_t) dt + \sigma_d(d_t) dW_{d,t}, \quad t \geq 0, \quad (3)$$

where $W_{r,t}$ and $W_{d,t}$ are independent standard Brownian motions, $\mu_i(i_t)$ and $\sigma_i(i_t)$, for $i = r, d$, are drift and diffusion coefficients, respectively. For technical reasons, we assume there exists a bounded set \mathcal{Y} such that $(r_t, d_t) \in \mathcal{Y}$ for all $t \geq 0$.² Thus, the demand D_t is also bounded.

Let c_t^F (\$/MWh) denote the power generation cost (primarily fuel cost) of the flexible resources at time t . The fuel (typically natural gas) is purchased from a supplier at a price adjusted on the monthly basis, which is a common practice in the industry. Thus, c_t^F is constant within each month and changes only across months.

3.3 Resource Operations

As discussed in Section 1, electric grids require supply and demand to be continuously balanced. We use a continuous-time model to formulate the resource operations problem. The advantage of this continuous-time model will become evident through the concise structure of the optimal policy.

Let $b_t \in [0, B]$ denote the amount of (usable) stored energy (in MWh) at time t . Let q_t^B (in MW) denote the rate of change in b_t :

$$db_t = q_t^B dt, \quad (4)$$

where $q_t^B > 0$ (< 0) represents the rate of charging (discharging) at time t . Due to the round-trip energy loss, raising the stored energy level at rate $q_t^B > 0$ requires q_t^B/α of power input, which must not exceed y_{in}^B , the charging power capacity defined in Section 3.1. When $q_t^B < 0$, $|q_t^B|$ is the power output from the battery, which is capped at y_{out}^B . Therefore, the storage operations are subject to the following state and rate constraints:

$$b_t \in [0, B], \quad (5)$$

$$q_t^B \in [-y_{\text{out}}^B, \alpha y_{\text{in}}^B]. \quad (6)$$

Let q_t^F and q_t^R denote the power output (in MW) of the flexible and renewable resources at time t , respectively. They must satisfy the capacity (rate) constraints:

$$q_t^F \in [0, y^F], \quad (7)$$

$$q_t^R \in [0, y^R R_t]. \quad (8)$$

Note that $y^R R_t - q_t^R$ represents renewable power curtailment.

In summary, the system's state variables include: time $t \geq 0$, stored energy level $b_t \in [0, B]$, stochastic components of the available renewable power and demand $(r_t, d_t) \in \mathcal{Y}$, and the (fuel) cost of flexible generation c_t^F . The control variables are q_t^R , q_t^F , and q_t^B , which control renewable output, flexible generation, and battery storage operations, respectively. We denote a control policy as $\pi = \{(q_t^R, q_t^F, q_t^B) : t \geq 0\}$.

²Proper diffusion coefficient functions $\sigma_r(r_t)$ and $\sigma_d(d_t)$ can ensure boundedness of (r_t, d_t) . The boundedness ensures the cost function in (10) is bounded, which is necessary for proving Lemma 2.

3.4 Operating Cost and Problem Formulation

Recall that D_t is the demand net the constant inflexible generation. Thus, the mismatch between the demand and the utility's total energy supply at time t is given by $D_t - q_t^R - q_t^F + \psi(q_t^B)$, where

$$\psi(q) = \begin{cases} q/\alpha, & \text{if } q \geq 0, \\ q, & \text{if } q < 0. \end{cases}$$

The system must not have over- or under-supply of energy. That is, (q_t^R, q_t^F, q_t^B) should satisfy

$$\Delta_t \equiv D_t - q_t^R - q_t^F + \psi(q_t^B) \geq 0, \quad (9)$$

and whenever $\Delta_t > 0$ (i.e., demand exceeds the utility's own power supply), the utility must import energy from an expensive peaking generator at a contracted price ξ (\$/MWh), which is assumed to be more expensive than the cost of flexible generation: $\xi > \sup_{t \geq 0} c_t^F$.

Therefore, the demand is met by five sources: (i) inflexible generation at a predetermined cost (excluded from optimization), (ii) flexible generation at marginal cost c_t^F , (iii) renewable generation at no operating cost, (iv) peak import at marginal cost ξ , and (v) energy storage. Given this operating cost structure and capacities (y^R, y^F, B) , the utility's problem is to control generation and storage operations by $\pi = \{(q_t^R, q_t^F, q_t^B) : t \geq 0\}$ to minimize the discounted operating cost.

We discount costs monthly, in accordance with industry practice. Because c_t^F is constant within a month, it is both practically relevant and analytically useful to solve for an optimal policy that minimizes the average cost for each month. Under an average cost objective, the optimal policy is more concise and easier to interpret (e.g., the initial system state is irrelevant), facilitating the derivation of operational insights for managing the system under continuously fluctuating demand and renewable generation. We formulate the average cost minimization problem under constant flexible generation cost c^F as follows:

$$\begin{aligned} \bar{C}(y^R, y^F, B, c^F) &= \inf_{\pi} \lim_{s \rightarrow \infty} \frac{1}{s} \mathbb{E} \left[\int_0^s (c^F q_t^F + \xi \Delta_t) dt \right], \\ &\text{s.t. (2)-(9),} \end{aligned} \quad (10)$$

where the limit exists because the integrand is bounded. In particular, Δ_t is bounded since D_t is bounded (discussed after (3)) and all controls are bounded.

Let there be M months over the planning horizon $[0, T]$, and let T_m mark the beginning of the m -th month ($0 = T_1 < T_2 < \dots < T_{M+1} = T$). The cost of flexible generation within the m -th month is denoted by $c_m^F \equiv c_t^F$, $t \in [T_m, T_{m+1})$. Let γ be the discount rate. Then, the discounted operating cost function in problem (1) can be expressed as:

$$C(y^R, y^F, B) = \sum_{m=1}^M e^{-\gamma T_m} (T_{m+1} - T_m) \mathbb{E}_{c_m^F} [\bar{C}(y^R, y^F, B, c_m^F)], \quad (11)$$

where the expectation is taken on c_m^F , which is random a priori.

4. Optimal Resource Operations Under Given Investment

In this section, we solve the optimal control problem in (10) and characterize the optimal policy.

4.1 Problem Transformation and Optimality Equation

First, we show that the problem in (10) can be transformed into a simpler one, in which we first optimize two controls q_t^F and q_t^B , and then determine q_t^R , as detailed in the following lemma.

Lemma 1. *The average cost $\bar{C}(y^R, y^F, B, c^F)$ in (10) can be determined by the following problem:*

$$\bar{C}(y^R, y^F, B, c^F) = \inf_{\{q_t^F, q_t^B, t \geq 0\}} \lim_{s \rightarrow \infty} \frac{1}{s} \mathbb{E} \left[\int_0^s \left(c^F q_t^F + \xi(D_t - y^R R_t - q_t^F + \psi(q_t^B))^+ \right) dt \right], \quad (12)$$

s.t. state equations: (2), (3), (4),

state constraint: (5),

control constraints: (6), (7).

Furthermore, if $\{(q_t^{F*}, q_t^{B*}) : t \geq 0\}$ is an optimal control for (12), then an optimal control for (10) is $\{(q_t^{R*} = \min\{y^R R_t, D_t + \psi(q_t^{B*})\}, q_t^{F*}, q_t^{B*}) : t \geq 0\}$, and the curtailed renewable power is $(y^R R_t - D_t - \psi(q_t^{B*}))^+$.

One of the challenges in solving the optimal control problem in (12) is handling the state constraint $b_t \in [0, B]$ in (5). An approach to solve such a problem with state constraints is to reformulate it using reflecting boundaries. We present the technical details of this approach in Online Appendix A; we also refer the reader to Harrison (1990) for theoretical foundations. The reflecting boundary approach allows us to derive the Hamilton-Jacob-Bellman (HJB) equation as well as the boundary conditions, as stated in the following lemma.

A few notations are used in the lemma. The system state is summarized by $x := (b, r, d)$ (battery state b , stochastic components of renewable potential r and demand d defined in (3)), $\mathcal{X} := [0, B] \times \mathcal{Y}$ denotes the state space, $\mathcal{U} := [0, y^F] \times [-y_{\text{out}}^B, \alpha y_{\text{in}}^B]$ denotes the feasible range of the controls, and $\mathcal{C}^2(P)$ is the set of twice continuously differentiable functions on a set P .

Lemma 2 (HJB Equation). *For given (y^R, y^F, B, c^F) , suppose*

- (a) *there exists a function $\phi(t, x) \in \mathcal{C}^2([0, t_0] \times \mathcal{X})$, such that $\phi(0, x) = \phi(t_0, x)$, for all $x \in \mathcal{X}$, and*
- (b) *there exists a constant $v \geq 0$ such that for all $t \in [0, t_0]$ and $x \in \mathcal{X}$, v and $\phi(t, x)$ satisfy*

$$v = \left\{ \inf_{(q^F, q^B) \in \mathcal{U}} \zeta(q^F, q^B, t, x) \right\} + \frac{\partial \phi(t, x)}{\partial t} + \sum_{i=r, d} \mu_i(i) \frac{\partial \phi(t, x)}{\partial i} + \frac{1}{2} \sum_{i=r, d} \sigma_i^2(i) \frac{\partial^2 \phi(t, x)}{\partial i^2}, \quad (13)$$

where $\zeta(q^F, q^B, t, x) = c^F q^F + \xi(f_d(\bar{D}_t, d) - y^R f_r(\bar{R}_t, r) - q^F + \psi(q^B))^+ + q^B \frac{\partial \phi(t, x)}{\partial b}$, with boundary

conditions

$$\frac{\partial \phi(t, 0, r, d)}{\partial b} = -\xi \quad \text{and} \quad \frac{\partial \phi(t, B, r, d)}{\partial b} = 0. \quad (14)$$

Then, $v = \bar{C}(y^R, y^F, B, c^F)$.

The function $\phi(t, x)$ is known as a relative cost function (or bias function).³ The difference $\phi(t, b_1, r, d) - \phi(t, b_2, r, d)$, with $b_1 < b_2$, represents the operating cost savings from having b_2 units of stored energy at time t compared to having only b_1 units of stored energy at time t , everything else being equal. Thus, $-\frac{\partial \phi(t, b, r, d)}{\partial b}$ represents the marginal value of stored energy at state (t, b, r, d) .

Although $\phi(t, x)$ is unknown a priori, its properties stated in the following lemma will allow us to derive the structures of the optimal policy in Section 4.2.

Lemma 3. *The relative cost function $\phi(t, b, r, d)$ has the following properties:*

- (i) $\phi(t, b, r, d)$ is convex and decreasing in b for any given $(t, r, d) \in [0, t_0] \times \mathcal{Y}$;
- (ii) $\frac{\partial \phi(t, b, r, d)}{\partial b} \in [-\xi, 0]$ for all $(t, b, r, d) \in [0, t_0] \times \mathcal{X}$.

Finally, we make a technical remark. Lemma 2 provides a sufficient condition that the average cost v and the bias function $\phi(t, x)$ need to satisfy. The HJB equation may not have a solution in \mathcal{C}^2 . In such a case, the optimal control problem has viscosity solutions; refer to Fleming and Soner (2006). Since the goal of this section is to understand the structure of the optimal resource operating policy, we omit the technical analysis related to viscosity solutions.

4.2 Structures of the Optimal Control and Storage Operations Decomposition

To derive the structures of the optimal control for (12), we first solve the optimization problem embedded in the HJB equation (13) and present the solution in Proposition 1. Since the HJB equation is for a problem with reflecting boundaries (Online Appendix A), we then adjust the solution at the boundaries to yield the optimal control for (12), as detailed in Theorem 1.

We begin by observing that the infimum in (13) is attainable due to the continuity of $\zeta(\cdot)$ and the compactness of \mathcal{U} . Thus, the minimization problem in (13) can be written as

$$\min_{(q^F, q^B) \in \mathcal{U}} c^F q^F + \xi (\tilde{D}(t, r, d) - q^F + \psi(q^B))^+ + \frac{\partial \phi(t, b, r, d)}{\partial b} q^B, \quad (15)$$

where $\tilde{D}(t, r, d) := D_t - y^R R_t = f_d(\bar{D}_t, d_t) - y^R f_r(\bar{R}_t, r_t)$ is the net demand on flexible resources. As we shall see in Proposition 1 and Theorem 1, whenever $b \in (0, B)$, the optimal decision at state (t, b, r, d) is indeed the solution to (15), which minimizes the sum of the flexible generation cost $c^F q^F$ (\$/hour), the import energy cost $\xi \Delta^+$ (\$/hour), and the opportunity cost (or gain) of storage operations. In view of (15), two observations are worth mentioning:

³The HJB equation (13) and the boundary conditions (14) are for the first- and second-order derivatives of $\phi(t, x)$, implying that any solution to the HJB equation plus a constant is also a solution. Thus, the value of $\phi(t, x)$ is meaningful only when compared to its value at another state or time.

- The instantaneous opportunity cost (or gain) of discharging (or charging) the storage is $\frac{\partial\phi}{\partial b}q^B$, which is linear in q^B ; this linear form is a result of the continuous-time framework. Online Appendix B shows a discrete-time version of this term, which does not lead to a concise solution.
- The problem in (15) depends on (t, b, r, d) only through $\tilde{D}(t, r, d)$ and $\partial\phi(t, b, r, d)/\partial b$. Thus, whenever $b \in (0, B)$, the optimal control of the resources depends on the state and time only through the net demand on flexible resources and the marginal value of stored energy.

For notational convenience, We write $\tilde{D}(t, r, d)$ as \tilde{D} and $\frac{\partial\phi(t, b, r, d)}{\partial b}$ as $\frac{\partial\phi}{\partial b}$ from this point onward. Instead of considering a high-dimensional state space, we only need to consider various cases of \tilde{D} and $\frac{\partial\phi}{\partial b}$ to solve (15), as formalized in Proposition 1 below.

In Proposition 1, \tilde{q}^B can be interpreted as the ideal battery operations if battery charging and discharging power capacities are not binding, and \tilde{q}^F is the desired flexible output considering the limited battery power capacity while ignoring the flexible capacity constraint. Then, equation (16) imposes capacity constraints on $(\tilde{q}^F, \tilde{q}^B)$ so that $(\tilde{q}^F, \tilde{q}^B)$ is feasible and proven optimal.

Proposition 1. *The optimal solution to (15), denoted as $(\tilde{q}^F, \tilde{q}^B)$, is given as follows:*

$$\tilde{q}^F = (\tilde{q}^F)^+ \wedge y^F \quad \text{and} \quad \tilde{q}^B = (\tilde{q}^B \vee (-y_{\text{out}}^B)) \wedge (\alpha y_{\text{in}}^B), \quad (16)$$

where \tilde{q}^F and \tilde{q}^B are determined as follows:

(a) If $\tilde{D} > y^F$,

$$(\tilde{q}^F, \tilde{q}^B) = \begin{cases} (y^F, & y^F - \tilde{D}), & \text{if } -\xi \leq \frac{\partial\phi}{\partial b} < -c^F, \\ (\tilde{D} - y_{\text{out}}^B, & -\tilde{D}), & \text{if } -c^F \leq \frac{\partial\phi}{\partial b} \leq 0. \end{cases} \quad (17)$$

(b) If $0 < \tilde{D} \leq y^F$,

$$(\tilde{q}^F, \tilde{q}^B) = \begin{cases} (\tilde{D} + y_{\text{in}}^B, & \alpha(y^F - \tilde{D})), & \text{if } -\xi \leq \frac{\partial\phi}{\partial b} < -\frac{c^F}{\alpha}, \\ (\tilde{D}, & 0), & \text{if } -\frac{c^F}{\alpha} \leq \frac{\partial\phi}{\partial b} < -c^F, \\ (\tilde{D} - y_{\text{out}}^B, & -\tilde{D}), & \text{if } -c^F \leq \frac{\partial\phi}{\partial b} \leq 0. \end{cases} \quad (18)$$

(c) If $\tilde{D} \leq 0$,

$$(\tilde{q}^F, \tilde{q}^B) = \begin{cases} (\tilde{D} + y_{\text{in}}^B, & \alpha(y^F - \tilde{D})), & \text{if } -\xi \leq \frac{\partial\phi}{\partial b} < -\frac{c^F}{\alpha}, \\ (0, & -\alpha\tilde{D}), & \text{if } -\frac{c^F}{\alpha} \leq \frac{\partial\phi}{\partial b} \leq 0. \end{cases} \quad (19)$$

In addition, the optimal decisions \tilde{q}^F and \tilde{q}^B have the following relation:

$$\tilde{q}^F = (\tilde{D} + \psi(\tilde{q}^B))^+ \wedge y^F. \quad (20)$$

In Online Appendix B, we analyze a discrete-time version of the model and show that its optimal policy structure is more complex but converges to the structure in Proposition 1 when the period

length approaches zero (see Figure B.1). Another advantage of the continuous-time model is that the concise decisions in Proposition 1 lend themselves to decomposition, which opens up new avenues for further analysis, as detailed next.

In our setting with three production sources (renewable, flexible, import), charging/discharging storage at any time may involve multiple sources. The optimal storage decisions in Proposition 1, however, do not reveal the sources for charging or sink for discharging. To derive further operational insights, we decompose the storage operations in Proposition 1 into the following four types based on their marginal cost or benefit:

- (i) **Charge using renewable output** (CR): Store renewable energy that would otherwise be curtailed. In this case, the marginal cost of charging is zero.
- (ii) **Charge using flexible output** (CF): Renewable output is already fully used or stored; storing more energy requires the flexible capacity to increase production. Thus, the marginal cost of charging is c^F/α (recall that raising b by 1 unit requires $1/\alpha$ units of input).
- (iii) **Discharge to reduce import** (DI): Discharge to meet demand that would otherwise be met by importing energy. The marginal benefit (i.e., cost saving) from discharging is ξ .
- (iv) **Discharge to reduce flexible output** (DF): Import is zero in this case; releasing more stored energy reduces the flexible output. The marginal benefit from discharging is thus c^F .

Clearly, CR is prioritized over CF, i.e., we charge battery using renewables before using flexible generation. Similarly, DI is prioritized over DF, i.e., we discharge battery to replace import first. Marginal values of storage operations have been discussed in the literature (see Secomandi 2010 and Zhou et al. 2019) but have not been used to decompose storage operations. In our setting, at any given time, if the potential amount of CR (or DI) operation is less than the optimal charging (or discharging) amount in Proposition 1, we know the remaining charging (or discharging) power is from CF (or DF) operations. Thus, we are able to decompose the charging decisions in Proposition 1 by sources and decompose the discharging decisions by sinks (i.e., replaced sources).⁴ Furthermore, we will pair up various types of storage operations to explain how storage creates value and how it drives investment relations in the next section.

Using the four types of storage operations, we can decompose some decisions in Proposition 1 to reveal the underlying insights, which are illustrate in Figure 1 when $b \in (0, B)$. Theorem 1 will confirm that the decisions in Proposition 1 are indeed optimal when $b \in (0, B)$.

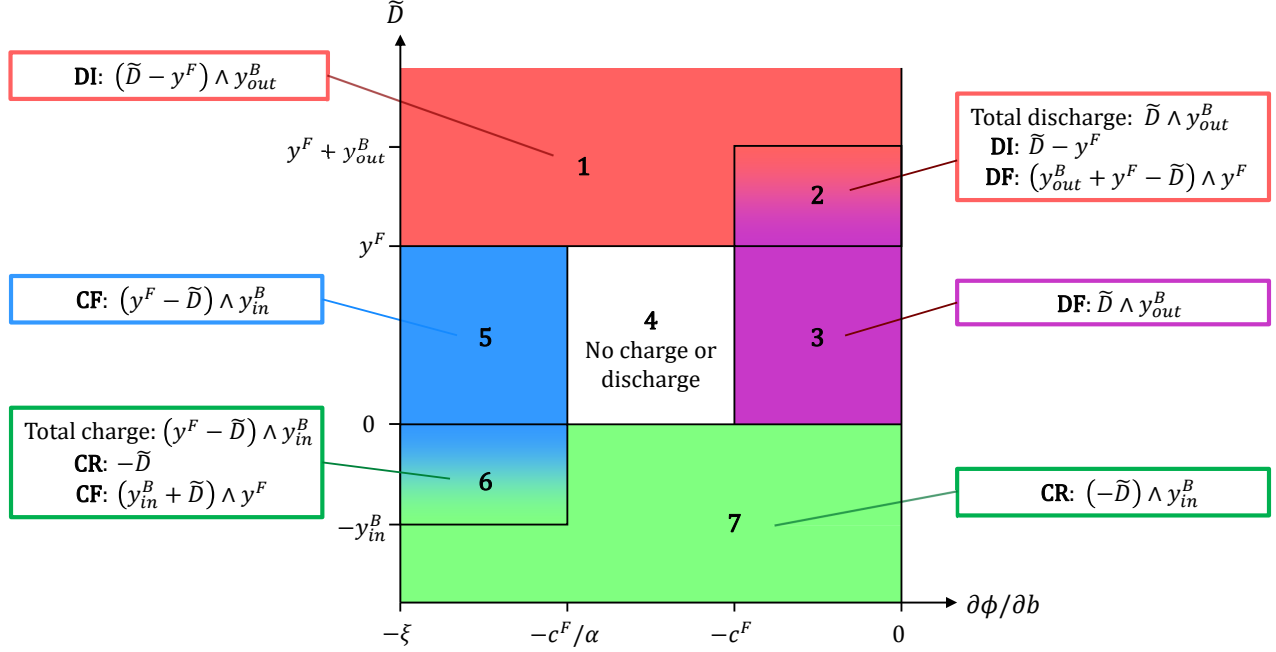
⁴To cement this point, consider the following example with $\alpha = 1$, $y^F = 10$ GW, $D_t = 3$ GW, $y^R R_t = 4$ GW, and thus net demand $\tilde{D}_t = -1$ GW. Then, we can charge storage using the excess renewable energy up to 1 GW, i.e., CR potential is 1 GW. If charging 2 GW, the sources must be 1 GW from renewables and 1 GW from flexible output.

For another example, $D_t = 10$ GW and supply conditions remain the same. The net demand $\tilde{D}_t = 6$ GW. Both CR and DI potentials are zero. If we operate the storage at $q_t^B \in (-6, 4)$ GW, then the flexible capacity must produce $6 + q_t^B$ GW. Therefore, the storage operation here is CF or DF because it directly impacts the flexible output.

Figure 1: The structure of the optimal storage operations (stored energy level $b \in (0, B)$)

DI = Discharge to reduce Import (red), DF = Discharge to reduce Flexible output (magenta),
 CR = Charge using Renewable output (green), CF = Charge using Flexible output (blue).

All expressions in the callouts are the power (MW) of storage operations. For DI and DF, the power is the rate of decrease in the stored energy level b . For CR and CF, α times the power is the rate of increase in b . The horizontal axis can be loosely considered as the stored energy level b since $\phi(\cdot)$ is convex in b .



(a) Case of $\tilde{D} > y^F$. Without using storage, the excess demand $\tilde{D} - y^F$ has to be met by energy import at cost ξ ; DI potential is $\tilde{D} - y^F$. As the opportunity cost of using stored energy ($-\frac{\partial \phi}{\partial b}$) is no higher than ξ (Lemma 3), it is desirable to perform DI as much as possible, i.e., discharge the storage at rate $(\tilde{D} - y^F) \wedge y_{out}^B$, as shown in Regions 1 and 2 in Figure 1.

If DI potential does not exceed the storage discharging capacity (i.e., $y_{out}^B - (\tilde{D} - y^F) > 0$), we can consider whether DF can further reduce cost by comparing the marginal benefit of DF (c^F) with the opportunity cost of discharging ($-\frac{\partial \phi}{\partial b}$). DF is desirable if and only if $-\frac{\partial \phi}{\partial b} < c^F$, as shown in Regions 1 and 2 in Figure 1 and (17). In Region 2, the total discharge amount is $\tilde{D} \wedge y_{out}^B$, which means that the storage is used to meet as much demand as possible, consistent with the second branch of (17).

If DI potential exceeds the storage discharging capacity ($\tilde{D} - y^F > y_{out}^B$), both branches of (17) lead to $\tilde{q}^F = y^F$ and $\tilde{q}^B = -y_{out}^B$ in (16); any remaining demand is met by import.

(b) Case of $\tilde{D} \in (0, y^F)$. This case corresponds to the middle band in Figure 1. The flexible resources can produce exactly \tilde{D} to meet the demand, but such a strategy is optimal only in Region 4. Region 3 is similar to Region 2 in that $-\frac{\partial \phi}{\partial b} < c^F$, implying that DF is desirable. Since there is

no need for DI here, we replace as much flexible output as possible by performing DF at rate $\tilde{D} \wedge y_{\text{out}}^B$, which is also confirmed by the third branch of (18).

In Region 5, the opportunity gain of charging ($-\frac{\partial \phi}{\partial b}$) exceeds the marginal cost of CF operation ($\frac{c^F}{\alpha}$), rendering CF operation to be desirable. Since the remaining flexible capacity (after meeting demand) is $y^F - \tilde{D}$, we perform CF as much as possible at rate $(y^F - \tilde{D}) \wedge y_m^B$, which is also reflected in the first branch of (18).

- (c) Case of $\tilde{D} < 0$. In this case where the potential renewable power exceeds the demand, one might expect that the flexible capacity should stop running and the battery should be charged using the excess renewable power—CR operation. Performing only CR is optimal in Region 7 (the second branch of (19)). However, in Region 6, because the opportunity gain of charging battery exceeds the marginal cost of CF, it is optimal to perform both CF and CR operations. The sum of CF and CR amount is $(y^F - \tilde{D}) \wedge y_m^B$, consistent with the first branch of (19).

The solution provided by Proposition 1 is the optimal control for a problem with reflecting boundaries. Using this solution, we can construct the optimal control for the original problem in (12), as detailed in Theorem 1. Online Appendix A provides the theory behind this construction. In Theorem 1, we emphasize the dependence of the policy on time and state $(t, x) \equiv (t, b, r, d)$.

Theorem 1. For $(t, x) \in [0, t_0] \times \mathcal{X}$, let $(\tilde{q}^F(t, x), \tilde{q}^B(t, x))$ be given by (16) in Proposition 1. Define

$$(q^{F*}(t, x), q^{B*}(t, x)) = \begin{cases} (\tilde{q}^F(t, x), \tilde{q}^B(t, x)), & \text{if } b \in (0, B), \\ (\tilde{q}^F(t, x), \tilde{q}^B(t, x) \vee 0), & \text{if } b = 0, \\ (\tilde{q}^F(t, x), \tilde{q}^B(t, x) \wedge 0), & \text{if } b = B. \end{cases} \quad (21)$$

Then, an optimal control policy for (12) is

$$\pi^* = \{(q^{F*}(t - \lfloor t/t_0 \rfloor, x), q^{B*}(t - \lfloor t/t_0 \rfloor, x)) : t \geq 0\}. \quad (22)$$

Note that the optimal control policy defined by (22) is cyclic with period t_0 , driven by the cyclic demand and renewable generation. Within each cycle, Proposition 1 prescribes the optimal control for $b \in (0, B)$. When b is on either boundary, the storage operation is modified according to (21), which is intuitive. What is less intuitive is that the flexible generation prescribed by Proposition 1 does not need to be modified. This is because if Proposition 1 calls for discharging but $b = 0$, then we are in Region 1, where q^F is already maxed at y^F ; if Proposition 1 calls for charging but $b = B$, then we are in Region 7, where q^F is already minimized at zero.

In summary, the optimal policy interweaves demand thresholds and cost thresholds, producing a structure with the following properties (\iff is read as “if and only if”):

- (i) First, perform: DI $\iff \tilde{D} > y^F$; CR $\iff \tilde{D} < 0$;

- (ii) If feasible,⁵ perform: $DF \iff -\frac{\partial\phi}{\partial b} < c^F$; $CF \iff -\frac{\partial\phi}{\partial b} > \frac{c^F}{\alpha}$.
- (iii) Energy flow balance: The total energy inflow (CR + CF) times α is equal to the total energy outflow (DI + DF) in the long run.

The four types of storage operations can form four pairs: (CR, DI), (CF, DI), (CR, DF), and (CF, DF). Part (i) highlights that CR and DI are purely driven by the net demand fluctuations: Charging when $\tilde{D} < 0$ and discharging when $\tilde{D} > y^F$ yields the largest cost saving (ξ per MWh). However, a policy that aims to perform *only* CR and DI is almost never optimal, because the amount of excess renewable energy rarely matches the amount of imported energy, in both long-term averages and daily cycles. Therefore, DF or CF operations are performed to enable more CR or DI operations, respectively. Specifically, CR and DF together yield a cost saving of c^F per MWh; CF and DI together yield a cost saving of $(\xi - \frac{c^F}{\alpha})$ per MWh. Thus, in contrast to CR and DI that are triggered by the exogenous net demand, CF and DF operations are driven by comparing the endogenous opportunity cost of storage with the cost of flexible generation, as confirmed in part (ii). Part (iii) asserts the long-run energy flow balance. The last pair (CF, DF) incurs a net loss of $c^F(\frac{1}{\alpha} - 1)$ and seems undesirable to perform at any time. However, interestingly, (CF, DF) is occasionally needed because the uncertain environment prevents us from perfectly matching CF with DI or matching DF with CR. We will illustrate the subtle role of (CF, DF) in the next section.

5. Capacity Investment Relations and Numerical Analysis

In this section, we analyze the problem in (1) and investigate the utility's optimal investment in storage, flexible, and renewable capacities. Our goal is to provide a deep understanding of how the optimal operations analyzed in Section 4 drive the investment relations among the three resources.

Formally, we define a binary relation among resources:

Definition 1 (Investment relation). *For any given optimal solution to (1), resource i substitutes (resp. complements) resource j if a marginal decrease in i 's investment cost leads to a marginal decrease (resp. increase) in j 's optimal investment level.*

Note that the investment relation is defined in a *local* sense, and the relation may change as the optimal investments change. Kök et al. (2020) show that this relation is symmetric (i.e., if resource i substitutes j , then j substitutes i) for their problem setting where operating costs can be derived. We generalize their result to a setting where the operating cost function $C(y^R, y^F, B)$ is unknown but satisfies some technical conditions, as stated in the following lemma.

⁵Feasibility simply means that a) the storage has capacity to perform DF or CF after performing DI or CR, b) $q^F > 0$ to allow DF, $q^F < y^F$ to allow CF.

Lemma 4. (i) Investment in a resource decreases in its own capacity cost, i.e., y^{R^*} (resp. y^{F^*} , B^*) decreases in k^R (resp. k^F , k^B).

(ii) If it is optimal to invest in all three resources (i.e., $y^{R^*} > y_0^R$, $y^{F^*} > y_0^F$, $B^* > B_0$) and the operating cost $C(y^R, y^F, B)$ is twice differentiable with a non-singular Hessian matrix at (y^{R^*}, y^{F^*}, B^*) , then the optimal investments are differentiable with respect to costs and satisfy:

$$\frac{\partial y^{R^*}}{\partial k^F} = \frac{\partial y^{F^*}}{\partial k^R}, \quad \frac{\partial y^{R^*}}{\partial k^B} = \frac{\partial B^*}{\partial k^R}, \quad \frac{\partial y^{F^*}}{\partial k^B} = \frac{\partial B^*}{\partial k^F}.$$

Note that if we fix one capacity and optimize the other two investment levels, a similar result holds (e.g., if we fix y^F and optimize y^R and B , then $\frac{\partial y^{R^*}}{\partial k^B} = \frac{\partial B^*}{\partial k^R}$). Lemma 4 ensures that the investment relations remain the same regardless of which investment cost we choose to vary.

5.1 The Role of Storage Operations in Investment Relations

In this section, we analyze how capacity investment relations are driven by the optimal storage operations. As discussed at the end of Section 4, storage reduces the system operating cost through three pairs of operations: (CR, DI), (CF, DI), and (CR, DF). The value of storage ties to its potential to execute these operational pairs. Thus, if investing in another resource increases (or decreases) the opportunities to perform these pairs, the value of the storage may be enhanced (or reduced).

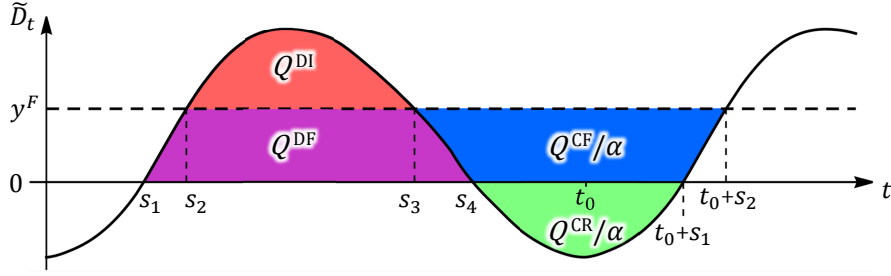
It is difficult to analytically characterize the investment relations under general settings, yet the fundamental relations can be captured by a special case specified in Assumption 1, which allows for explicit solution. We use this special case to demonstrate how operations drive investment relations.

Assumption 1 (Special case). (a) D_t and R_t are periodic deterministic processes with period t_0 ; (b) For any $y^R \geq 0$, the net demand process $\tilde{D}_t \equiv D_t - y^R R_t$ is unimodal in $[0, t_0]$. (c) The battery power capacity constraints are not binding.

Assumption 1(a) ensures analytical tractability and allows us to show that the basic investment relations are not driven by stochasticity; part (b) implies that the battery will be charged and discharged once per period; part (c) facilitates quantifying the charging and discharging potentials.

Under Assumption 1 and given y^F and y^R , there exist s_1, s_2, s_3, s_4 , such that $0 \leq s_1 \leq s_2 \leq s_3 \leq s_4 \leq t_0$, $\tilde{D}_t \in [0, y^F]$ for $t \in [s_1, s_2) \cup [s_3, s_4)$, $\tilde{D}_t \geq y^F$ for $t \in [s_2, s_3)$ and $\tilde{D}_t \leq 0$ for $t \in [0, s_1) \cup [s_4, t_0)$, as illustrated in Figure 2. If there were no storage, flexible resources would operate for $t \in [s_1, s_4]$, during which imports are needed for $t \in [s_2, s_3]$. We define four quantities: CR potential $Q^{\text{CR}} := -\alpha \int_{s_4}^{t_0+s_1} \tilde{D}_t dt$ is the maximum amount of charging from surplus renewable output, DI potential $Q^{\text{DI}} := \int_{s_2}^{s_3} (\tilde{D}_t - y^F) dt$ is the maximum amount of imports that can be displaced by storage, CF potential $Q^{\text{CF}} := \alpha \int_{s_3}^{t_0+s_2} (y^F - \tilde{D}_t^+) dt$ is the maximum amount of charging using flexible capacity, and DF potential $Q^{\text{DF}} := \int_{s_1}^{s_4} (\tilde{D}_t \wedge y^F) dt$ is the maximum amount of flexible generation that can be displaced by storage. All four quantities depend on y^F and y^R .

Figure 2: Net demand curve and charging and discharging potentials



A full analysis of the optimal operations is provided in Online Appendix C. Theorem 2 provides an explicit solution to the optimal storage investment under given flexible and renewable capacities.

Theorem 2. Let $\{c_m^F : m = 1, \dots, M\}$ have a stationary distribution represented by a random variable C^F , and define $A \equiv \sum_{m=1}^M e^{-\gamma T_m} (T_{m+1} - T_m) / t_0$. Then, under Assumption 1 and given y^F and y^R , the optimal storage investment B^* is given as follow:

(i) If $Q^{CR} \leq Q^{DI}$, then

$$B^* = \begin{cases} (Q^{CR} + Q^{CF}) \wedge Q^{DI}, & \text{if } k^B < A \left(\xi - \frac{\mathbb{E}[C^F]}{\alpha} \right), \\ Q^{CR}, & \text{if } A \left(\xi - \frac{\mathbb{E}[C^F]}{\alpha} \right) \leq k^B < A\xi, \\ 0, & \text{if } k^B \geq A\xi. \end{cases}$$

(ii) If $Q^{CR} > Q^{DI}$, then

$$B^* = \begin{cases} Q^{CR} \wedge (Q^{DI} + Q^{DF}), & \text{if } k^B < A\mathbb{E}[C^F], \\ Q^{DI}, & \text{if } A\mathbb{E}[C^F] \leq k^B < A\xi, \\ 0, & \text{if } k^B \geq A\xi. \end{cases}$$

Theorem 2 reveals how storage cost and its operating potentials determine the optimal storage size. The cost savings from executing one unit of (CR, DI), (CF, DI), and (CR, DF) operations are ξ , $\xi - \frac{\mathbb{E}[C^F]}{\alpha}$, and $\mathbb{E}[C^F]$ respectively. These savings are scaled by A to reflect the total savings when one unit of paired operations is performed every period throughout the planning horizon. We then compare the cost savings against storage capacity cost k^B to find the optimal storage capacity. Intuitively, in Theorem 2(i), where renewable surplus is insufficient to eliminate imports, storage creates value from (CR, DI) and (CF, DI) pairs. If only (CR, DI) is cost-effective (k^B falls within the second branch of Theorem 2(i)), the storage capacity should align with Q^{CR} . If both pairs are cost-effective, the optimal storage capacity is determined by the lesser of Q^{DI} and the total charging potential $Q^{CR} + Q^{CF}$. In Theorem 2(ii), where renewable surplus can fully remove imports, attention shifts to (CR, DI) and (CR, DF) pairs. The intuitive reasoning is similar. In all cases, the optimal storage size is dictated by the minimum of the charging and discharging potentials.

Leveraging Theorem 2, we examine the investment relations between storage and either renewable

or flexible capacities, as summarized in Corollary 1.

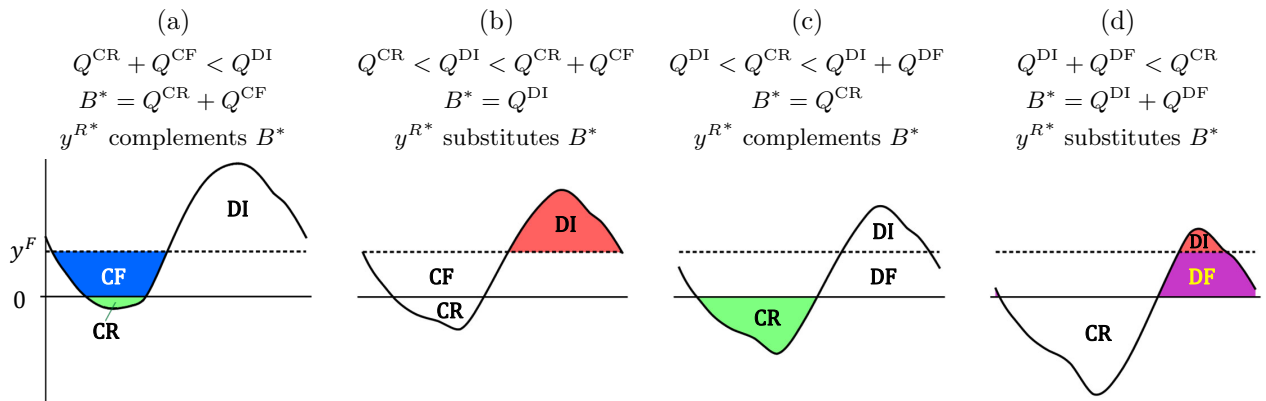
Corollary 1. *Under the assumptions of Theorem 2 and $(Q^{\text{CR}} + Q^{\text{CF}}) \neq Q^{\text{DI}} \neq Q^{\text{CR}} \neq (Q^{\text{DI}} + Q^{\text{DF}})$, we have the following investment relations (all relations are local, as in Definition 1):*

- (i) *Under fixed y^F , renewable capacity y^{R^*} and storage B^* are substitutes if $B^* = Q^{\text{DI}}$ or $B^* = Q^{\text{DI}} + Q^{\text{DF}}$, and are complements if $B^* = Q^{\text{CR}}$ or $B^* = Q^{\text{CR}} + Q^{\text{CF}}$;*
- (ii) *Under fixed y^R , flexible capacity y^{F^*} and storage B^* are substitutes if $B^* = Q^{\text{DI}}$, and are complements if $B^* = Q^{\text{CR}} + Q^{\text{CF}}$.*

We illustrate investment relations in Corollary 1(i) for the case where storage investment is cost-effective for all three operations pairs, i.e., $k^B < A \min\{\mathbb{E}[C^F], \xi - \mathbb{E}[C^F]/\alpha\}$. When the combined charging potential $Q^{\text{CR}} + Q^{\text{CF}}$ is limited (Figure 3(a)), an increase in renewable capacity reduces net demand, enhancing the charging potential $Q^{\text{CR}} + Q^{\text{CF}} = B^*$, leading to a complementary relation between renewable and storage capacities. As charging potential further expands with renewable capacity, discharging potential Q^{DI} becomes the limiting factor (Figure 3(b)), changing the relations between the two capacities to substitutes. Additional renewable capacity then phrases out (CF, DI) operation and brings into play (CR, DF) operation (Figure 3(c)), where the charging potential Q^{CR} is the limiting factor, reintroducing a complementary relation between renewable and storage capacities. Finally, with a substantial renewable investment (Figure 3(d)), the storage capacity is determined by the combined discharging potential $Q^{\text{DI}} + Q^{\text{DF}}$, reverting to a substitutive relation with the renewable capacity.

Figure 3: Optimal storage investment under various renewable capacities

In each panel, active operations are labeled, and the colored area determines the optimal storage size. Panels (a) and (b) correspond to Theorem 2(i); panels (c) and (d) correspond to Theorem 2(ii).



Investment relations under different flexible capacity y^F can be simpler. For example, if $y^F \equiv 0$, then we only have CR and DI operations, and only Figure 3(a) and (d) remain. Thus, the renewable and storage capacities switches from complements to substitutes as the renewable capacity increases.

Conversely, if y^F is large, the scenario in Figure 3(a) may never occur, and (d) is unlikely to be cost-effective. Thus, the renewable and storage capacities switches from substitutes in (b) to complements in (c) as the renewable investment increases. This is what we will observe in the numerical analysis.

For general settings, it is challenging to analytically characterize the optimal capacities as well as the charging and discharging potentials. In the rest of this section, we consider a realistic setting, numerically solve for the optimal control policy, and explore the investment relations. Our numerical analysis shows that the insights gleaned from Theorem 2 apply to broader contexts.

5.2 Data Sources and Model Calibration

We choose a representative utility in Florida, Florida Power & Light (FPL). We consider the optimal investment in flexible (natural gas), renewable (solar)⁶ and storage (battery) capacities using the electricity generation and demand data from FPL. Our goal is not to evaluate FPL’s current portfolio, but to validate our main theoretical results and explore additional insights.

5.2.1 Resource Parameters

To solve the utility’s investment problem stated in (1), we need to determine the cost parameters of all resources as well as the technology parameters of the battery.

Battery technology: The key parameters of the battery technology introduced in Section 3.4 are specified as follows. We assume that the one-way efficiency is 0.95 so that the round-trip efficiency is $\alpha = 0.9025$, which is in the range of energy efficiency of Li-ion batteries used as grid-scale energy storage (Li and Tsing 2015). EIA (2021b) reports that the national average duration of large-scale batteries is 2.3 hours. Thus, we set charging and discharging duration to be $L = L^c = 2.3$ hours. The maximum depth-of-discharge for lithium-ion batteries is about $l_{\max} = 0.85$.

Investment costs: We discount all yearly maintenance costs to the beginning of the planning horizon to compute the flexible capacity cost k^F . Using the data in EIA (2019), we find $k^F = \$1.17/\text{W}$. We fix k^F at this value and vary the investment costs of the solar and storage as described below. According to Feldman et al. (2021), the cost of utility-scale fixed-tilt solar PV systems has declined to $\$1.28/\text{W}_{\text{ac}}$ in 2020.⁷ Our analysis considers the capacity cost k^R ranging from $\$1.4/\text{W}_{\text{ac}}$ to a futuristic value of $\$0.2/\text{W}_{\text{ac}}$. Cole et al. (2021) detail the cost of utility-scale Li-ion batteries and project that the investment cost of two-hour batteries range from $\$0.4/\text{Wh}$ in 2020 to less than $\$0.2/\text{Wh}$ in 2050. We consider the capacity cost of battery k^B from $\$0.15/\text{Wh}$ to $\$0.3/\text{Wh}$. As

⁶Our theoretical model can be extended to include multiple types of renewable energy, but we choose study one type of renewable energy in the numerical analysis, so that the investment relations among storage, flexible, and renewable resources can be clearly delineated.

⁷Solar power produces direct current (DC). The DC-to-AC ratio for utility-scale solar is 1.37 (Feldman et al. 2021). These costs are comprehensive, including permits, inspection, interconnection, PV modules, structural and electrical components, inverter, installation, overhead, etc.

discussed in Section 3.1, we study one-time resource investment problem; the above investment costs are incurred at the beginning of the planning horizon.

Operating costs: The operating cost c_t^F (\$/MWh) of flexible generation is obtained by multiplying the natural gas price (\$/MBtu) by a heat rate of 6.82 MBtu/MWh, which implies a 50% efficiency, typical for a natural gas combined cycle plant. We assume a high cost $\xi = \$400/\text{MWh}$ for imports.⁸

Finally, we assume the planning horizon is $T = 30$ years and the annual discount rate is $\gamma = 5\%$. We remark that, resources have ramping constraints in reality. Although we simplify the resources into fully flexible and inflexible ones in the theoretical model, we investigated the effect of ramping constraints in numerical analysis; results are available upon request. As the qualitative insights remain unchanged, we report the results without ramping constraints.

5.2.2 Uncertainty Models

This section details how we estimate the models for the three sources of uncertainties introduced in Section 3.2. All parameters are estimated for the summer and winter seasons separately and are reported in Online Appendix D.

We derive an empirical distribution of Henry Hub natural gas spot prices from 2006 to 2020 for summer (April to September) and winter (October to March). Then, we construct a discrete price distribution over 9 price points with equal probabilities by matching the cumulative distribution functions of the discrete distribution and the empirical distribution. We assume that the natural gas price is in steady state throughout the planning horizon. These 9 prices, multiplied by the heat rate as mentioned earlier, serve to compute the operating cost in (11).

We specify the renewable capacity factor model in (2) as $R_t = \bar{R}_t \frac{e^{r_t}}{1 + e^{r_t}}$. The deterministic process \bar{R}_t represents the diurnal variations of the maximum solar power under clear sky conditions; the stochastic multiplier $s_t \equiv \frac{e^{r_t}}{1 + e^{r_t}} \in (0, 1)$ models the intermittency of solar power (s_t approaches 1 under clear sky and nears 0 under heavy clouds). Our data shows that $r_t = \log \frac{s_t}{1 - s_t}$ exhibits Gaussian distribution. Thus, we model r_t as an AR(1) process, the discrete-time analogue of an Ornstein-Uhlenbeck process (see similar approach in Kim and Powell 2011 and Wu et al. 2023).

As of December 2020, FPL has 32 solar PV sites with total capacity of 2.27 GW. We use FPL's Ten-Year Power Plant Site Plans⁹ to identify these 32 sites and 7 other sites planned for solar. We use Google Map to find the coordinate of each site; refer to Figure D.1 in Online Appendix D for the locations of these 39 sites. For each site, we use its coordinate to obtain the hourly solar radiation data in 2020, as described below.

⁸Our numerical results show that, under $\xi = \$400/\text{MWh}$, only 0.03% to 0.43% of the demand is met by imports. This is consistent with the electricity spot price: Based on electricity wholesale prices from EIA, in 2019, prices above \$400/MWh occurred in 0.06% of the trading periods, whereas for 2020 it occurred in 0.5% of trading periods.

⁹Available at <http://www.psc.state.fl.us/ElectricNaturalGas/TenYearSitePlans>

The National Solar Radiation Database provides detailed solar radiation data for the entire U.S. in two measures: the maximum radiation under clear sky and the actual radiation received at the ground level, denoted as $S_{i,t}^{\text{clear-sky}}$ and $S_{i,t}^{\text{ground}}$, respectively, where i represents a location by latitude and longitude. We then calculate the total solar radiation for FLP’s 39 sites: $S_t^{\text{clear-sky}} = \sum_{i=1}^{39} y_i S_{i,t}^{\text{clear-sky}}$ and $S_t^{\text{ground}} = \sum_{i=1}^{39} y_i S_{i,t}^{\text{ground}}$, where y_i is the nameplate PV capacity of site i . From these, we compute $\bar{R}_t = S_t^{\text{clear-sky}} / \max_t S_t^{\text{clear-sky}}$ and $s_t = S_t^{\text{ground}} / S_t^{\text{clear-sky}}$. The computed \bar{R}_t contains both diurnal and seasonal variations. To simplify the computation for solving the HJB equation, we average \bar{R}_t over the same hour of day for each season (summer/winter) to obtain a 24-point diurnal profile, creating a periodic process with a 24-hour cycle. The multiplier s_t is translated into r_t as previously described and fitted to an AR(1) model.

We specify the demand process in (2) as $\log D_t = \bar{D}_t + d_t$. The deterministic component \bar{D}_t captures both time-of-day and day-of-week effects; thus \bar{D}_t is a periodic process with period $t_0 = 168$ hours. The logarithm transformation of the demand data normalizes the stochastic component d_t , which is modeled as an AR(1) process. To calibrate the demand model, we obtain the hourly data for FPL’s total electricity demand from the U.S. Energy Information Administration (www.eia.gov/opa). The FPL’s demand has been generally stable over the past five years, so we assume the same demand pattern going forward. All estimates are reported in Online Appendix D.

5.2.3 Discretization and Computation Method

The solution of the optimal investment problem (1) involves computing the operating cost in (11) using the solution to the stochastic control problem in (12). We solve the HJB equation of the problem in (12) numerically following Kushner and Dupuis (2001), who use a Markov chain with a discrete state space to approximate the stochastic control problem. The main idea is to discretize the state space and use finite differences to approximate the derivatives of the value function. We discretize the state space of the stochastic component r_t into 21 levels; the state space of d_t is also discretized similarly. Since the problem is cyclic with a period of 168 hours, we discretize the time space into 168 levels. The storage space is discretized into 50-200 levels depending on the storage capacity. The controlled Markov chain approximating the original stochastic control problem is solved using an iterative method, which combines approximations in policy space and in value space; see Chapter 6 of Kushner and Dupuis (2001). We leverage the structure of the optimal control in Section 4.2 to expedite the search for the optimal policy in each iteration.

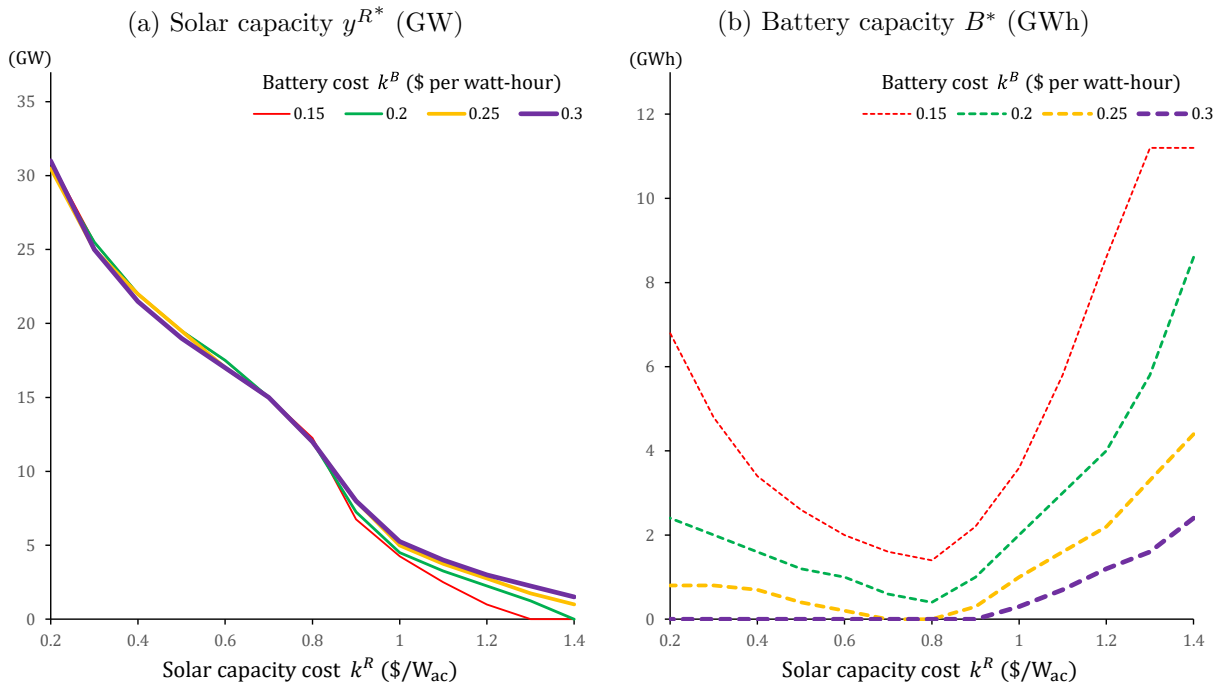
The investment problem (1) is optimized numerically by exhaustive enumeration of renewable capacity $y^R \in [0, 60]$ GW, flexible capacity $y^F \in [0, 25]$ GW, and storage size $B \in [0, 80]$ GWh. For every given capacity (y^R, y^F, B) , we compute the monthly operating cost in (12) for each value of c^F . We then compute the expected discounted operating cost as in (11).

5.3 Optimal Investment in Renewables and Battery (Fixed Flexible Capacity)

In this section, we consider a situation where the utility possesses a significant amount of existing flexible generation capacity that will not retire in the planning horizon. The utility’s investment focus is on solar and battery capacities only, solving (1) under a predetermined y^F .

To convey the scale, the average summer demand for FPL is 17.38 GW (see Appendix D). Deducting the inflexible (nuclear and coal) output of 4.11 GW, our portfolio needs to meet an average summer demand of 13.27 GW, with significant diurnal and stochastic variations. To investigate the relation between solar and battery investments, we consider 13 solar investment cost levels and 4 battery cost levels. For each cost combination, we find the optimal solar and battery capacities, (y^{R*}, B^*) under fixed flexible capacity $y^F = 18$ GW. The results are illustrated in Figure 4.

Figure 4: Optimal investment in solar and battery under flexible capacity $y^F = 18$ GW

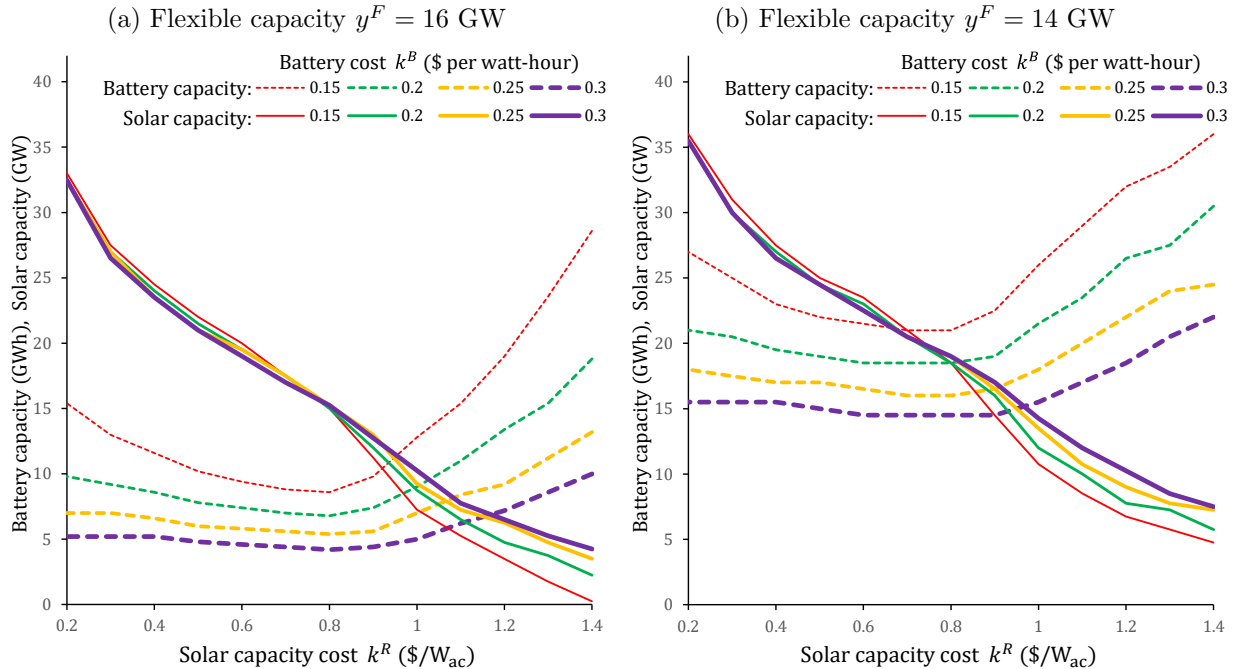


It is evident from Figure 4(a) that a lower cost of solar capacity raises its optimal investment. Figure 4(b) shows that the optimal battery capacity first decreases and then increases as the cost of solar decreases (except for the case of high battery cost $k^B = 0.3$ /Wh, where not investing in battery is optimal for a range of solar capacity costs). Therefore, solar and battery are substitutes when the solar cost is high, whereas they are complements at low solar cost.

Figure 5 depicts the cases with flexible capacity fixed at 16 GW and 14 GW, confirming that the qualitative trends and relations between battery and solar investments are consistent with those observed in Figure 4. These results verify the statements in Theorem 2 that solar and battery

capacities can be substitutes or complements; also refer to Figure 3 and its discussion in Section 5.1. Next, we analyze underlying operations that drive these investment relations.

Figure 5: Optimal investment in solar and battery under fixed flexible capacity



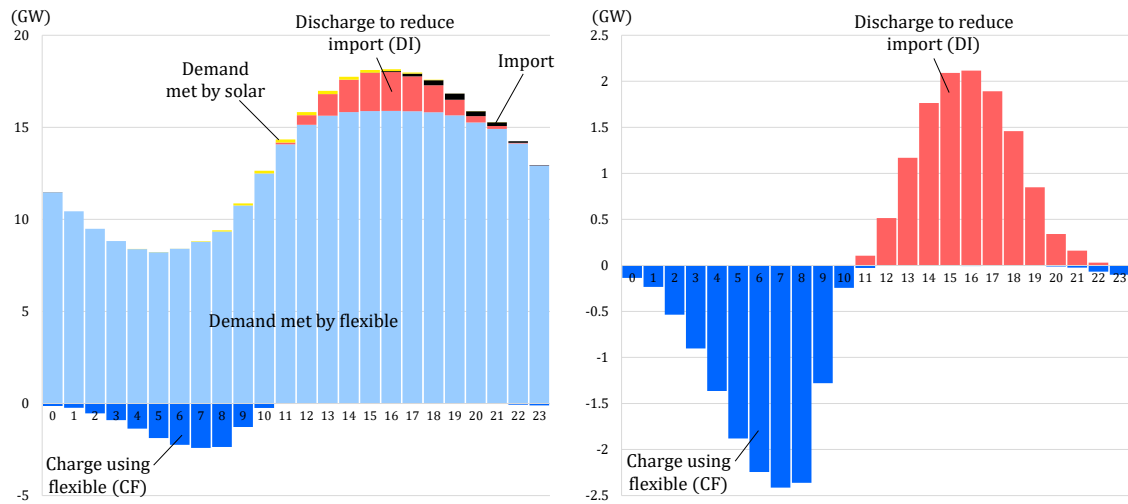
We consider operational details of three representative cases: high solar cost ($\$1.4/W_{ac}$), medium solar cost ($\$0.8/W_{ac}$), and low solar cost ($\$0.2/W_{ac}$). All three cases have battery cost $k^B = \$0.15/Wh$ and fixed flexible capacity $y^F = 16$ GW. The optimal capacity investments for these three cases are on the red curves in Figure 5(a). Specifically, the optimal solar capacities y^{R*} for the three cases are 0.25 GW, 15 GW, and 33 GW, respectively; the optimal battery capacities B^* are 28.6 GWh, 8.6 GWh, and 15.4 GWh, respectively.

The summer average hourly operations for these three representative cases are presented in Figure 6. In the left panels, the positive bars illustrate how much of the demand is met by flexible (light blue), solar (yellow), battery discharge (red for DI, magenta for DF), and imported energy (black). The positive bars stack up to exactly the average demand. The negative bars represent energy in excess of the demand: flexible generators may produce excess energy to charge the battery (blue for CF), excess solar energy may be used to charge battery (green for CR) or curtailed (grey). The right panels in Figure 6 zoom into the battery operations. These figures are similar to the cases studied in EIA (2022a) in terms of resource proportions.

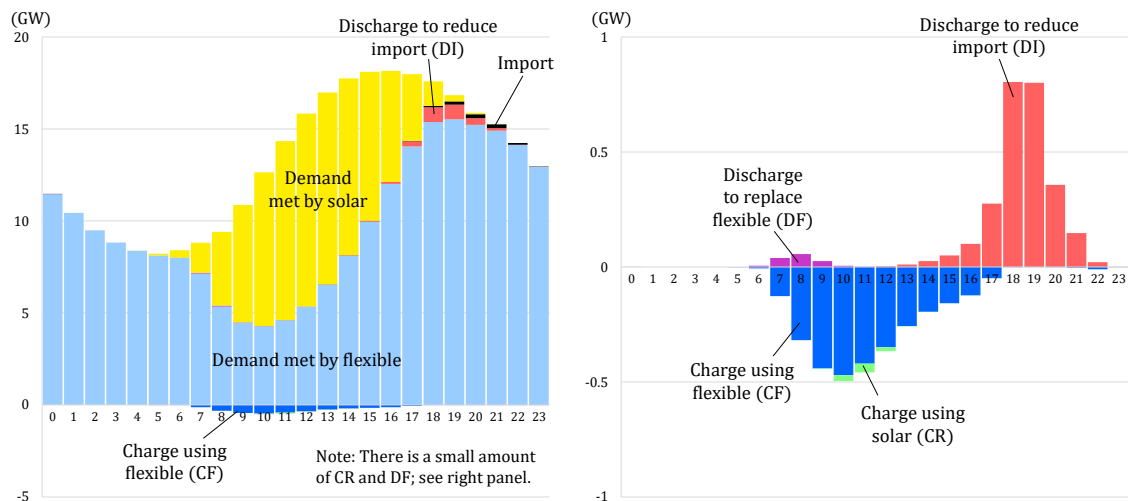
Case of high solar cost: In Figure 6(a), 0.25 GW of solar capacity supplies for 0.42% of demand on average. As the solar output never exceeds the demand in this case, the battery creates value only through (CF, DI) pair. CF operation can run whenever 16 GW of flexible capacity is not fully used.

Figure 6: Summer average hourly energy resource operations: $y^F = 16$ GW, $k^B = \$0.15/\text{Wh}$

(a) High solar cost: $k^R = \$1.4/\text{W}_{ac}$, $y^{R^*} = 0.25$ GW, $B^* = 28.6$ GWh



(b) Medium solar cost: $k^R = \$0.8/\text{W}_{ac}$, $y^{R^*} = 15$ GW, $B^* = 8.6$ GWh



(c) Low solar cost: $k^R = \$0.2/\text{W}_{ac}$, $y^{R^*} = 33$ GW, $B^* = 15.4$ GWh

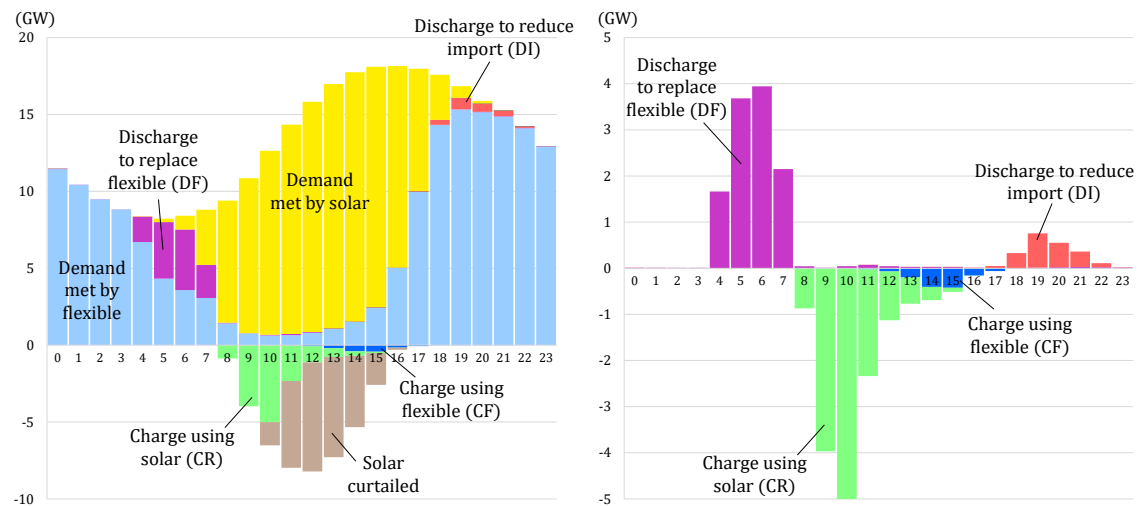


Figure 6(a) shows plenty of unused flexible capacity before noon, whereas DI potential corresponds to the bars marked as DI and import. Thus, the potential cost saving from (CF, DI) pair is limited by DI potential, corresponding to Figure 3(b) without CR. Under such a *discharging-constrained* case, the battery and renewable capacities are substitutes, confirming the substitution relation observed in Figures 4 and 5 under high solar cost.

Because of expensive energy import and demand uncertainty, it is optimal to size the battery to cover most of the demand in the extreme high-demand days. This implies that a large battery (28.6 GWh in this case) is desirable, and buffering for uncertainty is an important use of the battery. In fact, the average daily battery discharge (the sum of the red bars for DI in Figure 6(a)) is 12.49 GWh, which is only 43.7% of the battery's energy capacity, implying a significant buffer for uncertainty. Such buffering effectively mitigates the high cost of import during demand surges. As a result, only 0.43% of the total demand is met by imported energy.

Case of medium solar cost: In Figure 6(b), it is optimal to install 15 GW of solar capacity to supply 25.3% of the total demand. The solar energy reduces the daytime net demand, significantly reducing the DI potential. The battery's primary role is still to time-shift flexible generation via (CF, DI) pair, but at a much smaller quantity compared to the case in Figure 6(a). As a result, the optimal battery capacity, 8.6 GWh, is also much smaller. This is exactly why the battery and solar are substitutes when the potential benefit of the battery is constrained by DI potential.

It is worth noting that although solar energy cannot satisfy demand on average, solar energy at times exceeds demand due to uncertainties (in this case, 0.13% of the total solar energy is in excess of demand). The battery serves as a buffer not only for meeting peak demand but also for storing the excess solar power, reflected by CR in the right panel of Figure 6(b).

To prepare for CR operation, the battery performs DF operation in the early morning so that it has adequate room for storing solar energy. Interestingly, we find that the average daily amount of DF operation is 130 MWh, which exceeds 77 MWh of CR operation. This is because after DF operation creates room for CR operations, the uncertainties in both solar power and demand may prevent CR operation from refilling the room. Consequently, the remaining room (created by DF) is filled by CF operation to enable more DI operation later in the day. Here, although (CF, DF) pair leads to a (small) net loss, it is tactically and optimally performed to increase the chance of performing other cost-saving pairs.

Storage operations under uncertainties are also reflected in two other aspects. First, for some hours, battery may be charged or discharged depending on how uncertainties unfold. Thus, charging and discharging occur "together" during some hours in the right panel of Figure 6(b). We can also observe this to a lesser extent in Figure 6(a) and (c). Second, the average discharge over a day is 2.74

GWh, which is only 31.7% of the battery capacity. As explained before, the low battery utilization reflects the battery's role in buffering uncertainties in both demand and solar power.

Case of low solar cost: Figure 6(c) shows a case where a large amount of solar capacity is installed, supplying 42.6% of the demand directly. The amount of excess solar energy is much more than in the previous case. The surplus solar energy per day, measured by the bars marked as CR and solar curtailed in Figure 6(c), is exactly the CR potential. There is plenty of DF potential, as the flexible generation is the primary source of energy after sunset. Thus, the potential benefit of battery is limited by CR operation, corresponding to Figure 3(c). Under such a *charging-constrained* case, battery and renewable capacities are complements, confirming the complementary relations observed in Figures 4 and 5. In this case, solar and battery still compete in meeting peak demand, but this substitution effect is dominated by their complementary operations in storing surplus renewable generation (CR). Note that the CR potential in Figure 6(c) seems underused. This is because of uncertainty and cost concerns, as explained next.

In this case, one might expect that more solar output requires more buffer for uncertainty. However, it may be surprising that the battery utilization is actually 90.8%. Unlike the previous two cases where the battery reduces costs primarily through (CR, DI) pair, here additional investments in battery need to be traded off with a smaller marginal benefit from (CR, DF) pair. Consequently, a higher battery capacity utilization is needed to justify the investment. Figure 6(c) shows how a high battery utilization is operationalized: discharging occurs mostly in the early morning to create room for storing solar energy as much as possible in the day; the battery is primarily charged by solar power, and the remaining excess solar power must be curtailed.

Case of very low solar cost: In a futuristic case when the cost of renewable capacity is drastically lower and the renewable capacity is very high, the role of the battery is to store excess renewable output to replace ideally all fossil generation. In such a case, CR potential is expected to exceed discharging potential, i.e., the potential benefit of storage is limited by discharging operation, corresponding to Figure 3(d). Then, the battery and renewable capacities return to substitutes, as they compete to replace fossil energy.

Summary: Solar and battery capacities substitute each other in reducing the cost of serving peak demand or replacing fossil energy, whereas the battery complements solar by storing solar surplus. These two interactions may coexist. At high or very low solar costs, the substitution effect dominates; at a low (but not very low) solar cost, the complementary effect is more prominent.

5.4 Optimal Flexible-Renewable-Storage Portfolio

In this section, we consider a situation where all three resources—battery, renewable and flexible resources—are to be invested. We are interested in several aspects of the investment: First, does

the substitution and complementary relations observed under fixed flexible capacity continue to hold when the flexible capacity is jointly optimized? Second, since solar or battery alone can substitute flexible capacity, do solar and battery capacities *compete* against or *cooperate* with each other to substitute flexible capacity, and how?

We vary the solar cost k^R and battery cost k^B in the same ranges as in Section 5.3; we include an additional case where the battery is expensive and not invested; the flexible capacity cost is $k^F = \$1.17/\text{W}$ (see Section 5.2). We solve for the optimal investment problem in (1) for all cost combinations. The results are shown in Figure 7.

Figure 7: Optimal capacity investment

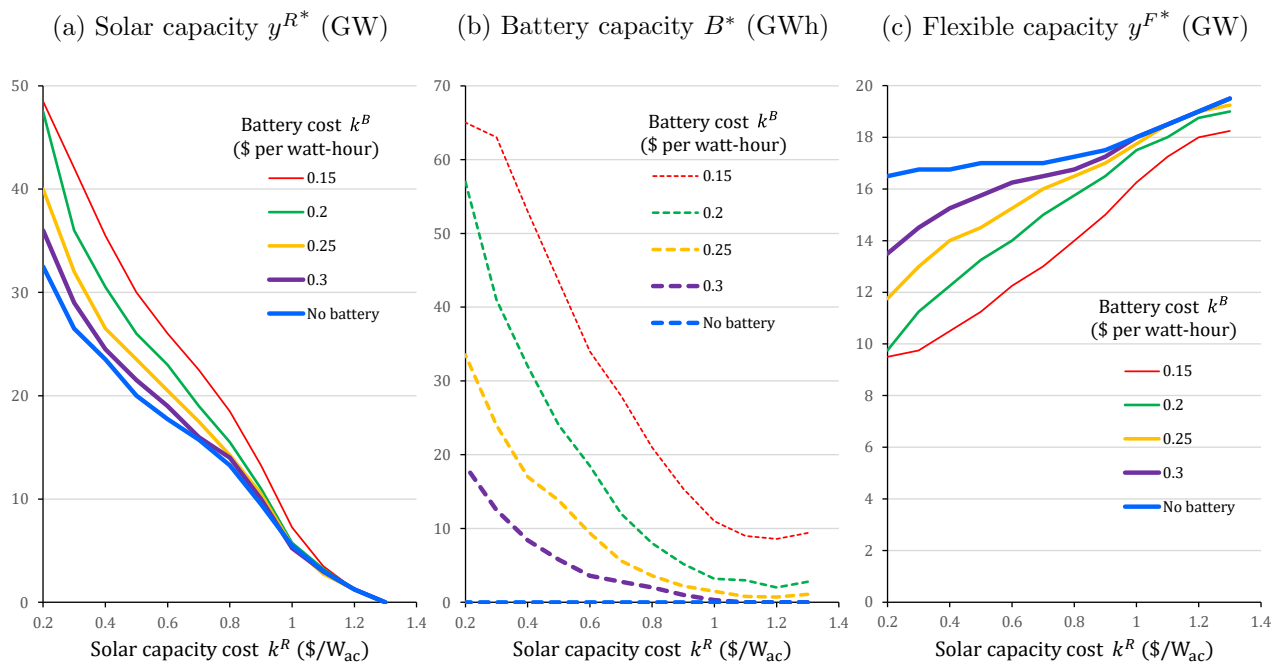


Figure 7(b) shows that the substitution and complementary relations between solar and battery discussed Section 5.3 continue to co-exist when flexible capacity is jointly optimized. However, the substitution effect dominates only under very high cost of solar (above $\$1.2/\text{W}_{ac}$). When the solar cost is below $\$1.2/\text{W}_{ac}$, the complementary effect not only dominates, but also appears to be much stronger than if the flexible capacity is fixed, which is evident from comparing Figure 7(b) with Figures 4(b) and 5. Importantly, Figure 7(c) shows how the flexible capacity declines as the solar cost decreases. We can see that the curve tends to be steeper when the battery cost is lower, implying that the battery complements solar in substituting the flexible capacity.

One reason for the observed strong complementary relation between battery and solar is that the battery can time-shift solar energy to peak-demand hours, thereby substituting the flexible capacity. In other words, the large amount of curtailed solar observed previously in Figure 6(c) can now be

time-shifted to reduce the need for flexible generation in early evenings. Thus, the reduction in flexible capacity investment can now justify a high investment in battery, which in turn encourages more investment in solar.

Reduced solar curtailment, however, only explains the strong complementary relation when there is a lot of excess solar (i.e., when solar cost is below $\$0.8/W_{ac}$). It does not explain why the two are complements when the solar cost is between $\$0.8/W_{ac}$ and $\$1.2/W_{ac}$, for which the optimal solar capacity is no more than 18.5 GW, implying a very small amount of excess solar. Indeed, the complementary effect between battery and solar goes beyond just curtailment reduction; they can complement each other even when solar does not exceed the demand, as we explain below. In Figure 6(a), the flexible capacity is operating at its capacity in the afternoon and early evening. If we would like to replace 1 GW of flexible capacity by battery, we would need to add a large battery and time-shift about 8 GWh of flexible generation to shave this “wide” peak. In contrast, in Figure 6(b), solar output reshapes the net demand profile, creating a “pointy” peak. As a result, a much smaller battery can time-shift an adequate amount of flexible generation to replace 1 GW of flexible capacity. Note that, in this case of high solar cost, solar output does not exceed the demand and thus is not time-shifted or smoothed by the battery. In short, although solar alone has limited ability to reduce the maximum net demand level to substitute flexible capacity, solar makes it easier for battery to shave the peak demand, forging a complementary relation with battery to together substitute flexible capacity.

6. Concluding Remarks

Renewable, flexible, and storage resources make up most of the new investments in the electricity industry. This paper explores the optimal operations of these three resources and their joint investment relations. At the operational level, we employ stochastic optimal control theory to provide a concise structured policy for the renewable-flexible-storage resource control problem. At the investment level, we analyze how operations drive investment relations and numerically solve a realistic model calibrated using real-world data.

We summarize the key operational insights as follows. First, storage operations can be decomposed to identify the energy source for charging and the energy displaced by discharging. Such decomposition crystallizes the structure of the optimal storage operations: Charging using renewable (CR) and discharging to replace import (DI) are driven only by net demand, whereas charging using flexible (CF) and discharging to replace flexible (DF) are performed opportunistically by comparing the marginal value of stored energy and the cost of flexible generation. Second, storage reduces cost via different pairs of charging and discharging operations; whether storage complements or substitutes other resources hinges on the operational pairs involved and whether executing these pairs is

constrained by charging or discharging. In addition, a storage operation pair that seems to incur a loss may still be part of the optimal strategy to facilitate other pairs of storage operations.

The key investment relations we have identified are: 1) storage and renewables are substitutes in meeting peak demand; 2) storage complements renewables by storing excess renewable output; 3) renewables (solar in particular) complement battery by compressing the peak period, making it easier for battery to displace flexible capacity; 4) when all resources are jointly optimized, the combined complementary effects in 2) and 3) are often stronger than the substitution effect in 1), resulting in synergies between renewable and storage that together substitute flexible capacity.

These investment relations have important implications for practice. As the government stimulates renewable or storage investment, the impact on different regions and utilities are bound to be different. In areas where renewable penetration is low and flexible capacity is difficult to be displaced due to low fuel costs, stimulating investment in storage or renewable can discourage each other due to their substitution effect (they compete in meeting the peak demand). In such situations, policy makers should be aware of the potential negative impact of renewable subsidies on storage investment and vice versa. On the other hand, our research also informs the government, utilities, and investors that this negative effect between renewable and storage is short-lived. As either investment cost declines, storage and renewables can complement each other in shaving the peak demand and thus reducing the need for flexible capacity. Our research also clarifies a myth that storage helps renewable energy only in storing excess renewable generation. Although that is an important source of storage value, when there is little excess renewable energy, storage can still cooperate with renewables to effectively displace fossil energy generation.

Our analysis gives rise to a few future research directions. First, our model currently has two conventional energy sources: flexible and import. In reality, different generators have different marginal cost levels; the resulting optimal storage operating policy can involve more thresholds. In such a case, the storage decomposition method continues to work, but it will result in more types of storage operations, leading to more intricate investment relations. Second, we consider only a one-time investment in this paper. In reality, as the cost of resources gradually declines, a dynamic investment model is needed to optimize the timing of investments.

References

- Aflaki, S., S. Netessine. 2017. Strategic investment in renewable energy sources: The effect of supply intermittency. *Manufacturing & Service Operations Management* **19**(3) 489–507.
- Al-Gwaiz, M., X. Chao, O. Q. Wu. 2017. Understanding how generation flexibility and renewable energy affect power market competition. *Manufacturing & Service Operations Management* **19**(1) 114–131.
- Alizamir, S., F. de Véricourt, P. Sun. 2016. Efficient feed-in-tariff policies for renewable energy technologies. *Operations Research* **64**(1) 52–66.

- Anderson, D. 1972. Models for determining least-cost investments in electricity supply. *The Bell Journal of Economics and Management Science* **3**(1) 267–299.
- Angelus, A. 2021. Distributed renewable power generation and implications for capacity investment and electricity prices. *Production and Operations Management* **30**(12) 4614–4634.
- Avci, H., E. C. Karakoyun, A. S. Kocaman, E. Nadar, P. Toufani. 2021. Integration of pumped hydro energy storage and wind energy generation: Structural analysis and algorithms. Working paper, Bilkent University.
- Babich, V., R. Lobel, Ş. Yücel. 2020. Promoting solar panel investments: Feed-in-tariff vs. tax-rebate policies. *Manufacturing & Service Operations Management* **22**(6) 1148–1164.
- Bertsimas, D., R. Cory-Wright, V. Digalakis. 2023. Decarbonizing OCP. *Manufacturing & Service Operations Management*, forthcoming doi:10.1287/msom.2022.0467.
- Billionnet, A., M. Costa, P. Poirion. 2016. Robust optimal sizing of a hybrid energy stand-alone system. *European Journal of Operational Research* **254**(2) 565–575.
- Brown, P., A. P. Lopes, J. Matos. 2008. Optimization of pumped storage capacity in an isolated power system with large renewable penetration. *IEEE Transactions on Power systems* **23**(2) 523–531.
- Bruno, S., S. Ahmed, A. Shapiro, A. Street. 2016. Risk neutral and risk averse approaches to multistage renewable investment planning under uncertainty. *European Journal of Operational Research* **250**(3) 979–989.
- Budischak, C., D. Sewell, H. Thomson, L. Mach, D. Veron, W. Kempton. 2013. Cost-minimized combinations of wind power, solar power and electrochemical storage, powering the grid up to 99.9% of the time. *Journal of Power Sources* **225** 60–74.
- Buttel, L. 2023. America’s electricity generation capacity: 2023 update. American Public Power Association. <https://www.publicpower.org/resource/americas-electricity-generating-capacity>.
- Castronuovo, E. D., J. A. P. Lopes. 2004. On the optimization of the daily operation of a wind-hydro power plant. *IEEE Transactions on Power systems* **19**(3) 1599–1606.
- Cho, N. R., Y. Kim, K. Murali, M. Yavuz. 2023. Drivers and implications of combined investment in renewables and energy storage in the residential sector. *Decision Sciences*, forthcoming doi:https://doi.org/10.1111/dec.12589.
- Cole, W., A. W. Frazier, C. Augustine. 2021. Cost projections for utility-scale battery storage: 2021 update. National Renewable Energy Laboratory, Golden, CO.
- Cruise, J., L. Flatley, R. Gibbens, S. Zachary. 2019. Control of energy storage with market impact: Lagrangian approach and horizons. *Operations Research* **67**(1) 1–9.
- Del Granado, P., S. Wallace, Z. Pang. 2014. The value of electricity storage in domestic homes: A smart grid perspective. *Energy Systems* **5**(2) 220–226.
- Drake, D. F., J. G. York. 2021. Kicking ash: Who (or what) is winning the “war on coal”? *Production and Operations Management* **30**(7) 2162–2187.
- EIA. 2019. Cost and performance characteristics of new generating technologies, annual energy outlook. Technical report. U.S. Energy Information Administration.
- EIA. 2021a. Annual Energy Outlook 2021. U.S. Energy Information Administration. <https://www.eia.gov/outlooks/aeo>.
- EIA. 2021b. Battery storage in the United States: An update on market trends. U.S. Energy Information Administration. <https://www.eia.gov/analysis/studies/electricity/batterystorage>.
- EIA. 2022a. Annual Energy Outlook 2022. U.S. Energy Information Administration. <https://www.eia.gov/outlooks/aeo>.
- EIA. 2022b. U.S. battery storage capacity will increase significantly by 2025. U.S. Energy Information Administration. <https://www.eia.gov/todayinenergy/detail.php?id=54939>.
- EIA. 2024. U.S. battery storage capacity expected to nearly double in 2024. U.S. Energy Information Admin-

- istration. <https://www.eia.gov/todayinenergy/detail.php?id=61202>.
- Feldman, D., V. Ramasamy, R. Fu, A. Ramdas, J. Desai, R. Margolis. 2021. U.S. solar photovoltaic system and energy storage cost benchmark: Q1 2020. National Renewable Energy Laboratory, Golden, CO. <https://www.nrel.gov/docs/fy21osti/77324.pdf>.
- Fertig, E., J. Apt. 2011. Economics of compressed air energy storage to integrate wind power: A case study in ERCOT. *Energy Policy* **39**(5) 2330–2342.
- Fleming, W. H., H. Soner. 2006. *Controlled Markov Processes and Viscosity Solutions*. 2nd ed. Springer.
- Gao, Z., K. Alshehri, J. R. Birge. 2024. Aggregating distributed energy resources: Efficiency and market power. *Manufacturing & Service Operations Management* Forthcoming.
- Garcia-Gonzalez, J., R. Moraga, L. Matres-Santos, A. Mateo. 2008. Stochastic joint optimization of wind generation and pumped-storage units in an electricity market. *IEEE Transactions on Power systems* **23**(2) 460–468.
- Goodarzi, S., S. Aflaki, A. Masini. 2019. Optimal feed-in tariff policies: The impact of market structure and technology characteristics. *Production and Operations Management* **28**(5) 1108–1128.
- Guaajardo, J. A. 2018. Third-party ownership business models and the operational performance of solar energy systems. *Manufacturing & Service Operations Management* **20**(4) 788–800.
- Harrison, J. M. 1990. *Brownian Motion and Stochastic Flow Systems*. 2nd ed. Krieger Publishing Company.
- Harsha, P., M. Daleh. 2015. Optimal management and sizing of energy storage under dynamic pricing for the efficient integration of renewable energy. *IEEE Transactions on Power Systems* **30**(3) 1164–1181.
- Hu, S., G. C. Souza, M. E. Ferguson, W. Wang. 2015. Capacity investment in renewable energy technology with supply intermittency: Data granularity matters! *Manufacturing & Service Operations Management* **17**(4) 480–494.
- Huang, H., N. Sunar, J. M. Swaminathan, R. Roy. 2023. Do noisy customer reviews discourage platform sellers? Empirical analysis of an online solar marketplace. *Manufacturing & Service Operations Management* **25**(6) 2195–2215.
- Jiang, D. R., W. B. Powell. 2015. Optimal hour-ahead bidding in the real-time electricity market with battery storage using approximate dynamic programming. *INFORMS Journal on Computing* **27**(3) 525–543.
- Kamdem, B. G., E. Shittu. 2017. Optimal commitment strategies for distributed generation systems under regulation and multiple uncertainties. *Renewable and Sustainable Energy Reviews* **80** 1597–1612.
- Kaps, C., S. Marinesi, S. Netessine. 2023. When should the off-grid sun shine at night? Optimum renewable generation and energy storage investments. *Management Science* **69**(12) 7633–7650.
- Kim, J. H., W. Powell. 2011. Optimal energy commitments with storage and intermittent supply. *Operations Research* **59**(6) 1347–1360.
- Kök, A. G., K. Shang, Ş. Yücel. 2018. Impact of electricity pricing policies on renewable energy investments and carbon emissions. *Management Science* **64**(1) 131–148.
- Kök, A. G., K. Shang, Ş. Yücel. 2020. Investments in renewable and conventional energy: The role of operational flexibility. *Manufacturing & Service Operations Management* **22**(5) 925–941.
- Korpaas, M., A. Holen, R. Hildrum. 2003. Operation and sizing of energy storage for wind power plants in a market system. *Electrical Power and Energy Systems* **25** 599–606.
- Kushner, H. J., P. Dupuis. 2001. *Numerical Methods for Stochastic Control Problems in Continuous Time*. 2nd ed. Springer, New York, NY.
- Kuznia, L., B. Zeng, G. Centeno, Z. Miao. 2013. Stochastic optimization for power system configuration with renewable energy in remote areas. *Annals of Operations Research* **210**(1) 411–432.
- Li, K., K. Tsing. 2015. Energy efficiency of lithium-ion battery used as battery storage devices in micro-grid. *IECON 2015 - 41st Annual Conference of the IEEE Industrial Electronics Society*. 005235–005240.
- Mak, H.-Y. 2022. Enabling smarter cities with operations management. *Manufacturing & Service Operations Management* **24**(1) 24–39.

- Paine, N., F. Homans, M. Pollak, J. Bielicki, E. Wilson. 2014. Why market rules matter: Optimizing pumped hydroelectric storage when compensation rules differ. *Energy Economics* **46** 10–19.
- Parker, G., B. Tan, O. Kazan. 2019. Electric power industry: Operational and public policy challenges and opportunities. *Production and Operations Management* **28**(11) 2738–2777.
- Parpas, P., M. Webster. 2014. A stochastic multiscale model for electricity generation capacity expansion. *European Journal of Operational Research* **232**(2) 359–374.
- Peura, H., D. W. Bunn. 2021. Renewable power and electricity prices: The impact of forward markets. *Management Science* **67**(8) 4772–4788.
- Qi, W., Y. Liang, Z.-J. M. Shen. 2015. Joint planning of energy storage and transmission for wind energy generation. *Operations Research* **63**(6) 1280–1293.
- Ritzenhofen, I., J. R. Birge, S. Spinler. 2016. The structural impact of renewable portfolio standards and feed-in tariffs on electricity markets. *European Journal of Operational Research* **255**(1) 224–242.
- Secomandi, N. 2010. Optimal commodity trading with a capacitated storage asset. *Management Science* **56**(3) 449–467.
- Sharma, V., M. H. Haque, S. M. Aziz. 2019. Energy cost minimization for net zero energy homes through optimal sizing of battery storage system. *Renewable Energy* **141** 278–286.
- Siddiqui, A. S., M. Tanaka, Y. Chen. 2016. Are targets for renewable portfolio standards too low? The impact of market structure on energy policy. *European Journal of Operational Research* **250**(1) 328–341.
- Singh, S. P., A. Scheller-Wolf. 2022. That’s not fair: Tariff structures for electric utilities with rooftop solar. *Manufacturing & Service Operations Management* **24**(1) 40–58.
- Sunar, N., J. M. Swaminathan. 2021. Net-metered distributed renewable energy: A peril for utilities? *Management Science* **67**(11) 6716–6733.
- Sunar, N., J. R. Birge. 2019. Strategic commitment to a production schedule with uncertain supply and demand: Renewable energy in day-ahead electricity markets. *Management Science* **65**(2) 714–734.
- Sunar, N., J. M. Swaminathan. 2022. Socially relevant and inclusive operations management. *Production and Operations Management* **31**(12) 4379–4392.
- U.S. Environmental Protection Agency. 2024. Greenhouse gas inventory data explorer. <https://cfpub.epa.gov/ghgdata/inventoryexplorer/#allsectors/allsectors/allgas/econsect/all>.
- van de Ven, P. M., N. Hegde, L. Massoulié, T. Salonidis. 2013. Optimal control of end-user energy storage. *IEEE Transactions Smart Grid* **4**(2) 789–797.
- Weigelt, C., E. Shittu. 2016. Competition, regulatory policy, and firms’ resource investments: The case of renewable energy technologies. *Academy of Management Journal* **59**(2) 678–704.
- Welling, A. 2016. The paradox effects of uncertainty and flexibility on investment in renewables under governmental support. *European Journal of Operational Research* **251**(3) 1016–1028.
- World Resources Institute. 2024. Climate watch historical GHG emissions. <https://www.climatewatchdata.org/ghg-emissions>.
- Wu, O. Q., R. Kapuscinski, S. Suresh. 2023. On the distributed energy storage investment and operations. *Manufacturing & Service Operations Management* **25**(6) 2277–2297. doi:10.1287/msom.2020.0652.
- Wu, O. Q., Ş. Yücel, Y. Zhou. 2022. Smart charging of electric vehicles: An innovative business model for utility firms. *Manufacturing & Service Operations Management* **24**(5) 2481–2499.
- Xi, X., R. Sioshansi, V. Marano. 2014. A stochastic dynamic programming model for co-optimization of distributed energy storage. *Energy Systems* **5**(3) 575–505.
- Zhou, Y., A. Scheller-Wolf, N. Secomandi, S. Smith. 2016. Electricity trading and negative prices: Storage vs. disposal. *Management Science* **62**(3) 880–898.
- Zhou, Y., A. Scheller-Wolf, N. Secomandi, S. Smith. 2019. Managing wind-based electricity generation in the presence of storage and transmission capacity. *Production and Operations Management* **28**(4) 970–989.

Online Supplements

A. Reflecting Boundary Approach

One of the challenges in solving the optimal control problem in (12) is handling the state boundary constraint $b_t \in [0, B]$ in (5), which requires us to derive boundary conditions satisfied by the value function; see Chapter II of Fleming and Soner (2006). In this appendix, we use reflecting boundaries to reformulate the optimal control problem in (12). The new formulation constructs two reflecting processes to regulate the storage level so that this state constraint is automatically satisfied. The additional optimality condition imposed on the two reflecting processes allows us to derive the boundary conditions of the HJB equation, stated in Lemma 2 in the paper.

The reflecting boundary method essentially handles the state constraint $b_t \in [0, B]$ by constructing two reflecting processes. These reflecting processes ensure that the storage level stays within $[0, B]$ by “nudging” the storage process to stay on the boundary if it is about to drift out of the boundary. Such reflecting boundaries always exist and are unique for continuous paths; see Chapter 2 of Harrison (1990). The amount of nudge has intuitive interpretation, which we will explain after the reformulation below.

$$\inf_{\{\tilde{q}_t^F, \tilde{q}_t^B, t \geq 0\}} \lim_{s \rightarrow \infty} \frac{1}{s} \mathbb{E} \left[\int_0^s \left(c^F \tilde{q}_t^F + \xi (D_t - y^R R_t - \tilde{q}_t^F + \psi(\tilde{q}_t^B))^+ \right) dt + \xi I_s \right], \quad (\text{A.1})$$

$$\text{s.t. } (2), (3), (5),$$

$$d\tilde{b}_t = \tilde{q}_t^B dt + dI_t - dU_t, \quad \tilde{b}_0 = b_0 \in [0, B], \quad (\text{A.2})$$

$$\tilde{q}_t^F \in [0, y^F] \quad \text{and} \quad \tilde{q}_t^B \in [-y_{\text{out}}^B, \alpha y_{\text{in}}^B], \quad (\text{A.3})$$

$$I_t \text{ and } U_t \text{ are increasing and continuous with } I_0 = U_0 = 0, \quad (\text{A.4})$$

$$\int_0^\infty \tilde{b}_t dI_t = 0, \quad \int_0^\infty (B - \tilde{b}_t) dU_t = 0. \quad (\text{A.5})$$

Compared to the formulation in (12), we construct two reflecting processes I_t and U_t in the new formulation. The storage state equation (4) is replaced by (A.2). The two reflecting processes I_t and U_t only change when the storage level hits the two boundaries. The state constraint (5) is supplemented by (A.4)-(A.5). The two reflecting processes I_t and U_t constructed from conditions (A.4)-(A.5) ensure that the regulated storage level \tilde{b}_t always satisfies the state constraint (5).

For a given policy $\{(\tilde{q}_t^F, \tilde{q}_t^B) : t \geq 0\}$, the processes I_t and U_t regulate the process \tilde{b}_t as follows. The first (resp. second) integral constraint in (A.5) allows I_t (resp. U_t) to increase only when $\tilde{b}_t = 0$ (resp. $\tilde{b}_t = B$). Thus, if $\tilde{b}_t \in (0, B)$, then $dI_t = dU_t = 0$ and \tilde{b}_t is solely driven by \tilde{q}_t^B . When \tilde{b}_t reaches 0, \tilde{q}_t^B can still be negative, while I_t increases at the same rate as the negative part of \tilde{q}_t^B to ensure that \tilde{b}_t does not drop below 0 (i.e., battery cannot be overdrifted). Thus, the process I_t can be interpreted as the cumulative amount of energy that must be imported to prevent overdrifting the storage under the policy $\{(\tilde{q}_t^F, \tilde{q}_t^B) : t \geq 0\}$. Hence, a cost ξI_s is added in the objective in (A.1).

On the other hand, when \tilde{b}_t reaches B , the control \tilde{q}_t^B can still be positive, while U_t increases at the same rate as the positive part of \tilde{q}_t^B to ensure that \tilde{b}_t does not exceed B (i.e., battery does not get overcharged). Intuitively, when the storage is full but there is still excessive renewable energy, we would wish to store it (hence $\tilde{q}_t^B > 0$) but $\tilde{q}_t^B > 0$ will not raise the storage level above B , i.e., the excess energy that we wish to

charge is actually wasted. Thus, the process U_t represents the cumulative amount of renewable energy we intend to store under policy $\{(\tilde{q}_t^F, \tilde{q}_t^B) : t \geq 0\}$ but is actually curtailed because the battery is full.

The following lemma shows that we can obtain an optimal policy for the original formulation (12) by solving the new formulation.

Lemma A.1. *The Brownian control problem stated in (A.1)-(A.5) is equivalent to the formulation (12) in the following sense:*

(i) *Every feasible policy for (12) is a feasible policy for (A.1)-(A.5) with the same cost and with $I_t = 0$ and $U_t = 0$ for all $t \geq 0$.*

(ii) *Every optimal policy for (A.1)-(A.5) yields a feasible policy for (12) with the same cost. Specifically, if $(\tilde{q}_t^F, \tilde{q}_t^B)$ with associated reflecting processes I_t and U_t is an optimal policy for (A.1)-(A.5), then $(\tilde{q}_t^F, \tilde{q}_t^B + I_t' - U_t')$ is an optimal policy for (12).*

Lemma A.1(i) implies that the minimum cost of (A.1) is no higher than that of (12). Part (ii) then states if a policy achieves the minimum cost of (A.1), we can construct a policy for (12) to achieve the same cost. Therefore, solving (A.1)-(A.5) is equivalent to solving (12).

Since the boundary condition is automatically satisfied with the two reflecting process, the reformulated problem in (A.1)-(A.5) using reflecting boundaries has state-independent feasible range of the control variables: $(\tilde{q}_t^F, \tilde{q}_t^B) \in \mathcal{U} \equiv [0, y^F] \times [-y_{\text{out}}^B, \alpha y_{\text{in}}^B]$. (In (12), the constraints $b_t \in [0, B]$ render the feasible controls to be state dependent.) In addition, the reflecting processes I_t and U_t impose additional conditions that the optimal value function needs to satisfy. This allows us to write down the Hamilton-Jacob-Bellman (HJB) equation as well as the boundary conditions that the value function satisfies, as given in Lemma 2 in the paper.

Proof of Lemma A.1: (i) It is straightforward to see that every feasible policy for (12) is feasible for (A.1)-(A.5) with $I_t = U_t = 0$ for all $t \geq 0$. In addition, the two problems yield the same cost since $I_t = 0$ adds no cost to the objective in (A.1).

(ii) It follows from Chapter 2.4 of Harrison (1990) that, for any given feasible solution $(\tilde{q}_t^B, \tilde{q}_t^F)$ to (A.1)-(A.5) there exist unique I_t and U_t that satisfy equations (5), (A.2), (A.4), and (A.5).

Let $I_t' = (\tilde{q}_t^B)^- \mathbb{I}_{\tilde{b}_t=0}$ and $U_t' = (q_t^B)^+ \mathbb{I}_{\tilde{b}_t=B}$, where \mathbb{I}_A is an indicator function that equals one if A is true and equals zero otherwise, $x^- = \max(0, -x)$ and $x^+ = \max(0, x)$. Let

$$I_t = \int_0^t I_s' ds \quad \text{and} \quad U_t = \int_0^t U_s' ds.$$

It is easy to verify that the constructed I_t and U_t satisfy equations (A.2) and (A.4)-(A.5).

We now construct a policy that is feasible for (12). Let $q_t^F = \tilde{q}_t^F$ and $q_t^B = \tilde{q}_t^B + I_t' - U_t'$ for $t \geq 0$. Then it follow from (A.2) that $b_t = \tilde{b}_t$ for all $t \geq 0$. Thus, the two systems have the same dynamics. We will complete the proof by showing that the two systems also yield the same cost if the policy $(\tilde{q}_t^B, \tilde{q}_t^F)$ is optimal. We consider the following three cases:

If $I_t' = U_t' = 0$, then the two systems incur the costs at the same rate because the operating decisions in both systems are identical.

If $I_t' > 0$ and $U_t' = 0$, it implies that $\tilde{q}_t^B < 0$ and $\tilde{b}_t = 0$. In this case, $q_t^F = \tilde{q}_t^F$ and $q_t^B = \tilde{q}_t^B + I_t'$. To show that the two systems incur the costs at the same rate, we show that $\Delta_t^+ = \tilde{\Delta}_t^+ + I_t'$, where $\tilde{\Delta}_t =$

$D_t - y_I - y^R R_t - \tilde{q}_t^F - \psi(\tilde{q}_t^B)$ and $\Delta_t = D_t - y_I - y^R R_t - q_t^F - \psi(q_t^B)$. It follows from $q_t^F = \tilde{q}_t^F$ and $q_t^B = \tilde{q}_t^B + I_t'$ that $\Delta_t = \tilde{\Delta}_t + I_t'$.

To show that $\Delta_t^+ = \tilde{\Delta}_t^+ + I_t'$, it suffices to show that $\tilde{\Delta}_t \geq 0$. We show this by contradiction. Suppose that $\tilde{\Delta}_t < 0$. If we replace \tilde{q}_t^B by $\tilde{q}_t^B + \epsilon$ for a small $\epsilon > 0$ such that $\tilde{\Delta}_t + \epsilon < 0$ and $\tilde{q}_t^B + \epsilon < 0$, then the system incurs the cost at a rate of $\tilde{q}_t^F + (\tilde{q}_t^B + \epsilon)^- < \tilde{q}_t^F + (\tilde{q}_t^B)^-$. This contradicts to the assumption that the given policy is optimal.

If $I_t' = 0$ and $U_t' < 0$, it implies that $\tilde{q}_t^B > 0$ and $\tilde{b}_t = B$. To show that the two systems incur the costs at the same rate, we show that $\Delta_t^+ = \tilde{\Delta}_t^+$. Since $\Delta_t = \tilde{\Delta}_t - U_t'$, it suffices to show that $\tilde{\Delta}_t \leq 0$. We show this by contradiction. Suppose that $\tilde{\Delta}_t > 0$. If we replace \tilde{q}_t^B by $\tilde{q}_t^B - \epsilon$ for a small $\epsilon > 0$ such that $\tilde{\Delta}_t - \epsilon/\alpha > 0$ and $\tilde{q}_t^B - \epsilon > 0$, then the system incurs the cost at a rate of $\tilde{q}_t^F + \tilde{\Delta}_t - \epsilon/\alpha < \tilde{q}_t^F + \tilde{\Delta}_t$. This contradicts the assumption that the given policy $(\tilde{q}_t^B, \tilde{q}_t^F)$ is optimal.

In sum, the two systems incur the costs at the same rate under all cases for all $t \geq 0$ if the given policy $(\tilde{q}_t^B, \tilde{q}_t^F)$ is optimal. \square

B. The Discrete-Time Model

This section formulates and analyzes a discrete-time model to demonstrate the conciseness and usefulness of the continuous-time model in the paper.

First, we present the discrete-time counterpart of the continuous-time model in (12), highlighting only the elements that differ. Let $t \in \mathcal{T} := \{0, 1, 2, \dots\}$ index time periods, and the length of each period is $\delta > 0$. Thus, period t is the time interval $[t\delta, (t+1)\delta)$. Demand in period t is $D_t\delta$. That is, D_t is still measured in MW, so is all the power capacities. Similarly, renewable output in period t is $R_t\delta$. The stochastic components of the demand and renewable generation, d_t and r_t , are Markovian processes characterized by the Markov kernels $p_d(x, y)$ and $p_r(x, y)$, respectively. In particular,

$$\mathbb{P}(r_{t+1} \in A | r_t = x) = \int_{y \in A} k_r(y, x) dy \quad \text{and} \quad \mathbb{P}(d_{t+1} \in A | d_t = x) = \int_{y \in A} k_d(y, x) dy. \quad (\text{B.1})$$

At the beginning of each period t , the utility observes D_t , R_t , and the stored energy level b_t , and then decides the flexible generation rate q_t^F , renewable generation rate q_t^R , and the storage charging/discharging rate q_t^B in period t . The stored energy level evolves according to

$$b_{t+1} = b_t + q_t^B \delta. \quad (\text{B.2})$$

We consider a discrete-time analogue of the model in (10). Using the same procedure described in Section 4.1, we can transform the problem into the discrete-time version of the problem in (12):

$$\begin{aligned} \bar{C}(y^R, y^F, B, c^F) = & \inf_{\{q_t^F, q_t^B, t \in \mathcal{T}\}} \lim_{s \rightarrow \infty} \frac{1}{s\delta} \mathbb{E} \left[\sum_{t=0}^s \left(c^F q_t^F + \xi(D_t - y^R R_t - q_t^F + \psi(q_t^B))^+ \right) \delta \right], & (\text{B.3}) \\ \text{s.t.} & \quad \text{state equations: (2), (B.1), (B.2),} \\ & \quad \text{state constraint: (5),} \\ & \quad \text{control constraints: (6), (7).} \end{aligned}$$

Next, we derive the Bellman equation that the optimal average cost $v = \bar{C}(y^R, y^F, B, c^F)$ and the relative

cost function $\phi_t(b, r, d)$ must satisfy: For $(b_t, r_t, d_t) \in \mathcal{X}$,

$$\phi_t(b_t, r_t, d_t) = \min_{q^F \in [0, y^F], q^B \in [q_t^B, \bar{q}_t^B]} \left\{ c^F q^F + \xi(\tilde{D}_t + \psi(q^B) - q^F)^+ - v + \tilde{\phi}_t(b_t + q^B \delta, r_t, d_t) \right\}, \quad (\text{B.4})$$

where $\tilde{D}_t = f_d(\bar{D}_t, d_t) - y^R f_r(\bar{R}_t, r_t)$, $q_t^B = \max(-y_{\text{out}}^B, -b_t/\delta)$ and $\bar{q}_t^B = \min((B - b_t)/\delta, \alpha y_{\text{in}}^B)$, and $\tilde{\phi}_t(b, r, d) = \mathbb{E}[\phi_{t+1}(b, r_{t+1}, d_{t+1}) | r_t = r, d_t = d]$. The definition of the function $\tilde{\phi}_t$ fixes the value of the battery energy level b in period $t + 1$ while taking the expectation conditional on the values of r_t and d_t in period t . Similarly, we state a lemma that characterizes the important properties of the relative cost function.

Lemma 3'. $\phi_t(b, r, d)$ is convex and decreasing in b , for any given (t, r, d) . Therefore, $\phi_t(b, r, d)$ is differentiable almost everywhere with $\partial\phi_t(b, r, d)/\partial b \in [-\xi/\delta, 0]$.

We omit the proof of Lemma 3' because it follows the same but tedious argument in the proof of Lemma 3. Thus, we have the following immediate properties of $\tilde{\phi}(\cdot)$.

Corollary 2. $\tilde{\phi}_t(b, r, d)$ is convex and decreasing in b , for any given (t, r, d) . Therefore, $\tilde{\phi}_t(b, r, d)$ is differentiable almost everywhere with $\partial\tilde{\phi}_t(b, r, d)/\partial b \in [-\xi, 0]$.

We provide the solution to the Bellman equation for comparison; see Appendix F for the detailed proof. To facilitate stating the proposition, we write $\partial\tilde{\phi}_t(b_t, r_t, d_t)/\partial b$ as $\partial\tilde{\phi}_t/\partial b$ in short. In addition, define two constants $\bar{b}_t(r, d)$ and $\underline{b}_t(r, d)$ as follows:

$$\begin{aligned} \bar{b}_t(r, d) &= \sup \left\{ b \in [0, B] : \frac{\partial\tilde{\phi}_t(b, r, d)}{\partial b} = -c^F \right\}, \\ \underline{b}_t(r, d) &= \inf \left\{ b \in [0, B] : \frac{\partial\tilde{\phi}_t(b, r, d)}{\partial b} = -\frac{c^F}{\alpha} \right\}. \end{aligned}$$

Proposition 1'. The optimal dispatch rate q_t^{F*} and charging rate q_t^{B*} satisfy: Given the system state $(b_t, r_t, d_t) \in \mathcal{X}$, $q_t^{B*} = (q_t^B \vee \hat{q}^B) \wedge \bar{q}_t^B$ and $q_t^{F*} = (\tilde{D} + \psi(q_t^{B*}))^+ \wedge y^F$, where

(a) $\tilde{D} > y^F$:

$$\hat{q}^B = \begin{cases} y^F - \tilde{D}, & \text{if } -\xi \leq \frac{\partial\tilde{\phi}_t}{\partial b} < -c^F, \\ (y^F - \tilde{D}) \wedge [-(\tilde{D} \wedge ((b - \bar{b}_t)/\delta))], & \text{if } -c^F \leq \frac{\partial\tilde{\phi}_t}{\partial b} \leq 0. \end{cases} \quad (\text{B.5})$$

(b) $0 < \tilde{D} \leq y^F$:

$$\hat{q}^B = \begin{cases} ((\underline{b}_t - b)/\delta) \wedge (\alpha(y^F - \tilde{D})), & \text{if } -\xi \leq \frac{\partial\tilde{\phi}_t}{\partial b} < -\frac{c^F}{\alpha}, \\ 0, & \text{if } -\frac{c^F}{\alpha} \leq \frac{\partial\tilde{\phi}_t}{\partial b} < -c^F, \\ -((b - \bar{b}_t)/\delta) \wedge \tilde{D}, & \text{if } -c^F \leq \frac{\partial\tilde{\phi}_t}{\partial b} \leq 0. \end{cases}$$

(c) $\tilde{D} \leq 0$:

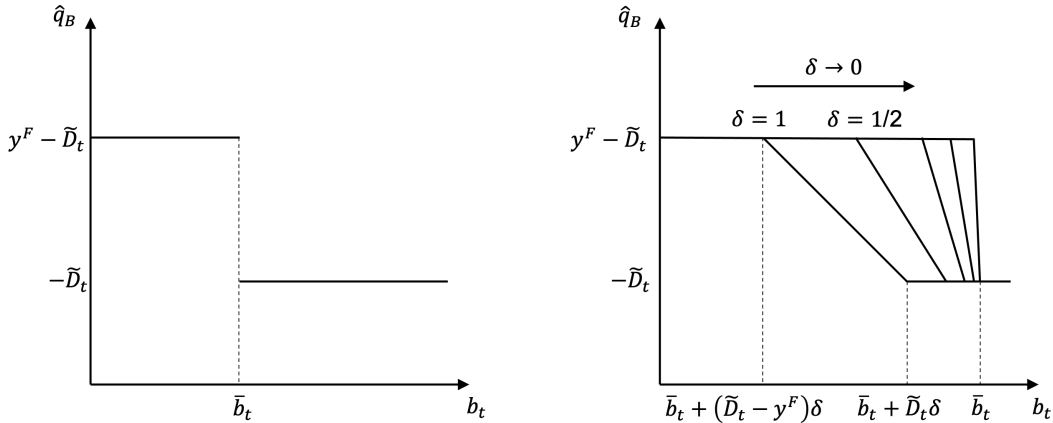
$$\hat{q}^B = \begin{cases} [(\underline{b}_t - b)^+/\delta] \wedge (\alpha(y^F - \tilde{D})), & \text{if } -\xi \leq \frac{\partial\tilde{\phi}_t}{\partial b} < -\frac{c^F}{\alpha}, \\ -\alpha\tilde{D}, & \text{if } -c^F/\alpha \leq \frac{\partial\tilde{\phi}_t}{\partial b} \leq 0. \end{cases}$$

Comparing the optimal solution provided in Proposition 1 and Proposition 1', we find that the continuous-time model has a simpler structure in its solution. There are two key differences between the solutions of the discrete-time and continuous-time models. The first one is that the solution of the discrete-time model suggests

that the battery level stays in the same region next period. If the suggested discharging/charging rate moves the battery level to a different region, the optimal solution is adjusted so that the battery level stays on the boundary between two regions. For example, in case (a) when net demand \tilde{D} is high, we charge the battery to meet the unmet demand. The minimum charging rate (without considering the maximum discharging rate) is $|y^F - \tilde{D}|$, which is the rate to meet the extra demand after exhausting all energy sources. However, the battery may be preferable than the flexible source if the marginal value of energy in the battery $|\partial\tilde{\phi}_t/\partial b|$ is low. In this case, we may use the battery first to meet all the net demand \tilde{D} . However, discharging the battery at rate \tilde{D} may bring down the energy level in the battery to the region where the flexible source is preferred. Therefore, to keep the energy level in the same region, we should discharge at rate either $|-(\tilde{D} \wedge [(b - \bar{b}_t))/\delta]|$ or the minimum discharging rate $|y^F - \tilde{D}|$, whichever is larger. Figure B.1 shows that the solution of the continuous-time model has a bang-bang structure while that of the discrete-time model smooths out the rate changes at the boundary. As the period length δ becomes smaller and smaller, the solution of the discrete-time model converges to that of the continuous-time model.

Figure B.1: Optimal solutions in the continuous-time and discrete-time models

(a) Optimal \hat{q}_B in continuous time model ($\tilde{D}_t \geq y^F$) (b) Optimal \hat{q}_B in discrete time model ($\tilde{D}_t \geq y^F$)



The second difference between the solutions of the discrete-time and continuous-time models is the behavior at the boundary. In the continuous-time model, we only impose constraints on the charging rate q_t^B when the battery level hits the boundary zero or B as shown in Theorem 1. The constraint requires that we never charge when the battery is full and never discharge when the battery is empty. However, the boundary constraint in the discrete-time model may affect the solution when the battery level is nearly full or empty. The boundary constraint is accounted in the definitions of the discharging and charging limits \underline{q}_t^B and \bar{q}_t^B . To be specific, the battery constraint starts to affect the optimal solution when $b_t < y_{\text{out}}^B \delta$ and $b_t > B - \alpha y_{\text{in}}^B \delta$. The maximum amount that is allowed to charge/discharge depends on current battery level.

C. Optimal Investments of the Special Case in Section 5.1

This appendix solves the special case under Assumption 1. Proposition C.1 provides explicit expressions for the optimal average operating cost by solving the HJB equation in Lemma 2 under given resources capacities (y^R, y^F, B) .

Proposition C.1. *Under Assumption 1, the average operating cost defined in (10) is given as follows:*

(i) If $B \leq \min(Q^{\text{CR}}, Q^{\text{DI}})$,

$$\bar{C}(y^R, y^F, B, c^F) = \frac{c^F Q^{\text{DF}} + \xi(Q^{\text{DI}} - B)}{t_0}.$$

(ii) If $Q^{\text{CR}} \leq Q^{\text{DI}}$ and $B \geq Q^{\text{CR}}$,

$$\bar{C}(y^R, y^F, B, c^F) = \begin{cases} \frac{c^F Q^{\text{DF}} + \xi(Q^{\text{DI}} - B) + c^F(B - Q^{\text{CR}})/\alpha}{t_0}, & \text{if } B \leq \min(Q^{\text{CR}} + Q^{\text{CF}}, Q^{\text{DI}}), \\ \frac{c^F Q^{\text{DF}} + \xi(Q^{\text{DI}} - Q^{\text{CR}} - Q^{\text{CF}})^+ + c^F(Q^{\text{CF}} \wedge (Q^{\text{DI}} - Q^{\text{CR}}))/\alpha}{t_0}, & \text{if } B \geq \min(Q^{\text{CR}} + Q^{\text{CF}}, Q^{\text{DI}}). \end{cases}$$

(iii) If $Q^{\text{DI}} \leq Q^{\text{CR}}$ and $B \geq Q^{\text{DI}}$,

$$\bar{C}(y^R, y^F, B, c^F) = \begin{cases} \frac{c^F Q^{\text{DF}} - c^F(B - Q^{\text{DI}})}{t_0}, & \text{if } B \leq \min(Q^{\text{CR}}, Q^{\text{DI}} + Q^{\text{DF}}), \\ \frac{c^F(Q^{\text{DI}} + Q^{\text{DF}} - Q^{\text{CR}})^+}{t_0}, & \text{if } B \geq \min(Q^{\text{CR}}, Q^{\text{DI}} + Q^{\text{DF}}). \end{cases}$$

In addition, if $\{c_m^F : m = 1, \dots, M\}$ has a stationary distribution represented by random variable C^F , the discounted operation cost defined in (11) is given by $C(y^R, y^F, B) = At_0 \mathbb{E}[\bar{C}(y^R, y^F, B, C^F)]$, where the expectation is taken on C^F and A is the constant given in Theorem 2.

Proof. We solve the optimal control problem for given capacities y^R, y^F and B . We seek to find the gain and the bias function for $t \in [s_4, t_0 + s_4)$. Without stochasticity, we can drop r and d in the state descriptor and let (t, b) denote the state of the system. Moreover, the HJB equation in (13) simplifies to the following: For $b \in (0, B)$ and $t \in [s_2, t_0 + s_2)$,

$$v - \frac{\partial \phi(t, b)}{\partial t} + H\left(t, b, \frac{\partial \phi(t, b)}{\partial b}\right) = 0 \text{ with } \frac{\partial \phi(t, 0)}{\partial b} = -\xi \text{ and } \frac{\partial \phi(t, B)}{\partial b} = 0, \quad (\text{C.1})$$

where

$$H(t, b, p) = - \inf_{q^F \in [0, y^F], q^B \in \mathbb{R}} \{\zeta(t, b, q^F, q^B) + pq^B\},$$

where $\zeta(t, b, q^F, q^B) = c^F q^F + \xi(\tilde{D}_t - q^F + \psi(q^B))^+$. By substituting the solution in Proposition 1 with $y_{\text{in}}^B = y_{\text{out}}^B = +\infty$, we obtain that: For $t \in [s_4, t_0 + s_1)$ where $\tilde{D}_t < 0$,

$$H(t, b, p) = \begin{cases} +\infty, & \text{if } p < -\frac{\xi}{\alpha}, \\ -c^F y^F - \alpha p(y^F - \tilde{D}_t), & \text{if } -\frac{\xi}{\alpha} \leq p \leq -\frac{c^F}{\alpha}, \\ \alpha p \tilde{D}_t, & \text{if } -\frac{c^F}{\alpha} \leq p \leq 0, \\ +\infty, & \text{if } p > 0, \end{cases} \quad (\text{C.2})$$

for $t \in [s_1, s_2) \cup [s_3, s_4)$ where $0 < \tilde{D}_t < y^F$,

$$H(t, b, p) = \begin{cases} +\infty, & \text{if } p < -\xi, \\ -c^F y^F - \alpha p(y^F - \tilde{D}_t), & \text{if } -\xi \leq p \leq -\frac{c^F}{\alpha}, \\ -c^F \tilde{D}_t, & \text{if } -\frac{c^F}{\alpha} \leq p \leq -c^F, \\ p \tilde{D}_t, & \text{if } -c^F \leq p \leq 0, \\ +\infty, & \text{if } p > 0, \end{cases} \quad (\text{C.3})$$

and for $t \in [s_2, s_3)$ where $\tilde{D}_t \geq y^F$,

$$H(t, b, p) = \begin{cases} +\infty, & \text{if } p < -\xi, \\ -c^F y^F - p(y^F - \tilde{D}_t), & \text{if } -\xi \leq p \leq -c^F, \\ p \tilde{D}_t, & \text{if } -c^F \leq p \leq 0, \\ +\infty, & \text{if } p > 0. \end{cases} \quad (\text{C.4})$$

If there is a function $\phi(t, b) \in C^1([s_2, t_0 + s_2) \times [0, B])$ and a constant $v \geq 0$ satisfying equation (C.1), then we have $\bar{C}(0, y^R, B, c^R) = v$ where $C^1(\cdot)$ is the space of continuously differentiable functions. Unfortunately, this problem does not have a classical solution, i.e., a solution that is continuously differentiable functions. In what follows, we will prove by construction. Note that the bias function is piece-wise differentiable. When the bias function is differentiable, it has to satisfy condition (C.1). Thus, we construct a parameterized function that is continuous and piece-wise differentiable, and satisfies condition (C.1). Then, we use the the continuity conditions to find the parameters for different scenarios. Lastly, we verify from the first principle that the constructed function is actually the bias function and the resulting charging/discharging policy is optimal.

In what follows, we first construct a function $\phi(t, b)$ that satisfies (C.1) at differentiable points. To facilitate the analysis to follow, the define the following functions:

$$\begin{aligned} y_1(t, \tau) &= \left(\xi - \frac{c^F}{\alpha} \right) \alpha y^F(t - \tau) + \xi \int_t^\tau \alpha \tilde{D}_s ds, \\ y_2(t, \tau) &= c^F \int_t^\tau \tilde{D}_s ds, \\ y_3(t, \tau) &= (\xi - c^F) y^F(t - \tau) + \xi \int_t^\tau \tilde{D}_s ds, \\ z_1(t, \tau) &= - \int_t^\tau (y^F - \tilde{D}_s) ds, \\ z_2(t, \tau) &= \int_t^\tau \tilde{D}_s ds. \end{aligned}$$

Also, we summarize the important properties of functions z_1 and z_2 as follows: (z-property)

- (i) For $t \in [s_4, t_0 + s_1)$ and $\tau = t_0 + s_1$, $z_1(t, \tau)$, $z_2(t, \tau)$ and $z_1(t, \tau) - z_2(t, \tau)$ increase in t .
- (ii) For $t \in [t_0 + s_1, t_0 + s_2)$ and $\tau = t_0 + s_2$, $z_1(t, \tau)$ increases in t while $z_2(t, \tau)$ decrease in t .
- (iii) For $t \in [t_0 + s_2, t_0 + s_3)$ and $\tau = t_0 + s_3$, $z_1(t, \tau)$, $z_2(t, \tau)$ and $z_2(t, \tau) - z_1(t, \tau)$ decrease in t .
- (iv) For $t \in [t_0 + s_3, t_0 + s_4)$ and $\tau = t_0 + s_4$, $z_1(t, \tau)$ increases in t while $z_2(t, \tau)$ decrease in t .

Now we define a parameterized function $\phi(t, b)$ for $t \geq 0$ and $b \in [0, B]$. The function ϕ is divided into four cases. Within one case, ϕ is differentiable. The boundaries of the four cases are the non-differentiable. We also define the charging/discharging policies, denoted by π_* , for each cases. For $t \in [s_4, t_0 + s_1)$ and

$a_1 \leq a_2 \leq a_3 \leq B$, let

$$\phi(t, b) = vt + \begin{cases} A_1 - \xi b + y_1(t, t_0 + s_1), & \text{if } b \leq a_1 + \alpha z_1(t, t_0 + s_1), \\ A_2 - \frac{c^F}{\alpha} b + y_2(t, t_0 + s_1), & \text{if } a_1 + \alpha z_1(t, t_0 + s_1) < b \leq a_2 + \alpha z_2(t, t_0 + s_1), \\ c^F a_3 - c^F b + \alpha y_2(t, t_0 + s_1), & \text{if } a_2 + \alpha z_2(t, t_0 + s_1) < b \leq a_3 + \alpha z_2(t, t_0 + s_1), \\ 0, & \text{if } b > a_3 + \alpha z_2(t, t_0 + s_1), \end{cases} \quad (\text{C.5})$$

where $A_1 = \left(\xi - \frac{c^F}{\alpha}\right) a_1 + \left(\frac{c^F}{\alpha} - c^F\right) a_2 + c^F a_3$ and $A_2 = \left(\frac{c^F}{\alpha} - c^F\right) a_2 + c^F a_3$. The first case is the CF+CR region, where the second and cases are the CR region. The last case is when the stored energy is too much and has a margin of zero. There is no charging in this region. For $t \in [t_0 + s_1, t_0 + s_2)$ and constants such that $b_1 \leq b_2 \leq b_3$ and $b_1 \leq B$ and $b_3 \geq 0$, let

$$\phi(t, b) = vt + \begin{cases} B_1 - \xi b + y_1(t, t_0 + s_2), & \text{if } b \leq b_1 + \alpha z_1(t, t_0 + s_2), \\ B_2 - \frac{c^F}{\alpha} b + y_2(t, t_0 + s_2), & \text{if } b_1 + \alpha z_1(t, t_0 + s_2) \leq b \leq b_2, \\ c^F b_3 + b_4 - c^F b + y_2(t, t_0 + s_2), & \text{if } b_2 < b \leq b_3 + z_2(t, t_0 + s_2), \\ b_4, & \text{if } b \geq b_3 + z_2(t, t_0 + s_2), \end{cases} \quad (\text{C.6})$$

where $B_1 = \left(\xi - \frac{c^F}{\alpha}\right) b_1 + \left(\frac{c^F}{\alpha} - c^F\right) b_2 + c^F b_3 + b_4$ and $B_2 = \left(\frac{c^F}{\alpha} - c^F\right) b_2 + c^F b_3 + b_4$. The first three cases are the CF, no charging/discharging, and DF regions, respectively. The last regions are also DF regions. For $t \in [t_0 + s_2, t_0 + s_3)$ and constants such that $0 \leq c_1 \leq c_2 \leq c_3$, let

$$\phi(t, b) = vt + \begin{cases} C_1 - \xi b + y_3(t, t_0 + s_3), & \text{if } b \leq c_1 + z_1(t, t_0 + s_1), \\ C_2 - \frac{c^F}{\alpha} b + y_3(t, t_0 + s_3), & \text{if } c_1 + z_1(t, t_0 + s_1) < b \leq c_2 + z_1(t, t_0 + s_1), \\ c^F c_3 + c_4 - c^F b + y_2(t, t_0 + s_3), & \text{if } c_2 + z_1(t, t_0 + s_1) < b \leq c_3 + z_2(t, t_0 + s_3), \\ c_4, & \text{if } b > c_3 + z_2(t, t_0 + s_3), \end{cases} \quad (\text{C.7})$$

where $C_1 = \left(\xi - \frac{c^F}{\alpha}\right) c_1 + \left(\frac{c^F}{\alpha} - c^F\right) c_2 + c^F c_3 + c_4$ and $C_2 = \left(\frac{c^F}{\alpha} - c^F\right) c_2 + c^F c_3 + c_4$. The first two cases are the DI regions, where the third cases and fourth cases are the DI+DF region. For $t \in [t_0 + s_3, t_0 + s_4)$ and constants such that $d_1 \leq d_2 \leq d_3$ and $d_1 \leq B$, $d_3 \geq 0$, let

$$\phi(t, b) = vt + \begin{cases} D_1 - \xi b + y_1(t, t_0 + s_4), & \text{if } b \leq d_1 + \alpha z_1(t, t_0 + s_4), \\ D_2 - \frac{c^F}{\alpha} b + y_2(t, t_0 + s_r), & \text{if } d_1 + \alpha z_1(t, t_0 + s_4) < b \leq d_2, \\ c^F d_3 + d_4 - c^F b + y_2(t, t_0 + s_4), & \text{if } d_2 \leq b \leq b_3 + z_2(t, t_0 + s_4), \\ d_4, & \text{if } b > d_3 + z_2(t, t_0 + s_4), \end{cases} \quad (\text{C.8})$$

where $D_1 = \left(\xi - \frac{c^F}{\alpha}\right) d_1 + \left(\frac{c^F}{\alpha} - c^F\right) d_2 + c^F d_3 + d_4$ and $D_2 = \left(\frac{c^F}{\alpha} - c^F\right) d_2 + c^F d_3 + d_4$. The charging/discharging policy is the same as the one in $[t_0 + s_1, t_0 + s_2)$.

Note that the function ϕ has four cases for different values of b . The continuity conditions simply require that the boundaries of the four cases match at $t = s_4, t_0 + s_1, t_0 + s_2, t_0 + s_3$ if the boundaries are in $[0, B]$. Moreover, by the z-properties, the boundaries of are well-defined, i.e., the boundaries never cross. Since $\frac{\partial y_2}{\partial t} = \frac{\alpha \partial y_2}{\partial t}$ for $t = t_0 + s_1$ and $t = t_0 + s_4$ and $\frac{\partial y_2}{\partial t} = \frac{\partial y_3}{\partial t}$ for $t = t_0 + s_2$ and $t = t_0 + s_3$, $\phi(t, b)$ is differentiable for $t = s_1, s_2, s_3, s_4$ if b is not on the boundaries. The last observation is that once the trajectory of b hits one of the boundaries. The trajectory of b will move along the boundaries under policy π_* .

Next, we find suitable parameters and $v \geq 0$ such that $\phi(t, b)$ is continuous for $b \in [0, B]$. We want to note that the choice of the parameters may not be unique. Note that ϕ is a periodic function, so we require that

$\phi(s_4, b) = \phi(t_0 + s_4, b)$ for all $b \in [0, B]$. In addition, we define the following constants:

$$Q_1^{\text{CF}} = \int_{s_1}^{s_2} \alpha(y^F - \tilde{D}_t) dt, \quad Q_2^{\text{CF}} = \int_{s_3}^{s_4} \alpha(y^F - \tilde{D}_t) dt, \quad Q_3^{\text{CF}} = \alpha y^F(t_0 + s_1 - s_4),$$

and

$$Q_1^{\text{DF}} = \int_{s_1}^{s_2} \tilde{D}_t dt, \quad Q_2^{\text{DF}} = \int_{s_3}^{s_4} \tilde{D}_t dt, \quad Q_3^{\text{DF}} = y^F(s_3 - s_2).$$

The parameters are given as follow:

1. $B \leq \min(Q^{\text{CR}}, Q^{\text{DI}})$. $a_1 = B - Q_1^{\text{CF}}$, $a_2 = a_3 = B$, $b_1 = b_2 = b_3 = B$, $c_1 = c_2 = 0$, $c_3 = Q_2^{\text{DF}}$, $d_2 = d_3 = 0$, and $d_1 = B - Q^{\text{CR}} - Q_1^{\text{CF}} - Q_3^{\text{CF}}$. Moreover, we have that $b_4 = c^F Q_1^{\text{DF}}$ and $c_4 = d_4 = c^F Q^{\text{DF}} + \xi(Q^{\text{DI}} - B)$. By the continuity at s_4 , we have that $v = [c^F Q^{\text{DF}} + \xi(Q^{\text{DI}} - B)]/t_0$.
2. $Q^{\text{CR}} \leq Q^{\text{DI}}$ and $B \geq Q^{\text{CR}}$. In this case, we have $a_2 = a_3 = B$, $b_2 = b_3 = B$, $c_2 = B - Q^{\text{CR}}$, $c_3 = B - Q^{\text{CR}} + Q_2^{\text{DF}}$, and $d_2 = d_3 = B - Q^{\text{CR}}$. There are a few sub-cases.
 - (a) $Q^{\text{CR}} \leq B \leq \min(Q^{\text{CR}} + Q^{\text{CF}}, Q^{\text{DI}})$. We have $a_1 = B - Q_1^{\text{CF}}$, $b_1 = B$, $c_1 = 0$, $d_1 = B - Q^{\text{CR}} - Q_1^{\text{CF}} - Q_3^{\text{CF}}$. Moreover, we have $v = (c^F Q^{\text{DF}} + \xi(Q^{\text{DI}} - B) + c^F(B - Q^{\text{CR}})/\alpha)/t_0$.
 - (b) $Q^{\text{DI}} \leq Q^{\text{CR}} + Q^{\text{CF}}$ and $B \geq Q^{\text{DI}}$. We have $a_1 = Q^{\text{DI}} - Q_1^{\text{CF}}$, $b_1 = Q^{\text{DI}}$, $c_1 = 0$, $d_1 = Q^{\text{DI}} - Q^{\text{CR}} - Q_1^{\text{CF}} - Q_3^{\text{CF}}$. Moreover, we have $v = (c^F Q^{\text{DF}} + c^F(Q^{\text{DI}} - Q^{\text{CR}})/\alpha)/t_0$.
 - (c) $Q^{\text{CR}} + Q^{\text{CF}} \leq Q^{\text{DI}}$ and $B \geq Q^{\text{CR}} + Q^{\text{CF}}$. We have $a_1 = B - Q_1^{\text{CF}}$, $b_1 = B$, $c_1 = B - Q^{\text{CR}} - Q^{\text{CF}}$, $d_1 = B - Q^{\text{CR}} - Q_1^{\text{CF}} - Q_3^{\text{CF}}$ and $v = (c^F Q^{\text{DF}} + \xi(Q^{\text{DI}} - Q^{\text{CR}} - Q^{\text{CF}}) + c^F Q^{\text{CF}}/\alpha)/t_0$.
3. $Q^{\text{DI}} \leq Q^{\text{CR}}$ and $B \geq Q^{\text{DI}}$. In this case, we have $a_1 = Q^{\text{DI}} - Q_1^{\text{DF}}$, $a_2 = Q^{\text{DI}}$, $b_1 = b_2 = Q^{\text{DI}}$, $c_1 = c_2 = 0$, $d_1 = d_2 = 0$. There are three sub-cases:
 - (a) $Q^{\text{DI}} \leq B \leq \min(Q^{\text{CR}}, Q^{\text{DI}} + Q^{\text{DF}})$. $a_3 = B$, $b_3 = Q^{\text{DI}} + Q_2^{\text{DF}} + Q_3^{\text{DF}}$, $c_3 = Q_2^{\text{DF}}$ and $d_3 = 0$. We have $v = (c^F Q^{\text{DF}} - c^F(B - Q^{\text{DI}}))/t_0$.
 - (b) $Q^{\text{CR}} \leq Q^{\text{DI}} + Q^{\text{DF}}$ and $B \geq Q^{\text{CR}}$. We have $a_3 = B$, $b_3 = B - Q^{\text{CR}} + Q^{\text{DI}} + Q_2^{\text{DF}} + Q_3^{\text{DF}}$, $c_3 = B - Q^{\text{CR}} + Q_2^{\text{DF}}$, and $d_3 = B - Q^{\text{CR}}$. We also have $v = c^F(Q^{\text{DI}} + Q^{\text{DF}} - Q^{\text{CR}})/t_0$.
 - (c) $Q^{\text{DI}} + Q^{\text{DF}} \leq Q^{\text{CR}}$ and $B \geq Q^{\text{DI}} + Q^{\text{DF}}$. We have $a_3 = Q^{\text{DF}} + Q^{\text{DI}}$, $b_3 = Q^{\text{DI}} + Q_2^{\text{DF}} + Q_3^{\text{DF}}$, $c_3 = Q_2^{\text{DF}}$ and $d_3 = 0$. We also have $b_4 = c_4 = d_4 = v = 0$.

Lastly, we verify that the constructed function $\phi(t, b)$ and the constant v are actually the bias function and the gain. First, we use b_t^* to denote the trajectory under the policy $\pi_* = (q_*^F(t, b), q_*^B(t, b))$. The following always hold: for $t \geq t_0$ and $b_{t_0}^* = b_0$,

$$\phi(t_0, b_0) - \phi(t, b_t^*) = -v(t - t_0) + \int_{t_0}^t \zeta(t, b_s^*, q_*^F(s, b_s^*), q_*^B(s, b_s^*)) ds.$$

When b_t^* is not moving along any of the non-differentiable boundaries of the function ϕ , this follows immediately from condition C.1. By comparing both sides of the equation, we note that this also holds if the trajectory b_t^* is moving along one of the non-differentiable boundaries. Suppose there is a policy $\tilde{\pi} = (\tilde{q}^F(t, b), \tilde{q}^B(t, b))$. The trajectory under policy $\tilde{\pi}$ is \tilde{b}_t with $\tilde{b}_{t_0} = b_0$. For $t \geq t_0$, define a function $\tilde{M}(t)$

$$\tilde{M}(t) = \int_{t_0}^t \zeta(s, \tilde{b}_s, \tilde{q}^F(s, \tilde{b}_s), \tilde{q}^B(s, \tilde{b}_s)) ds + \phi(t, \tilde{b}_t) - v(t - t_0).$$

We first consider the case when \tilde{b}_s does not move along the non-differentiable boundaries in $[t_0, t]$. This $M'(t)$ exists for only finite points. It follows from (C.1) that for $s \in [0, t_0]$ and $M'(s)$ exists,

$$M'(s) = \zeta(s, \tilde{b}_s, \tilde{q}^F(t, \tilde{b}_t), \tilde{q}^B(t, \tilde{b}_t)) + \frac{\partial \phi(t, \tilde{b}_t)}{\partial t} + \frac{\partial \phi(s, \tilde{b}_s)}{\partial b} \tilde{q}^B(s, \tilde{b}_s) \geq 0.$$

Thus, we have that $M(t) = \int_0^t M'(s) ds + M(t_0) \geq M(t_0)$. Now we consider the case when \tilde{b}_s moves along one of the non-differentiable boundaries of function ϕ in $[t_0, t]$. In this case, the policy $\tilde{\pi}$ follows π_* in $[t_0, t]$. Thus, it follows from equation (C) that

$$\begin{aligned} M(t) &= \int_{t_0}^t \zeta(t, b_s^*, q_*^F(s, b_s^*), q_*^B(s, b_s^*) ds + \phi(t, b_t^*) - v(t - t_0) \\ &= \phi(t_0, b_0) - \phi(t, b_t^*) + \phi(t, b_t^*) = \phi(t_0, b_0) = M(t_0). \end{aligned}$$

The trajectory of \tilde{b}_s for general cases can be divided into several periods. Each of the periods can fall into one of the two cases discussed aforementioned. Thus, we have that $M(t) \geq M(t_0)$. Since ϕ is bounded, we let t goes to infinity and have the following:

$$\lim_{t \rightarrow \infty} \frac{M(t)}{t - t_0} = \lim_{t \rightarrow \infty} \frac{\int_{t_0}^t \zeta(s, \tilde{b}_s, \tilde{q}^F(s, \tilde{b}_s), \tilde{q}^B(s, \tilde{b}_s))}{t - t_0} - v \geq 0.$$

Thus, we have shown that the average cost under a given policy $\tilde{\pi}$ is greater than v . And all inequalities become equations under policy π_* . Letting $\bar{C}(y^R, y^F, B, c^F) = v$ completes the proof. The value of $C(y^R, y^F, B)$ follows from equation (11). \square

Proof of Theorem 2: Using the closed-form expressions for the optimal operating cost in Proposition C.1, we can find the marginal benefit of the battery capacity (in terms of the marginal reduction of the discounted cost) as follows:

1. If $Q^{\text{CR}} \leq Q^{\text{DI}}$,

$$-\frac{\partial C(y^R, y^F, B)}{\partial B} = \begin{cases} A\xi, & \text{if } 0 \leq B \leq Q^{\text{CR}}, \\ A\left(\xi - \frac{\mathbb{E}[C^F]}{\alpha}\right), & \text{if } Q^{\text{CR}} < B \leq \min(Q^{\text{CR}} + Q^{\text{CF}}, Q^{\text{DI}}), \\ 0, & \text{if } B > \min(Q^{\text{CR}} + Q^{\text{CF}}, Q^{\text{DI}}). \end{cases}$$

2. If $Q^{\text{CR}} > Q^{\text{DI}}$,

$$-\frac{\partial C(y^R, y^F, B)}{\partial B} = \begin{cases} A\xi, & \text{if } 0 \leq B \leq Q^{\text{DI}}, \\ A\mathbb{E}[C^F], & \text{if } Q^{\text{DI}} < B \leq \min(Q^{\text{CR}}, Q^{\text{DI}} + Q^{\text{DF}}), \\ 0, & \text{if } B > \min(Q^{\text{CR}}, Q^{\text{DI}} + Q^{\text{DF}}). \end{cases}$$

Then, the optimal investment in Theorem 2 follows immediately. \square

D. Data and Estimated Model Parameters for Numerical Analysis

Figure D.1: Florida Power & Light solar project sites

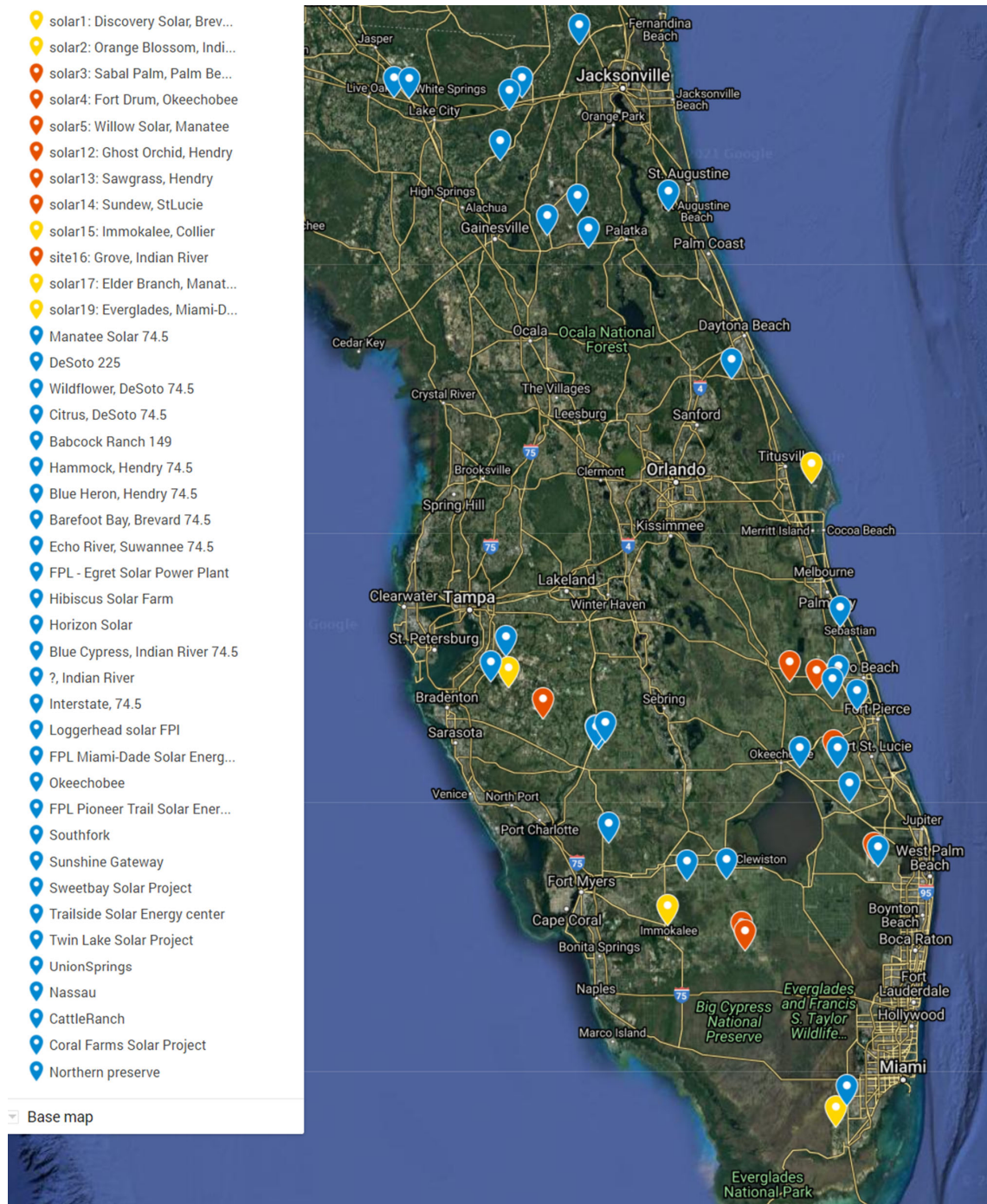


Table D.1: Summary statistics

	Monthly natural gas price (\$/MBtu)		Hourly demand (MWh)		Solar capacity factor under clear sky		Solar capacity factor on the ground	
	summer	winter	summer	winter	summer	winter	summer	winter
Mean	4.099	4.126	17381.9	12129.0	0.3202	0.2774	0.2414	0.1936
Std.dev.	2.205	1.850	3905.5	2434.1	0.3802	0.3535	0.2918	0.2526
q1	2.798	2.805	13740	9968.5	0	0	0	0
q2 (median)	3.405	3.580	17366	12340	0.0690	0.0265	0.0499	0.0114
q3	4.576	5.208	20686	13701	0.6888	0.6026	0.5075	0.4112
No. of obs.	90	90	2915	2184	2208	1440	2208	1440

Inflexible output from nuclear and coal is 4113 MW.

Table D.2: Estimated distribution of the natural gas price

Summer: \$4.099/MBtu on average

Price (\$/MBtu)	1.912	2.537	2.815	2.955	3.374	3.946	4.394	5.865	9.091
probability	1/9	1/9	1/9	1/9	1/9	1/9	1/9	1/9	1/9

Winter: \$4.126/MBtu on average

Price (\$/MBtu)	2.013	2.531	2.844	3.208	3.564	3.974	4.731	6.383	7.890
probability	1/9	1/9	1/9	1/9	1/9	1/9	1/9	1/9	1/9

Table D.3: Estimates for the solar output model

Solar output model: $R_t = \bar{R}_t \frac{e^{r_t}}{1 + e^{r_t}}$. Summer parameters are estimated using data from June to August 2020; winter parameters are estimated using data from January to February 2020. \bar{R}_t is the clear-sky capacity factor averaged over the same hour of day for each season.

		Summer (day light saving time)	Winter
Clear-sky capacity factor \bar{R}_t	0	0	0
	1	0	0
	2	0	0
	3	0	0
	4	0.00077	0
	5	0.00935	0.00015
	6	0.03865	0.06313
	7	0.15537	0.25906
	8	0.38106	0.48837
	9	0.60729	0.69485
	10	0.79765	0.84658
	11	0.93243	0.92931
	12	1.00000	0.93293
	13	0.99368	0.85722
	14	0.91414	0.71219
	15	0.76996	0.51123
	16	0.57327	0.28340
	17	0.34483	0.07942
	18	0.12692	0.00003
	19	0.03250	0
	20	0.00693	0
	21	0.00044	0
	22	0	0
	23	0	0
	Average	0.32022	0.27741
Random component $r_t = \bar{r} + e_t$, $e_{t+1} = \rho e_t + \varepsilon_t$	mean \bar{r}	1.10001	0.77348
	Autoregressive coef. ρ	0.82548	0.87455
	Std.dev. of error ε_t	0.69563	0.35432

Table D.4: Estimates for the demand model

Demand model: $\log D_t = \bar{D}_t + d_t$. We use the hourly FPL's demand data from June to September 2020 to estimate the parameters in summer and use the data from December 2019 to February 2020 to estimate the parameters in winter.

		Summer	Winter
Deterministic component \bar{D}_t is the sum of day-of-week and hour-of-day components	Day of week		
	Sun	9.62545	9.21082
	Mon	9.65529	9.27153
	Tue	9.66051	9.28676
	Wed	9.64463	9.29618
	Thu	9.65578	9.28125
	Fri	9.67026	9.25610
	Sat	9.63573	9.21338
	Hour of day		
	0	0	0
	1	-0.06798	-0.07010
	2	-0.13552	-0.13290
	3	-0.18580	-0.16953
	4	-0.21995	-0.18510
	5	-0.23346	-0.17234
	6	-0.21783	-0.10852
	7	-0.18653	-0.00565
	8	-0.14153	0.06945
	9	-0.03918	0.14367
	10	0.07291	0.20422
	11	0.16952	0.24397
	12	0.24719	0.26527
	13	0.30334	0.28300
	14	0.33901	0.29260
15	0.35554	0.29567	
16	0.35767	0.29507	
17	0.34984	0.28933	
18	0.33162	0.29464	
19	0.29642	0.32099	
20	0.24962	0.29349	
21	0.21864	0.24262	
22	0.16413	0.17341	
23	0.09141	0.09651	
Random component $d_{t+1} = \rho d_t + \varepsilon_t$	Autoregressive coef. ρ	0.92628	0.91423
	Std.dev. of error ε_t	0.03061	0.03900

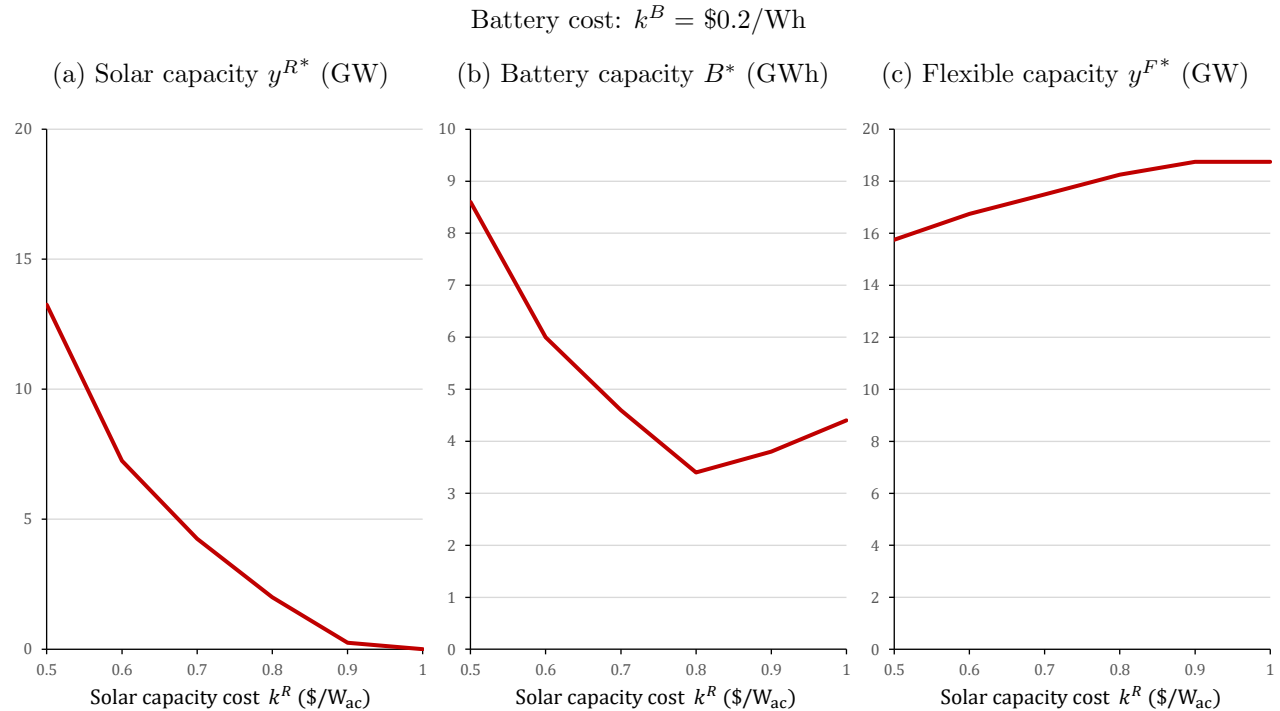
E. Additional Numerical Analysis on Investment Relations

In this section, we run the same portfolio optimization as in Figure 7 under different cost parameters: the natural gas prices are half of the values reported in Table D.2 and the investment cost for flexible capacity k^F is increased from \$1.17/W (in the paper) to \$1.287/W.

The optimal investment portfolios are illustrated in Figure E.1. When the cost of solar capacity is above (resp. below) \$0.8/W_{ac}, we observe a distinct substitution (resp. complementary) effect between solar and battery capacities. This substitution effect is more pronounced than what is observed in Figure 7 of the paper.

The reasons for the stronger substitution are twofold. First, the lower price of natural gas enhances the cost-effectiveness of flexible generation, leading to a reduction in the optimal renewable capacity compared to Figure 7. This decrease in renewable capacity weakens the complementary effect between renewable and battery, facilitating a more noticeable substitution effect, where renewables and battery compete to meet peak demand. Second, although battery and solar capacities can jointly displace flexible capacity (the second complementary effect discussed in the paper), the lower natural gas price coupled with a slightly increased cost for flexible capacity renders it more difficult to displace flexible capacity. Therefore, in this setting, the complementary effect is weakened, resulting in a more evident substitution effect between renewable and battery capacities when $k^R > \$0.8/W_{ac}$ in Figure E.1.

Figure E.1: Optimal capacity investment



F. Proofs

Proof of Lemma 1: We will prove the following two statements:

- (i) The average cost $\bar{C}(y^R, y^F, B, c^F)$ in (10) can be determined by the following problem with a modified objective and without constraint (9):

$$\bar{C}(y^R, y^F, B, c^F) = \inf_{\pi} \lim_{s \rightarrow \infty} \frac{1}{s} \mathbb{E} \left[\int_0^s (c^F q_t^F + \xi \Delta_t^+) dt \right], \quad (\text{F.1})$$

s.t. (2)-(8).

- (ii) There exists an optimal control for (F.1) such that renewable energy is fully used: $q_t^R = y^R R_t$.

These two statements essentially transform the original problem of simultaneously deciding three controls in (10) into a simpler auxiliary problem in (F.1), in which we do not lose optimality by setting $q_t^R = y^R R_t$. Then, replacing q_t^R in (F.1) by the full potential renewable output $y^R R_t$ leads to the problem in (12).

To show (i), note that any feasible policy of problem (10) is also feasible for problem (F.1). Moreover, since $\Delta_t \geq 0$ under any feasible policy of problem (10), the objectives in (10) and (F.1) are the same under any feasible policy of problem (10). Therefore, the cost under the optimal policy of (F.1) is no higher than that in (10) because (F.1) allows for a larger set of feasible policies. To show that the two problems yield the same optimal cost, it suffices to show that for any optimal policy of (F.1), we can construct a feasible policy for (10) that yields the same cost as in (F.1).

Let $\{(q_t^{R*}, q_t^{F*}, q_t^{B*}) : t \geq 0\}$ be an optimal policy for (F.1). We define $\pi = \{(q_t^R, q_t^F, q_t^B) : t \geq 0\}$ such that $q_t^R = \min\{q_t^{R*}, D_t - q_t^{F*} + \psi(q_t^{B*})\}$, $q_t^F = q_t^{F*}$, and $q_t^B = q_t^{B*}$.

First we need to show that π is feasible for (10). Note that the construction ensures $\Delta_t \geq 0$ under policy π for all t . Thus, if $q_t^R = \min\{q_t^{R*}, D_t - q_t^{F*} + \psi(q_t^{B*})\} \geq 0$ for all t , then π is feasible for (10). We show this by contradiction. Suppose $D_t - q_t^{F*} + \psi(q_t^{B*}) < 0$ for $t \in [t_1, t_2]$. We will show that we can construct a new policy $\tilde{\pi}$ with a lower cost in (F.1), which contradicts to the optimality of $(q_t^{R*}, q_t^{F*}, q_t^{B*})$ in (F.1). We use “ \sim ” to denote all the decisions and the associated storage state under the new policy $\tilde{\pi}$. In addition, let $\Delta_t^* = (D_t - q_t^{R*} - q_t^{F*} + \psi(q_t^{B*}))^+$. Since we assume $D_t - q_t^{F*} + \psi(q_t^{B*}) < 0$, we have $\Delta_t^* = 0$ for $t \in [t_1, t_2]$. We discuss two scenarios.

Scenario 1. If there exists an interval $[t_3, t_4] \subseteq [t_1, t_2]$ such that $q_t^{F*} > 0$ in $[t_3, t_4]$. Then let $\tilde{q}_t^R = q_t^{R*}$, $\tilde{q}_t^B = q_t^{B*}$ for all t , and let $\tilde{q}_t^F = (D_t + \psi(q_t^{B*}))^+$ for $t \in [t_1, t_2]$ and $\tilde{q}_t^F = q_t^{F*}$ for other t . The system has the same dynamics under policy $(q_t^{R*}, q_t^{F*}, q_t^{B*})$ and policy $\tilde{\pi}$. Since $\tilde{q}_t^F \leq q_t^{F*}$ for all t , the system incurs a (weakly) lower cost under policy $\tilde{\pi}$.

Scenario 2. If there exists no such interval $[t_3, t_4]$, then $q_t^{F*} = 0$ for almost all $t \in [t_1, t_2]$. Thus it follows from $D_t - q_t^{F*} + \psi(q_t^{B*}) < 0$ and $D_t \geq 0$ that $q_t^{B*} < -D_t \leq 0$ for $t \in [t_1, t_2]$. Let $d > 0$ be a small amount. Define the time t' as follows:

$$t' = \sup \left\{ t \in [t_1, t_2] : \int_{t'}^{t_2} D_s ds \geq d \right\}.$$

Let $\tilde{q}_t^F = q_t^{F*}$ and $\tilde{q}_t^R = q_t^{R*}$ for all $t \leq t_2$. Let $\tilde{q}_t^B = q_t^{B*}$ for $t \leq t'$ and $\tilde{q}_t^B = q_t^{B*} + D_s \in [-y_{\text{out}}^B, 0]$ for $t \in [t', t_2]$. Under the new policy, the storage level at time t_2 is $\tilde{b}_{t_2} = b_{t_2} + d$. In addition, note that $\tilde{D}_t \leq 0$ and thus $\tilde{\Delta}_t^+ = (\Delta_t^*)^+$ for all $t \in [t_1, t_2]$. Next define t'' as follows:

$$t'' = \inf \left\{ t \geq t_2 : \int_{t_2}^t \min(q_s^{F*} + q_s^{R*}, y_{\text{out}}^B + q_s^{B*}) ds \geq d \right\}.$$

We construct a new policy $\tilde{\pi}$ for this case as follows. Let

$$\tilde{q}_t^B = \max(-y_{\text{out}}^B, q_t^{B*} - (q_t^{F*} + q_t^{R*})),$$

$\tilde{q}_t^F = (q_t^{F*} - \alpha(q_t^{B*} - \tilde{q}_t^B)/2)^+$ and $\tilde{q}_t^R = (q_t^{R*} - \alpha(q_t^{B*} - \tilde{q}_t^B)/2)^+$ for $t \in (t_2, t'')$. In addition, let $\tilde{q}_t^F = q_t^{F*}$, $\tilde{q}_t^R = q_t^{R*}$ and $\tilde{q}_t^B = q_t^{B*}$ for $t \geq t''$. Under the new policy, $\tilde{q}_t^F \leq q_t^{F*}$, $\tilde{\Delta}_t \leq \Delta_t^*$ for $t \in [t_2, t'']$. In addition, $\tilde{b}_{t''} - \tilde{b}_{t_2} = b_{t''} - b_{t_2} - d$, which implies $\tilde{b}_{t''} = b_{t''}$. In sum, under the policy $\tilde{\pi}$, the system dynamics and rate of cost incurred to the system are the same as those under the policy $(q_t^{R*}, q_t^{F*}, q_t^{B*})$ for $t \leq t'$ and $t \geq t''$. Note that $\tilde{q}_t^F \leq q_t^{F*}$ and $\tilde{\Delta}_t^+ \leq (\Delta_t^*)^+$ for $t \in [t', t'']$. Thus, the system yields a lower cost under the new policy $\tilde{\pi}$.

In both scenarios, if $D_t - q_t^{F*} + \psi(q_t^{B*}) < 0$ during interval $[t_1, t_2]$, we are able to construct a new policy $\tilde{\pi}$ which yields a lower cost in (F.1). This contradicts to the fact that $(q_t^{R*}, q_t^{F*}, q_t^{B*})$ is an optimal policy. Therefore, $D_t - q_t^{F*} + \psi(q_t^{B*}) \geq 0$ for all t , and π is feasible for (10).

Next, we show that the cost of (10) under π is the same as that of (F.1) under $(q_t^{R*}, q_t^{F*}, q_t^{B*})$. Since $q_t^F = q_t^{F*}$ and $q_t^B = q_t^{B*}$, the two systems have the same dynamics. We only need to show that the cost rates of the two systems are the same at any time t . It suffices to show that $\Delta_t = (\Delta_t^*)^+$. In other words, we want to show that

$$D_t - q_t^R - q_t^F + \psi(q_t^B) = \left(D_t - q_t^{R*} - q_t^{F*} + \psi(q_t^{B*}) \right)^+.$$

Note that if $D_t - q_t^R - q_t^F + \psi(q_t^B) > 0$, i.e., $q_t^{R*} \leq D_t - q_t^{F*} + \psi(q_t^{B*})$, then $q_t^R = q_t^{R*}$ and the above equation holds. Otherwise, both sides of the equation are zero. This completes the proof of statement (i).

To show (ii), we show that for any given policy π that solves (F.1), there exists a policy $\hat{\pi}$ with a (weakly) lower cost such that $\hat{q}_t^R = y^R R_t$. Let $\hat{q}_t^B = q_t^B$ and $\hat{q}_t^F = q_t^F$. Since the charging/discharging rate remains the same under the new policy, the system dynamics remain the same as that under the policy $\hat{\pi}$. Note that $\hat{\Delta}_t \leq \Delta_t$ and thus $\hat{\Delta}_t^+ \leq \Delta_t^+$ under the policy $\hat{\pi}$. Thus, the system yields a (weakly) lower cost under the new policy $\hat{\pi}$.

From statements (i) and (ii), we see that the average cost $\bar{C}(y^R, y^F, B, c^F)$ in (10) can be determined by the problem in (12).

To prove the last statement in the lemma, let $\{(y^R R_t, q_t^{F*}, q_t^{B*}) : t \geq 0\}$ be an optimal policy for (F.1), which implies that $\{(q_t^{F*}, q_t^{B*}) : t \geq 0\}$ is optimal for (12). Then, from the proof of (i) and (ii), we know that the optimal renewable energy use is $q_t^{R*} = \min\{y^R R_t, D_t - q_t^{F*} + \psi(q_t^{B*})\}$. Thus, to show that $q_t^{R*} = \min\{y^R R_t, D_t + \psi(q_t^{B*})\}$ is an equivalent expression, we only need to show that if $q_t^{F*} > 0$, then $y^R R_t \leq D_t - q_t^{F*} + \psi(q_t^{B*})$. We prove this by contraction. Suppose $q_t^{F*} > 0$ and $D_t - q_t^{F*} + \psi(q_t^{B*}) < y^R R_t$ for $t \in [t_1, t_2]$. Then, there exists $\hat{q}_t^F < q_t^{F*}$ such that $\hat{q}_t^F > 0$ and $D_t - \hat{q}_t^F + \psi(q_t^{B*}) < y^R R_t$ for $t \in [t_1, t_2]$. Then, if we modify the policy such that \hat{q}_t^F is used in place of q_t^{F*} for $t \in [t_1, t_2]$, the policy is still feasible for (F.1) and the system dynamics remain the same. However, the modified policy yields a strictly lower cost than $\{(y^R R_t, q_t^{F*}, q_t^{B*}) : t \geq 0\}$, which contradicts its optimality for (F.1). \square

Proof of Lemma 2: We consider the equivalent problem defined in Appendix A. It follows from Lemma A.1 that this formulation with reflecting boundaries is the same as the original problem to solve. Let us fix a policy $\tilde{\pi} = (\tilde{q}_t^F, \tilde{q}_t^B)$ and initial state (s, r, d, b) and define a function $M(s)$ (for $s \geq s$) as follows:

$$M(s') = \int_s^{s'} [c^F \tilde{q}_t^F + \xi(\tilde{D}_t - \tilde{q}_t^F + \psi(\tilde{q}_t^B))^+] dt + \xi I_{s'} + \phi(t_{s'}, b_{s'}, r_{s'}, d_{s'}) - v(s' - s),$$

where $t_{s'} = s - \lfloor \frac{s'}{t_0} \rfloor t_0$ and $\tilde{D}_t = f_d(\bar{D}_t, d_t) - y^R f_r(\bar{R}_t, r_t)$. Thus, $t_{s'} \in [0, t_0]$.

Then by Ito's lemma, we have the following:

$$\begin{aligned} dM(s') &= [c^F \tilde{q}_{s'}^F + \xi(\tilde{D}_{s'} - \tilde{q}_{s'}^F + \psi(\tilde{q}_{s'}^B))]^+ ds + \xi dI_{s'} \\ &+ \left[\frac{\partial \phi(t_{s'}, x_{s'})}{\partial t} + \tilde{q}_B^s \frac{\partial \phi(t_{s'}, x_{s'})}{\partial b} + \sum_{i=r,d} \mu_i(i) \frac{\partial \phi(t_{s'}, x_{s'})}{\partial i} + \frac{1}{2} \sum_{i=r,d} \sigma^2(i) \frac{\partial^2 \phi(t_{s'}, x_{s'})}{\partial i^2} \right] ds' - v ds' \\ &+ \frac{\partial \phi(t_{s'}, x_{s'})}{\partial b} dI_{s'} - \frac{\partial \phi(t_{s'}, x_{s'})}{\partial b} dU_{s'} + \sum_{i=r,d} \sigma(i) \frac{\partial \phi(t_{s'}, x_{s'})}{\partial i} dW_{i,s'}, \end{aligned}$$

where $x_{s'} = (r_{s'}, d_{s'}, b_{s'})$. It follows from (13) that

$$v \leq \zeta(\tilde{q}^F, \tilde{q}^B; t, x) + \frac{\partial \phi(t_{s'}, x_{s'})}{\partial t} + \sum_{i=r,d} \mu_i(i) \frac{\partial \phi(t_{s'}, x_{s'})}{\partial i} + \frac{1}{2} \sum_{i=r,d} \sigma^2(i) \frac{\partial^2 \phi(t_{s'}, x_{s'})}{\partial i^2}.$$

Thus, we have that

$$\begin{aligned} dM(s') &\geq \xi dI_{s'} + \frac{\partial \phi(t_{s'}, x_{s'})}{\partial b} dI_{s'} - \frac{\partial \phi(t_{s'}, x_{s'})}{\partial b} dU_{s'} + \sum_{i=r,d} \sigma(i) \frac{\partial \phi(t_{s'}, x_{s'})}{\partial i} dW_{i,s'} \\ &= \sum_{i=r,d} \sigma(i) \frac{\partial \phi(t_{s'}, x_{s'})}{\partial i} dW_{i,s'}, \end{aligned}$$

where the equation in the second line from the fact that $I_{s'}$ ($U_{s'}$) increases only when $b_{s'} = 0$ ($b_{s'} = B$) and (14). Thus $M(s)$ is a supermartingale. This implies that

$$\mathbb{E}[M(s')] \geq \mathbb{E}[M(s)] = \phi(s, b, r, d). \quad (\text{F.2})$$

Since ϕ is bounded, dividing this inequality by $s' - s$ and letting s' go to infinity give that

$$\begin{aligned} &\lim_{s' \rightarrow \infty} \frac{1}{s' - s} \mathbb{E}^\pi \left[\int_s^{s'} [c^F \tilde{q}_t^F + \xi(\tilde{D}_t - \tilde{q}_t^F + \psi(\tilde{q}_t^B))]^+ dt + \xi I_s + \phi(t_{s'}, b_t, r_t, d_t) \right] - v \\ &= \lim_{s' \rightarrow \infty} \frac{1}{s' - s} \mathbb{E}^\pi \left[\int_s^{s'} [c^F \tilde{q}_t^F + \xi(\tilde{D}_t - \tilde{q}_t^F + \psi(\tilde{q}_t^B))]^+ dt + \xi I_s \right] - v \geq 0. \end{aligned}$$

In other words, $v \leq \bar{C}(y^R, y^F, B, c^F)$.

Since \mathcal{U} is a compact set, there exists $\tilde{q}_t^{F*}(x)$ and $\tilde{q}_t^{B*}(x)$ that

$$\zeta(\tilde{q}_t^{F*}(x), \tilde{q}_t^{B*}(x), t, x) = \inf_{\{(q^F, q^B) \in \mathcal{U}\}} \zeta(q^F, q^B, t, x) \text{ for all } t, x.$$

Let $\tilde{\pi}^* = (\tilde{q}_t^{F*}(x), \tilde{q}_t^{B*}(x))$ for all t, x . Then all inequalities in the proof become equations. Thus, we have that $v = \bar{C}(y^R, y^F, B, c^F)$. \square

Next we state and prove two lemmas that facilitate the proof of Lemma 3.

Lemma F.1. *There exists an optimal policy π^* such that the following holds for any initial state:*

$$\mathbb{P}(\inf\{t \geq 0 : b_t = 0\} < \infty) = 1.$$

Proof. This can be proved by contradiction. Suppose that

$$\mathbb{P}(\inf\{t \geq 0 : b_t = 0\} = \infty) > 0.$$

Then, there exists $\epsilon > 0$ such that

$$\mathbb{P}(\inf\{t \geq 0 : b_t \leq \epsilon\} = \infty) = c_0 > 0.$$

Now consider all sample paths that $b_t \geq \epsilon$ for all $t \geq 0$. Let q_t^F and q_t^B denote the optimal control decisions at time t under the optimal policy π^* . Then we construct a new policy $\hat{\pi} = (\hat{q}_t^F, \hat{q}_t^B)$ for this sample path.

Letting $\delta_t = (q_t^F \wedge (q_t^B + y_{\text{out}}^B))^+ \geq 0$, define $\hat{q}_t^F = q_t^F - \delta_t$ and $\hat{q}_t^B = q_t^B - \alpha\delta_t$. Then we see that

$$\begin{aligned} & c^F \hat{q}_t^F + \xi(f_d(\bar{D}_t, d_t) - y^R f_r(\bar{R}_t, r_t) - \hat{q}_t^F + \psi(\hat{q}_t^B))^+ \\ & \leq c^F \hat{q}_t^F + \xi(f_d(\bar{D}_t, d_t) - y^R f_r(\bar{R}_t, r_t) - q_t^F + \psi(q_t^B))^+ \\ & = c^F q_t^F - c^F \delta_t \xi(f_d(\bar{D}_t, d_t) - y^R f_r(\bar{R}_t, r_t) - q_t^F + \psi(q_t^B))^+. \end{aligned}$$

where the inequality follows from the fact that $-\hat{q}_t^F + \psi(\hat{q}_t^B) \geq q_t^F + \psi(q_t^B)$. We implement the until t' where

$$t' = \inf \left\{ t \geq 0 : \int_0^t \delta_s ds = \epsilon \right\}.$$

Then after t' , let $\hat{q}_t^F = q_t^F$ and $\hat{q}_t^B = q_t^B$. Note that the new policy satisfies the control constraints and the battery level is always greater than $\epsilon - \alpha\epsilon > 0$. Therefore, the policy $\hat{\pi}$ is an admissible policy. In addition, the total cost incurred under $\hat{\pi}$ reduces the cost under policy π^* by $c^F \int_0^{t'} \delta_s ds = c^F \epsilon$. Thus, in expectation, the expected cost under $\hat{\pi}$ is reduced by

$$c^F \epsilon \mathbb{P}(\inf\{t \geq 0 : b_t \leq \epsilon\} = \infty) = c^F \epsilon c_0 > 0.$$

This contradicts to the fact that π^* is optimal. \square

For the following lemma, for $s > t_0$, define $t_s \equiv \tau - \lfloor \frac{s}{t_0} \rfloor t_0$. Thus, $t_s \in [0, t_0)$.

Lemma F.2. *For any stopping time $\tau > s$ that $\tau < \infty$ a.s., the following holds: For $s \in [0, t_0)$,*

$$\phi(s, x) \leq \mathbb{E}_{(s,x)}^\pi \left[\int_s^\tau \left(c^F q_t^F + \xi(\tilde{D}_t - y^R R_t - q_t^F + \psi(q_t^B))^+ \right) dt - v(\tau - s) + \phi(t_\tau, x_\tau) \right], \quad (\text{F.3})$$

where $\tilde{D}_t = f_d(\bar{D}_t, d_t) - y^R f_r(\bar{R}_t, r_t)$. The inequality becomes an equation under the policy π^* .

Proof. We prove the lemma for any fixed time $s' > s$. Then the lemma holds for any stopping time τ that $\tau < \infty$ due to strong Markovian property.

It follows from equation (F.2) in the proof Lemma 2 that for $x = (r, d, b)$

$$\mathbb{E}_{(s,x)}^\pi \left[\int_s^{s'} \left(c^F q_t^F + \xi(\tilde{D}_t - y^R R_t - q_t^F + \psi(q_t^B))^+ \right) dt + \xi I_{s'} - v(s' - s) + \phi(t_{s'}, x_{s'}) \right] \geq \phi(s, x). \quad (\text{F.4})$$

Given any admissible policy π , it follows from Lemma A.1 that $I_{s'} = 0$. This completes the proof. \square

Proof of Lemma 3: We first fix (s, r, d) and prove that $\phi(s, b, r, d)$ is convex in b . Let $b^{(1)} > b^{(2)} \in [0, B]$. We want to show for any $a \in (0, 1)$,

$$\phi\left(s, x^{(3)}\right) \leq a\phi\left(s, x^{(1)}\right) + (1-a)\phi\left(s, x^{(2)}\right)$$

where $x^{(1)} = (b^{(1)}, r, d)$, $x^{(2)} = (b^{(2)}, r, d)$ and $x^{(3)} = (ab^{(1)} + (1-a)b^{(2)}, r, d)$.

We show the convexity by constructing a pathwise control policy π for the process starting with the state $(s, x^{(3)})$. Note that the randomness of the system only comes from the demand d_t and the renewable generation r_t (for $t \geq s$). In addition, the evolution of (t, r_t, d_t) is independent of the battery level. Now we fix a sample path (t, r_t, d_t) and consider three systems: The first two systems start at the battery levels $b^{(1)}$ and $b^{(2)}$ and are running under the optimal control policy π^* . Given the sample path and the control policy, the two systems are now deterministic. Let $(q_t^{F(i)} q_t^{B(i)})$ (for $i = 1, 2$) denote the optimal decisions at time t for systems 1 and 2, respectively. The third system starts at the battery level $b^{(3)} = ab^{(1)} + (1-a)b^{(2)}$ and

under the control $(q_t^{F(3)}, q_t^{B(3)})$, where

$$q_t^{F(3)} = a q_t^{F(1)} + (1-a) q_t^{F(2)} \quad \text{and} \quad q_t^{B(3)} = a q_t^{B(1)} + (1-a) q_t^{B(2)}.$$

This control is admissible (though history dependent) because it satisfies the control constraints, and it also satisfies the state constraint:

$$b_t^{(3)} = a b^{(1)} + (1-a) b^{(2)} + \int_s^t a q_s^{B(1)} + (1-a) q_s^{B(2)} ds = a b_t^{(1)} + (1-a) b_t^{(2)} \in [0, B]$$

Let τ be the first time that the first two systems evolves to the same state, i.e.

$$\tau = \inf\{t \geq s : b_t^{(1)} = b_t^{(2)}\}.$$

Note that τ is a stopping time. It follows from Lemma F.1 that $\tau < \infty$ almost surely. Otherwise, if the two systems never reaches to the same battery level, then $b_t^{(1)} > b_t^{(2)} \geq 0$ for all $t \geq s$. This contradicts to Lemma F.1. Note that the three systems are identical after time τ . In addition, the following holds:

$$\begin{aligned} & \int_s^\tau \left(c^F q_t^{F(3)} + \xi(D_t - y^R R_t - q_t^{F(3)} + \psi(q_t^{B(3)})) \right)^+ dt \\ & \leq a \int_s^\tau \left(c^F q_t^{F(1)} + \xi(D_t - y^R R_t - q_t^{F(1)} + \psi(q_t^{B(1)})) \right)^+ dt \\ & \quad + (1-a) \int_s^\tau \left(c^F q_t^{F(2)} + \xi(D_t - y^R R_t - q_t^{F(2)} + \psi(q_t^{B(2)})) \right)^+ dt. \end{aligned}$$

The inequality follows from the fact that $(D_t - y^R R_t - q_t^F + \psi(q_t^B))^+$ is convex in (q_t^F, q_t^B) , since $\psi(\cdot)$ and $(\cdot)^+$ are both convex. Let π denote the policy that follows the prescribed control during $[0, \tau]$ and then follows the optimal policy afterwards. The inequality holds if we take the expectation under policy π on the left-hand side and take the expectation under policy π^* on the right-hand side. That is,

$$\begin{aligned} & \mathbb{E}_{(s, x^{(3)})}^\pi \left[\int_s^\tau \left(c^F q_t^{F(3)} + \xi(D_t - y^R R_t - q_t^{F(3)} + \psi(q_t^{B(3)})) \right)^+ dt \right] \\ & \leq a \mathbb{E}_{(s, x^{(1)})}^\pi \left[\int_s^\tau \left(c^F q_t^{F(1)} + \xi(D_t - y^R R_t - q_t^{F(1)} + \psi(q_t^{B(1)})) \right)^+ dt \right] \\ & \quad + (1-a) \mathbb{E}_{(s, x^{(2)})}^\pi \left[\int_s^\tau \left(c^F q_t^{F(2)} + \xi(D_t - y^R R_t - q_t^{F(2)} + \psi(q_t^{B(2)})) \right)^+ dt \right]. \end{aligned} \tag{F.5}$$

Therefore, it follows from Lemma F.2 that

$$\begin{aligned} \phi(s, x^{(3)}) & \leq \mathbb{E}_{(s, x^{(3)})}^\pi \left[\int_s^\tau \left(c^F q_t^F + \xi(D_t - y^R R_t - q_t^F + \psi(q_t^B)) \right)^+ dt + \phi(t_\tau, x_\tau) \right] \\ & \leq a \mathbb{E}_{(s, x^{(1)})}^{\pi^*} \left[\int_s^\tau \left(c^F q_t^F + \xi(D_t - y^R R_t - q_t^F + \psi(q_t^B)) \right)^+ dt + \phi(\tau, x_\tau) \right] \\ & \quad + (1-a) \mathbb{E}_{(s, x^{(2)})}^{\pi^*} \left[\int_s^\tau \left(c^F q_t^F + \xi(D_t - y^R R_t - q_t^F + \psi(q_t^B)) \right)^+ dt + \phi(\tau, x_\tau) \right] \\ & = a \phi(s, x^{(1)}) + (1-a) \phi(s, x^{(2)}). \end{aligned}$$

The first and last inequalities follows from Lemma F.2. The second equality follows from (F.5).

Since $\phi(t, b, r, d)$ is convex in b , $\partial\phi(t, b, r, d)/\partial b$ is increasing in b . It follows from the boundary condition $\partial\phi(t, 0, r, d)/\partial b = -\xi$ and $\partial\phi(t, B, r, d)/\partial b = 0$ that $\partial\phi(t, b, r, d)/\partial b \in [-\xi, 0]$ for all states. Obviously, $\phi(t, b, r, d)$ is decreasing in b . \square

Proof of Proposition 1: The problem (15) can be solved by optimizing q^F for every given q^B and then

optimizing q^B . Specifically, we first solve

$$f(q^B) = \min_{q^F \in [0, y^F]} c^F q^F + \xi(\tilde{D} + \psi(q^B) - q^F)^+ \quad (\text{F.6})$$

and then solve

$$\min_{q^B \in [-y_{\text{out}}^B, \alpha y_{\text{in}}^B]} f(q^B) + \frac{\partial \phi}{\partial b} q^B, \quad (\text{F.7})$$

To solve (F.6), since $\xi > c^F$ by assumption, the optimal q^F should reduce the second term $(\tilde{D} + \psi(q^B) - q^F)^+$ as much as possible if $\tilde{D} + \psi(q^B) > 0$. Therefore, the optimal solution to (F.6) is $q^{F*}(q^B) = (\tilde{D} + \psi(q^B))^+ \wedge y^F$. The corresponding optimal objective value is

$$f(q^B) = \begin{cases} 0, & \text{if } \tilde{D} + \psi(q^B) < 0, \\ c^F(\tilde{D} + \psi(q^B)), & \text{if } 0 \leq \tilde{D} + \psi(q^B) < y^F, \\ \xi(\tilde{D} + \psi(q^B)) + (c^F - \xi)y^F, & \text{if } \tilde{D} + \psi(q^B) \geq y^F. \end{cases} \quad (\text{F.8})$$

Next, to derive an explicit solution for (F.7), we rewrite the objective function in (F.8) for three different ranges of \tilde{D} :

(i). $\tilde{D} \geq y^F$:

$$f(q^B) = \begin{cases} 0, & \text{if } q^B < -\tilde{D}, \\ c^F(\tilde{D} + q^B), & \text{if } -\tilde{D} \leq q^B < y^F - \tilde{D}, \\ \xi q^B + \xi \tilde{D} + (c^F - \xi)y^F, & \text{if } y^F - \tilde{D} \leq q^B \leq 0, \\ \xi q^B / \alpha + \xi \tilde{D} + (c^F - \xi)y^F, & \text{if } q^B \geq 0. \end{cases} \quad (\text{F.9})$$

(ii). $0 \leq \tilde{D} < y^F$:

$$f(q^B) = \begin{cases} 0, & \text{if } q^B < -\tilde{D}, \\ c^F(\tilde{D} + q^B), & \text{if } -\tilde{D} \leq q^B < 0, \\ c^F(\tilde{D} + q^B / \alpha), & \text{if } 0 \leq q^B < \alpha(y^F - \tilde{D}), \\ \xi q^B / \alpha + \xi \tilde{D} + (c^F - \xi)y^F, & \text{if } q^B \geq \alpha(y^F - \tilde{D}). \end{cases} \quad (\text{F.10})$$

(iii). $\tilde{D} < 0$:

$$f(q^B) = \begin{cases} 0, & \text{if } q^B < -\alpha \tilde{D}, \\ c^F(\tilde{D} + q^B / \alpha), & \text{if } -\alpha \tilde{D} \leq q^B < \alpha(y^F - \tilde{D}), \\ \xi q^B / \alpha + \xi \tilde{D} + (c^F - \xi)y^F, & \text{if } q^B \geq \alpha(y^F - \tilde{D}). \end{cases} \quad (\text{F.11})$$

Note that, in all three cases, $f(q^B)$ is piecewise linear and convex in q^B , with minimum slope 0 and maximum slope ξ/α . On the other hand, the second term in (F.7), $\frac{\partial \phi}{\partial b} q^B$ is linear q^B with slope between $-\xi$ and 0. Therefore, the objective function in (F.7) is piecewise linear and convex in q^B , with minimum slope $\frac{\partial \phi}{\partial b} \leq 0$ and maximum slope $\xi/\alpha + \frac{\partial \phi}{\partial b} > 0$.

Therefore, we can solve (F.7) by first ignoring the constraint $q^B \in [-y_{\text{out}}^B, \alpha y_{\text{in}}^B]$ to obtain the unconstrained optimal \hat{q}^B , given as follows:

(i). If $\tilde{D} \geq y^F$, then the optimal charging/discharging rate is

$$\hat{q}^B = \begin{cases} y^F - \tilde{D}, & \text{if } -\xi \leq \frac{\partial \phi}{\partial b} < -c^F, \\ -\tilde{D}, & \text{if } -c^F \leq \frac{\partial \phi}{\partial b} \leq 0. \end{cases}$$

(ii). If $0 \leq \tilde{D} < y^F$, then the optimal charging/discharging rate is

$$\hat{q}^B = \begin{cases} \alpha(y^F - \tilde{D}), & \text{if } -\xi \leq \frac{\partial \phi}{\partial b} < -c^F/\alpha, \\ 0, & \text{if } -c^F/\alpha \leq \frac{\partial \phi}{\partial b} < -c^F, \\ -\tilde{D}, & \text{if } -c^F \leq \frac{\partial \phi}{\partial b} \leq 0; \end{cases}$$

(iii). If $\tilde{D} < 0$, then the optimal charging/discharging rate is

$$\hat{q}^B = \begin{cases} \alpha(y^F - \tilde{D}), & \text{if } -\xi \leq \frac{\partial \phi}{\partial b} < -c^F/\alpha, \\ -\alpha\tilde{D}, & \text{if } -c^F/\alpha \leq \frac{\partial \phi}{\partial b} \leq 0; \end{cases}$$

Since the objective function of (F.7) is convex, the optimal solution constrained by $q^B \in [-y_{\text{out}}^B, \alpha y_{\text{in}}^B]$ can be written immediately as $\tilde{q}^B = (\hat{q}^B \vee (-y_{\text{out}}^B)) \wedge (\alpha y_{\text{in}}^B)$.

The corresponding optimal q^F is $\tilde{q}^F(\tilde{q}^B) = (\tilde{D} + \psi(\tilde{q}^B))^+ \wedge y^F$, which are stated in the proposition statement. It can be easily verify that $\tilde{q}^F(\tilde{q}^B) = (\hat{q}^F)^+ \wedge y^F$ where \hat{q}^F is stated in equations (17)-(19). \square

Proof of Theorem 1: If $b = 0$, Lemma A.1 implies that $q_t^{B*}(b, \tilde{D}) = \tilde{q}^B + I_t'$. In the proof of Lemma A.1, we show that if $b = 0$, the process I_t satisfies $I_t' = (\tilde{q}_t^B)^-$ where $x^- = \max(0, -x)$. Therefore, we have that $q_t^{B*}(b, \tilde{D}) = \tilde{q}^B \vee 0$.

Since $\tilde{q}^B \geq 0$ for $\tilde{D} \leq y^F$, we only consider the case when $\tilde{D} > y^F$. It follows from the boundary condition in Lemma 2 that $\frac{\partial \phi}{\partial b} = -\xi$ when $b = 0$. In this case, it follows from Proposition 1 that $\tilde{q}^F = y^F$, which is independent of \tilde{q}^B . Therefore, $q_t^{F*}(b, \tilde{D}) = \tilde{q}^F = y^F$.

A similar argument shows that $q_t^{B*}(b, \tilde{D}) = \tilde{q}^B \wedge 0$ and $q_t^{F*}(b, \tilde{D}) = \tilde{q}^F = 0$. \square

Proof of Lemma 4: For (i), we prove that y^{R*} (weakly) decreases in k^R . The same argument can be applied to prove that y^{F*} decreases in k^F and B^* decreases in k^B . We fix capacity costs $k^B \geq 0$ and $k^F \geq 0$ and let $k_1^R > k_2^R \geq 0$. Let (y_i^R, y_i^F, B_i) denote the optimal solution to (1) under renewable capacity cost k_i^R , for $i = 1, 2$. By the optimality of (y_1^R, y_1^F, B_1) under investment costs k_1^R, k^F and k^B , we have

$$k_1^R y_1^R + k^F y_1^F + k^B B_1 + C(y_1^R, y_1^F, B_1) \leq k_1^R y_2^R + k^F y_2^F + k^B B_2 + C(y_2^R, y_2^F, B_2).$$

Subtracting $(k_1^R - k_2^R)y_2^R$ from both sides of the inequality yields the following:

$$k_2^R y_1^R + k^F y_1^F + k^B B_1 + C(y_1^R, y_1^F, B_1) + (k_1^R - k_2^R)(y_1^R - y_2^R) \leq k_2^R y_2^R + k^F y_2^F + k^B B_2 + C(y_2^R, y_2^F, B_2).$$

By the optimality of (y_2^R, y_2^F, B_2) under investment costs k_2^R, k^F and k^B , we have

$$k_2^R y_1^R + k^F y_1^F + k^B B_1 + C(y_1^R, y_1^F, B_1) \geq k_2^R y_2^R + k^F y_2^F + k^B B_2 + C(y_2^R, y_2^F, B_2).$$

The above two inequalities imply that $(k_1^R - k_2^R)(y_1^R - y_2^R) \leq 0$, i.e., $y_1^R \leq y_2^R$.

For (ii), we prove that the partial derivatives exist and $\partial y^{R*}/\partial k^F = \partial y^{F*}/k^R$. The other two equations can be proved in the same way. Since it optimal to invest in all three energy sources, the optimal solution to

(1) has an interior solution. It follows from the first-order condition of equation (1) that

$$\left(\frac{\partial C(y^{R*}, y^{F*}, B^*)}{\partial y^R}, \frac{\partial C(y^{R*}, y^{F*}, B^*)}{\partial y^F}, \frac{\partial C(y^{R*}, y^{F*}, B^*)}{\partial B} \right)^T = -(k^R, k^F, k^B)^T.$$

Thus, (y^{R*}, y^{F*}, B^*) is the inverse function of the function $(\frac{\partial C}{\partial y^R}, \frac{\partial C}{\partial y^F}, \frac{\partial C}{\partial B})$. Since the Hessian of C is singular, the inverse function theorem guarantees that (y^{R*}, y^{F*}, B^*) are differentiable. Moreover, if we take the derivative with respect to k^R on both sides of the equation, we obtain that

$$\begin{aligned} \sum_{i=y^R, y^F, B} \frac{\partial^2 C(y^{R*}, y^{F*}, B^*)}{\partial y^R \partial i} \frac{\partial i}{\partial k^R} &= -1, \\ \sum_{k=y^R, y^F, B} \frac{\partial^2 C(y^{R*}, y^{F*}, B^*)}{\partial y^F \partial k} \frac{\partial i}{\partial k^R} &= 0, \\ \sum_{k=y^R, y^F, B} \frac{\partial^2 C(y^{R*}, y^{F*}, B^*)}{\partial B \partial k} \frac{\partial i}{\partial k^R} &= 0. \end{aligned}$$

If we write it in the matrix form, we have that

$$H_C \begin{pmatrix} \frac{\partial y^R}{\partial k^R} & \frac{\partial y^F}{\partial k^R} & \frac{\partial B}{\partial k^R} \end{pmatrix} = (1, 0, 0)^T,$$

where H_C is the Hessian matrix of the cost function $C(\cdot)$ evaluated at (y^{R*}, y^{F*}, B^*) . Since H_C is non-singular, it has an inverse matrix. Let H_C^{-1} denote the inverse matrix of H_C . Then we have that $\frac{\partial y^F}{\partial k^R} = -(H_C^{-1})_{21}$. Similarly, we can show that $\frac{\partial y^R}{\partial k^F} = -(H_C^{-1})_{12}$. Since the Hessian H_C is symmetric, its inverse H_C^{-1} is also symmetric. This implies that $\frac{\partial y^F}{\partial k^R} = \frac{\partial y^R}{\partial k^F}$. We can prove that $\frac{\partial y^R}{\partial k^B} = \frac{\partial B}{\partial k^B}$ and $\frac{\partial y^F}{\partial k^B} = \frac{\partial B}{\partial k^B}$ in the same way. \square

Proof of Theorem 2: The proof is included in Appendix C. \square

Proof of Corollary 1: (i) Flexible capacity y^F is fixed. By Definition 1, to show substitutes (resp. complements) between y^{R*} and B^* , we need to show that a decrease in k^R leads to a decrease (resp. increase) in B^* . According to Lemma 4(i), a decrease in k^R leads to an increase in y^{R*} , which decreases the net demand \tilde{D}_t . As a result, the discharging potentials decrease, while the charging potentials increase. We can also see this from Figure 2, where we fix y^F and decrease the net demand curve. Therefore, if the optimal storage capacity is $B^* = Q^{\text{DI}}$ or $B^* = Q^{\text{DI}} + Q^{\text{DF}}$ based on Theorem 2, B^* would decrease, meaning that y^{R*} and B^* are substitutes. Similarly, if $B^* = Q^{\text{CR}}$ or $B^* = Q^{\text{CR}} + Q^{\text{CF}}$, then B^* would increase, implying that y^{R*} and B^* are complements.

(ii) Renewable capacity y^R is fixed. According to Lemma 4(i), a decrease in k^F leads to an increase in y^{F*} , which reduces Q^{DI} , has no impact on $Q^{\text{DI}} + Q^{\text{DF}}$ and Q^{CR} , but increases $Q^{\text{CR}} + Q^{\text{CF}}$. We can also see this from Figure 2, where we raise y^F while keeping the net demand unchanged. Therefore, if $B^* = Q^{\text{DI}}$ based on Theorem 2, B^* would decrease, meaning that y^{F*} and B^* are substitutes. If $B^* = Q^{\text{CR}} + Q^{\text{CF}}$, then B^* would increase, implying that y^{F*} and B^* are complements. \square

Proof of Proposition 1': We can solve (B.4) by optimizing q^F for every given q^B and then optimizing q^B . Specifically, we first solve

$$f(q^B) = \min_{q^F \in [0, y^F]} c^F q^F + \xi(\tilde{D} + \psi(q^B) - q^F)^+ \quad (\text{F.12})$$

and then solve

$$\min_{q^B \in [\underline{q}_t^B, \bar{q}_t^B]} f(q^B) + \tilde{\phi}_t(b_t + q^B \delta, r_t, d_t), \quad (\text{F.13})$$

Note that (F.12) is identical to the problem in (F.6), and the function $f(q^B)$ has an explicit expression as stated in (F.8)-(F.11) in the proof of Proposition 1.

The optimal solution to this problem is $q^F = \min((\tilde{D} + \psi(q^B))^+, y^F)$. The value of $f(q^B)$, which depends on the net demand \tilde{D} , is provided in equations (F.9)-(F.11) for three cases. Note that $f(q^B)$ is increasing and convex in q^B in all three cases. Since $\tilde{\phi}(b, r_t, d_t)$ is also convex in b for fixed r_t and d_t , equation (F.13) minimizes a convex function on a compact set. Therefore, we first relax the control bound $q_t^B \in [\underline{q}_t^B, \bar{q}_t^B]$ and solve

$$\min_{\hat{q}^B} f(q^B) - v + \tilde{\phi}_t(b_t + \hat{q}^B \delta, r_t, d_t). \quad (\text{F.14})$$

The optimal solution to equation (F.13) is $q_t^{B*} = \underline{q}_t^B \vee (\hat{q}^B \wedge \bar{q}_t^B)$ where \hat{q}^B is the optimal solution to equation (F.14). The rest of the proof is dedicated to find the optimal solution for equation (F.14).

The value of the function $f(\cdot)$ depends on the value of the net demand \tilde{D} , as shown in equations (F.9)-(F.11). In all three cases, it is a piecewise linear function. We derive the optimal solution (B.5) for the case $\tilde{D} > y^F$ in details next. We omit the discussion for other two case because the derivation follows the same steps.

Since $\partial \tilde{\phi}_t(b, r_t, d_t) / \partial b \in [-\xi / \delta, 0]$ for any $b \in [0, B]$ and $f'(q^B) \geq \xi$ for $q^B \geq y^F - \tilde{D}$, we have that

$$f'(q^B) + \frac{\partial \tilde{\phi}_t(b_t + q^B \delta, r_t, d_t)}{\partial b} \delta \geq 0 \quad \text{for } q^B \geq y^F - \tilde{D}.$$

In addition, we have that $f'(q^B) = 0$ for $q^B < -\tilde{D}$. This implies that

$$f'(q^B) + \frac{\partial \tilde{\phi}_t(b_t + q^B \delta, r_t, d_t)}{\partial b} \delta \leq 0 \quad \text{for } q^B < \tilde{D}.$$

Therefore, it suffices to consider the case when $q^B \in [-\tilde{D}, y^F - \tilde{D}]$. Note from equation (F.9) that $f'(q^B) = c^F$ for $q^B \in [-\tilde{D}, y^F - \tilde{D}]$. Now consider the following three cases:

1. $(\bar{b}_t - b_t) / \delta > y^F - \tilde{D}$. Then we have that $b_t + (y^F - \tilde{D}) \delta < \bar{b}_t$. Since $\partial \tilde{\phi}_t(\cdot) / \partial b$ is increasing in b , we have that for $q^B \in [-\tilde{D}, y^F - \tilde{D}]$,

$$\frac{\partial \tilde{\phi}_t(b_t + q^B \delta, r_t, d_t)}{\partial b} \leq \frac{\partial \tilde{\phi}_t(b_t + (y^F - \tilde{D}) \delta, r_t, d_t)}{\partial b} \leq \frac{\partial \tilde{\phi}_t(\bar{b}_t, r_t, d_t)}{\partial b} = -c^F.$$

This implies that $f(q^B) + \tilde{\phi}_t(b_t + q^B \delta, r_t, d_t)$ is decreasing in q^B for $q^B \in [-\tilde{D}, y^F - \tilde{D}]$. The optimal solution $\hat{q}_B = y^F - \tilde{D}$.

2. If $(\bar{b}_t - b_t) / \delta \in [y^F - \tilde{D}, -\tilde{D}]$. In this case, since $\tilde{\phi}_t(b_t + q^B \delta, r_t, d_t)$ is convex in q^B and

$$f'(\bar{b}_t - b_t) / \delta + \frac{\partial \tilde{\phi}_t(\bar{b}_t, r_t, d_t)}{\partial b} = 0,$$

the optimal solution is the interior solution $\hat{q}^B = (\bar{b}_t - b_t) / \delta$.

3. If $(\bar{b}_t - b_t) / \delta < -\tilde{D}$. In this case, since $\tilde{\phi}_t(b_t + q^B \delta, r_t, d_t)$ is convex in q^B , we have that for $q^B \in [-\tilde{D}, y^F - \tilde{D}]$,

$$\frac{\partial \tilde{\phi}_t(b_t + q^B \delta, r_t, d_t)}{\partial b} \geq \frac{\partial \tilde{\phi}_t(b_t + (-\tilde{D}) \delta, r_t, d_t)}{\partial b} \geq \frac{\partial \tilde{\phi}_t(\bar{b}_t, r_t, d_t)}{\partial b} = -c^F.$$

This implies that $f(q^B) + \tilde{\phi}_t(b_t + q^B \delta, r_t, d_t)$ is increasing in q^B for $q^B \in [-\tilde{D}, y^F - \tilde{D}]$. The optimal

solution is $\hat{q}^B = -\tilde{D}$.

In sum, the optimal solution is $\hat{q}^B = (y^F - \tilde{D}) \wedge [-(\tilde{D} \wedge ((b - \bar{b}_t)/\delta))]$. Note that if $\partial\phi_t(b_t, r_t, d_t) < -c^F$, then $b_t < \bar{b}_t$. In this case, $(\bar{b}_t - b_t)/\delta > 0 > y^F - \tilde{D}$. The optimal solution is just $\hat{q}^B = y^F - \tilde{D}$. This completes the derivation of the optimal solution in equation (B.5). The optimal policy considering the charging constraint is $q_t^{B*} = (\underline{q}_t^B \vee \hat{q}^B) \wedge \bar{q}_t^B$. In addition, $q^{F*} = (\tilde{D} + \psi(q_t^{B*}))^+ \wedge y^F$. \square